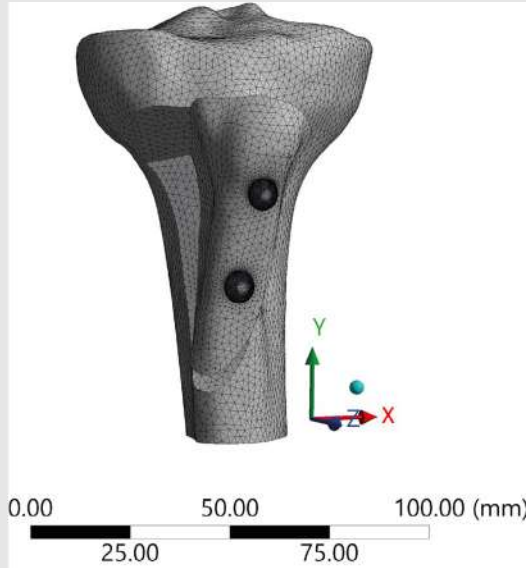


European Archives of Medical Research

Formerly Okmeydanı Medical Journal

Volume: 41 • Number: 3 • June 2025



See Page 167

Highlights

- **Perioperative Glycemic Control**
Mehmet Sahap, Beyza Nur Coban, Ikbâl Efnan Asik, Handan Gulec, Ezgi Erkilic
- **Dietary Inflammatory Index and Colorectal Cancer**
Noyan Kafaoglu, Engin Olcucuoglu, Ismail Oskay Kaya
- **Inflammatory Markers of Healing in Proximal Humerus Fractures**
Nazim Erkurt, Murat Cakar, Ali Yuce, Abdulhamit Misir, Tahsin Olgun Bayraktar, Serdar Aki
- **Temporal Evolution of LLMs for RECIST**
Esat Kaba, Davide Giardino, Arvin Naeimi, Merve Solak, Mehmet Beyazal, Fatma Beyazal Çeliker, Thomas Vogl
- **ASXL1 Gene Mutations in Myeloproliferative Neoplasms**
Neslihan Uslu, Veyssel Sabri Hancer, Reyhan Diz Kucukkaya
- **Fixation Performance in Fulkerson Osteotomy**
Ali Levent, Metin Yapti, Huseyin Kursat Celik, Mehmet Baris Ertan, Ozkan Kose
- **17 Schwannoma Cases: Cytology and FN**
Burcu Ozcan, Senay Erdogan Durmus, Zeynep Betul Erdem, Merve Cin
- **Effects of Laboratory Values in Stroke Rehabilitation**
Selda Ciftci Inceoglu, Aylin Ayyildiz, Cansu Adikti, Banu Kuran

European Archives of Medical Research

Formerly Okmeydanı Medical Journal

**Owner on behalf and Responsible Manager of University of Health Sciences Türkiye,
Prof. Dr. Cemil Taşcıoğlu City Hospital**

Ali Alemdar

Clinic of General Surgery, University of Health Sciences Türkiye, Prof. Dr. Cemil Taşcıoğlu City Hospital, İstanbul, Türkiye

Editor in Chief

İsmail Demirkale

Clinic of Orthopedics and Traumatology, University of Health Sciences Türkiye, Sisli Hamidiye Etfal Training and Research Hospital, İstanbul, Türkiye

ORCID ID: 0000-0001-7230-1599

Associate Editors

Asım Kalkan

Clinic of Emergency Medicine, University of Health Sciences Türkiye, Prof. Dr. Cemil Taşcıoğlu City Hospital, İstanbul, Türkiye

ORCID: orcid.org/0000-0002-5800-0201

Müjdat Adaş

Clinic of Orthopedics and Traumatology, University of Health Sciences Türkiye, Prof. Dr. Cemil Taşcıoğlu City Hospital, İstanbul, Türkiye

ORCID: orcid.org/0000-0003-3637-8876

Tamer Özülker

Clinic of Nuclear Medicine, University of Health Sciences Türkiye, Prof. Dr. Cemil Taşcıoğlu City Hospital, İstanbul, Türkiye

ORCID ID: 0000-0001-9521-683X

Namıgar Turgut

Clinic of Anesthesia and Reanimation, University of Health Sciences Türkiye, Prof. Dr. Cemil Taşcıoğlu City Hospital, İstanbul, Türkiye

ORCID: orcid.org/0000-0003-0252-3377

Özben Yalçın

Clinic of Pathology, University of Health Sciences Türkiye, Prof. Dr. Cemil Taşcıoğlu City Hospital, İstanbul, Türkiye

ORCID: orcid.org/0000-0002-0019-1922

Editorial Staff

Pelin İlhan

University of Health Sciences Türkiye, Prof. Dr. Cemil Taşcıoğlu City Hospital,

Department of Strategy Development, İstanbul, Türkiye

E-mail: stratejicemiltascioglu@gmail.com

ORCID ID: 0000-0001-9143-7512

Editorial Board

Achmet Ali

Department of Anesthesiology and Reanimation, İstanbul University Faculty

of Medicine, İstanbul, Türkiye

ORCID ID: 0000-0002-7224-6654

Ali Cahid Civelek

*Clinic of Radiology, Division of Nuclear Medicine, Johns Hopkins Medical
Instituons, Baltimore, USA*

ORCID ID: 0000-0003-4637-6292

Alper Ötünçtemur

Clinic of Urology, University of Health Sciences Türkiye, Prof. Dr. Cemil

Taşcıoğlu City Hospital, İstanbul, Türkiye

ORCID ID: 0000-0002-0553-3012

Andrej Nikolovski

Department of Visceral Surgery, University Surgery Clinic Sv. Naum Ohridski;

*Ss. Cyril and Methodius University in Skopje, Skopje, Republic of North
Macedonia*

ORCID ID: 0000-0002-5286-3532

Arzu Akan

Clinic of General Surgery, University of Health Sciences Türkiye, Prof. Dr.

Cemil Taşcıoğlu City Hospital, İstanbul, Türkiye

ORCID ID: 0000-0001-8435-9771

Berir Upcin

Institute of Anatomy and Cell Biology, Julius-Maximilians-University,

Würzburg, Germany

ORCID ID: 0000-0003-4853-9358

Berrin Hüner

*Clinic of Physical Therapy and Rehabilitation, Gaziosmanpaşa Training and
Research Hospital, İstanbul, Türkiye*

ORCID ID: 0000-0003-3584-8880

Burak Erden

Clinic of Eye Diseases, Dünya Göz Hospital Ataköy, İstanbul, Türkiye

ORCID ID: 0000-0003-0650-4552

Bülent Ozgonenel

*Clinic of Hematology Oncology, Children's Hospital of Michigan, Detroit,
United States*

ORCID ID: 0000-0001-8891-7646

Ekrem Üçer

*University Hospital Regensburg, Department of Cardiology, Regensburg,
Germany*

ORCID ID: 0000-0002-3935-1110

Funda Şimşek

*Clinic of Infectious Diseases and Departmental Microbiology, University of
Health Sciences Türkiye, Prof. Dr. Cemil Taşcıoğlu City Hospital, İstanbul,*

Türkiye

ORCID ID: 0000-0002-7387-5057

Gülcan Günütaş

*Department of Biochemistry, Faculty of Medicine, Kırklareli University,
Kırklareli Türkiye*

ORCID ID: 0000-0002-3638-4662

Hakan Önder

Clinic of Radiology, University of Health Sciences Türkiye, Prof. Dr. Cemil

Taşcıoğlu City Hospital, İstanbul, Türkiye

ORCID ID: 0000-0001-5207-3314

Hasan Dursun

Clinic of Pediatrics, University of Health Sciences Türkiye, Prof. Dr. Cemil

Taşcıoğlu City Hospital, İstanbul, Türkiye

ORCID ID: 0000-0002-8817-494X

European Archives of Medical Research

Formerly Okmeydanı Medical Journal

İlteriş Oğuz Topal

Clinic of Dermatology, University of Health Sciences Türkiye, Prof. Dr. Cemil Taşcıoğlu City Hospital, İstanbul, Türkiye

ORCID ID: 0000-0001-8735-9806

Kadriye Kılıçkesmez

Clinic of Cardiology, University of Health Sciences Türkiye, Prof. Dr. Cemil Taşcıoğlu City Hospital, İstanbul, Türkiye

ORCID ID: 0000-0002-2139-9909

Nurdan Gül

Department of Endocrinology, İstanbul University Faculty of Medicine, İstanbul, Türkiye

ORCID ID: 0000-0002-1187-944X

Mehmet Küçük

Clinic of Internal Medicine, University of Health Sciences Türkiye, Prof. Dr. Cemil Taşcıoğlu City Hospital, İstanbul, Türkiye

ORCID ID: 0000-0003-1720-3819

Mete Gürsoy

Clinic of Cardiovascular Surgery, University of Health Sciences Türkiye, Mehmet Akif Ersoy Chest and Cardiovascular Surgery Hospital, İstanbul, Türkiye

ORCID ID: 0000-0002-7083-476X

Metin Çetiner

Duisburg-essen University School Of Medicine, Division Of Pediatric Nephrology And Pediatric Sonography Hufelandstrasse

ORCID ID: 0000-0002-0918-9204

Mine Adaş

Clinic of Internal Medicine, University of Health Sciences Türkiye, Prof. Dr. Cemil Taşcıoğlu City Hospital, İstanbul, Türkiye

ORCID ID: 0000-0003-3008-6581

Murat Dursun

Department of Urology, İstanbul University Faculty of Medicine, İstanbul, Türkiye

ORCID ID: 0000-0001-9115-7203

Özge Kandemir Gürsel

Clinic of Radiation Oncology, University of Health Sciences Türkiye, Prof. Dr. Cemil Taşcıoğlu City Hospital, İstanbul, Türkiye

ORCID ID: 0000-0002-6960-4115

Seçil Arıca

Clinic of Family Practice, University of Health Sciences Türkiye, Prof. Dr. Cemil Taşcıoğlu City Hospital, İstanbul, Türkiye

ORCID ID: 0000-0003-0135-6909

Seçkin Aydın

Clinic of Brain Surgery, University of Health Sciences Türkiye, Prof. Dr. Cemil Taşcıoğlu City Hospital, İstanbul, Türkiye

ORCID ID: 0000-0003-1195-9084

Serdar Günaydın

Clinic of Cardiovascular Surgery, University of Health Sciences Türkiye, Ankara City Hospital, Ankara, Türkiye

ORCID ID: 0000-0002-9717-9793

Sezen Karakuş

Department of Ophthalmology, The Johns Hopkins Wilmer Eye Institute, Baltimore, USA

ORCID ID: 0000-0003-2951-995X

Sinan Akay

Department of Radiology, University of Iowa Health Care, 52242, Iowa City, IA

ORCID ID: 0000-0001-7201-475X

Şener Cihan

Department of Medical Oncology, İstinye University Faculty of Medicine, Medical Park Gaziosmanpaşa Hospital, İstanbul, Türkiye

ORCID ID: 0000-0002-3594-3661

Şerife Şimşek

Department of General Surgeon, Breast Surgeon, Fakeeh University Hospital, Dubai, UAE

ORCID ID: 0000-0003-0463-2710

Tolgar Lütfi Kumral

Clinic of Otorhinolaryngology, University of Health Sciences Türkiye, Prof. Dr. Cemil Taşcıoğlu City Hospital, İstanbul, Türkiye

ORCID ID: 0000-0001-8760-7216

Veli Mihanlı

Clinic of Gynecology and Obstetrics, University of Health Sciences Türkiye, Prof. Dr. Cemil Taşcıoğlu City Hospital, İstanbul, Türkiye

ORCID ID: 0000-0001-8701-8462

Yavuz Anacak

Department of Radiation Oncology, Ege University, İzmir, Türkiye

ORCID ID: 0000-0002-2548-1109

Yavuz Uyar

Clinic of Otorhinolaryngology, University of Health Sciences Türkiye, Prof. Dr. Cemil Taşcıoğlu City Hospital, İstanbul, Türkiye

ORCID ID: 0000-0001-8732-4208

Yücel Arman

Clinic of Internal Medicine, University of Health Sciences Türkiye, Prof. Dr. Cemil Taşcıoğlu City Hospital, İstanbul, Türkiye

ORCID ID: 0000-0002-9584-6644

Ziya Akçetin

KMG Klinikum Urology Clinic Chief, Luckenwalde, Germany

Statistics Editor

Zübeyde Arat

E-mail: zubeyde@aratistatistik.com

ORCID ID: 0009-0008-1751-686X

Social Media Editor

Caner Baran

Clinic of Urology, University of Health Sciences Türkiye, Prof. Dr. Cemil Taşcıoğlu City Hospital, İstanbul, Türkiye

E-mail: drcanerbaran@hotmail.com

ORCID ID: 0000-0002-6315-6518

Publisher Contact

Prof. Dr. Cemil Taşcıoğlu City Hospital
Address University of Health Sciences Türkiye, Prof. Dr. Cemil Taşcıoğlu City Hospital Clinical of E.N.T. / Okmeydanı / İstanbul
E-mail info@okmeydanitipdergisi.org
Website cemiltascioglush.saglik.gov.tr

Publishing House

Kare Publishing

Address Göztepe Mah. Fahrettin Kerim Gökay Caddesi No: 200/A D:2
Çemenzar - Kadıköy, İstanbul-Türkiye
Phone +90 216 550 61 11
Fax +90 216 550 61 12
Web www.karepb.com
E-mail kare@karepb.com

*For requests concerning advertising on printed versions and on the webpage of European Archives of Medical Research, please contact the publisher KARE Publishing.

European Archives of Medical Research

Formerly Okmeydanı Medical Journal

Please refer to the journal's webpage (<https://eurarchmedres.org/>) for "Aims and Scope", "Instructions to Authors" and "Ethical Policy".

The editorial and publication process of the European Archives of Medical Research are shaped in accordance with the guidelines of ICMJE, WAME, CSE, COPE, EASE, and NISO. The journal is in conformity with the Principles of Transparency and Best Practice in Scholarly Publishing.

European Archives of Medical Research is currently indexed in TUBITAK ULAKBIM TR Index, Gale, ProQuest, Türk Medline, Türkiye Atıf Dizini, J-GATE and EBSCO Host.

The journal is published online.

Owner: Ali ALEMDAR on Behalf of İstanbul Prof. Dr. Cemil Taşcıoğlu City Hospital

Responsible Manager: İsmail DEMİRKALE

European Archives of Medical Research

Formerly Okmeydanı Medical Journal

CONTENTS

REVIEW

125 Perioperative Management of Hyperglycemia and Hypoglycemia

Mehmet Sahap, Beyza Nur Coban, Ikbal Efnan Asik, Handan Gulec, Ezgi Erkilic; Ankara, Türkiye

ORIGINAL ARTICLES

131 The Relationship between the Dietary Inflammatory Index and Colorectal Cancer

Noyan Kafaoglu, Engin Olcucuoglu, Ismail Oskay Kaya; Giresun, Türkiye

138 Neutrophil-Lymphocyte Ratio and C-Reactive Protein-Albumin Ratio as Predictors of Union Complications in Proximal Humerus Fractures

Nazim Erkurt, Murat Cakar, Ali Yuce, Abdulhamit Misir, Tahsin Olgun Bayraktar, Serdar Aki; Istanbul, Türkiye

146 Temporal Evolution of Large Language Models For Response Evaluation Criteria in Solid Tumors-Based Response Evaluation After Locoregional Therapy

Esat Kaba, Davide Giardino, Arvin Naeimi, Merve Solak, Mehmet Beyazal, Fatma Beyazal Çeliker, Thomas Vogl; Rize, Türkiye

154 The Impact of ASXL1 Gene Mutations on Clinical Course and Prognosis in Myeloproliferative Neoplasms

Neslihan Uslu, Veysel Sabri Hancer, Reyhan Diz Kucukkaya; Istanbul, Türkiye

163 Comparison of Titanium, Magnesium, and Polymer-based Cortical Screw Fixation for Fulkerson Tibial Tubercle Osteotomy: A Finite Element Analysis

Ali Levent, Metin Yapti, Huseyin Kursat Celik, Mehmet Baris Ertan, Ozkan Kose; Sanliurfa, Türkiye

174 Clinicopathological, Cytological, and Immunocytochemical Characteristics of 17 Schwannoma Cases Diagnosed by Fine-Needle Aspiration Cytology

Burcu Ozcan, Senay Erdogan Durmus, Zeynep Betul Erdem, Merve Cin; Istanbul, Türkiye

183 Effects of Albumin, Uric Acid, Hemoglobin, and C-Reactive Protein Levels on Rehabilitation Outcomes in Stroke: A Retrospective Clinical Study

Selda Ciftci Inceoglu, Aylin Ayyildiz, Cansu Adikti, Banu Kuran; Istanbul, Türkiye

Perioperative Management of Hyperglycemia and Hypoglycemia

Id Mehmet Sahap,¹ Id Beyza Nur Coban,² Id Ikbal Efnan Asik,² Id Handan Gulec,¹ Id Ezgi Erkilic³

¹Department of Anesthesia and Resuscitation, Yildirim Beyazit University, Faculty of Medicine, Ankara Bilkent City Hospital, Ankara, Türkiye

²Department of Anesthesia and Resuscitation, Ankara Bilkent City Hospital, Ankara, Türkiye

³Department of Anesthesia and Resuscitation, Ankara City Hospital, University of Health Sciences, Ankara, Türkiye

ABSTRACT

Diabetes mellitus is a chronic metabolic disorder characterized by persistent hyperglycemia resulting from inadequate insulin secretion or impaired insulin action, leading to disturbances in carbohydrate, fat, and protein metabolism. In recent years, the prevalence of diabetes in Türkiye has significantly increased, posing a major public health concern and underscoring the need for early diagnosis and effective perioperative management. In the pre-operative period, diabetic patients require thorough evaluation to identify comorbidities, optimize glycemic control, and reduce the risk of perioperative complications. Key anesthetic considerations include assessing cardiovascular and renal status, evaluating for autonomic neuropathy, and determining the presence of delayed gastric emptying, which may influence airway management. Pre-operative optimization involves maintaining blood glucose within the recommended target range, adjusting or withholding oral hypoglycemic agents, and transitioning to intravenous insulin infusion if necessary. This review focuses on the principles of anesthesia management in diabetic patients, emphasizing pre-operative assessment, intraoperative glycemic control, and post-operative monitoring to improve surgical outcomes.

Keywords: Diabetes mellitus, Hyperglycemia, Hypoglycemia, Surgery

Cite this article as: Sahap M, Coban BN, Asik IE, Gulec H, Erkilic E. Perioperative Management of Hyperglycemia and Hypoglycemia. Eur Arch Med Res 2025;41(3):125–130.

INTRODUCTION

Diabetes mellitus (DM) is defined by the Turkish Society of Endocrinology and Metabolism as a metabolic disorder characterized by chronic hyperglycemia due to inadequate insulin secretion or impaired insulin action. This condition causes various abnormalities in carbohydrate, fat, and protein metabolism.^[1]

In recent years, the prevalence of diabetes in Türkiye has shown a significant increase. This has become a serious public

health concern and emphasizes the need for early diagnosis and effective management strategies.

According to the results of the Turkish Diabetes, Hypertension, and Obesity Prevalence Study (TURDEP)-I conducted in 1997–1998, the prevalence of diabetes among individuals aged 20 years and older was found to be 7.2%.^[2]

Twelve years later, the TURDEP-II, conducted in the same centers and among similar age groups, reported a prevalence rate of 13.7%.^[3]

Address for correspondence: Mehmet Sahap, Department of Anesthesia and Resuscitation, Yildirim Beyazit University, Faculty of Medicine, Ankara Bilkent City Hospital, Ankara, Türkiye

E-mail: drsahap@gmail.com **ORCID ID:** 0000-0003-3390-9336

Submitted: 08.07.2025 **Revised:** 11.08.2025 **Accepted:** 12.08.2025 **Available Online:** 12.09.2025

European Archives of Medical Research – Available online at www.eurarchmedres.org

OPEN ACCESS This work is licensed under a Creative Commons Attribution-NonCommercial 4.0 International License.



The difference between these two studies indicates that the prevalence of diabetes in Türkiye has nearly doubled, imposing a significant burden on public health. This increase is associated with factors such as lifestyle changes, urbanization, rising rates of obesity, and physical inactivity.

A similar situation is observed in the United States, where the prevalence of DM has significantly increased in recent years. According to national health surveys conducted in 1999–2000, the prevalence of diabetes among adults in the U.S. was reported to be 9.7%. However, recent evaluations conducted between August 2021, and August 2023, indicate that this figure has risen to 14.3%.^[4]

Diabetes is often diagnosed during pre-operative assessments. The American Diabetes Association recommends screening all overweight individuals with an additional risk factor for diabetes.

It has been reported that approximately 30–40% of patients undergoing cardiac surgery have a history of diabetes. Furthermore, in individuals without a prior diagnosis, stress hyperglycemia – defined as a blood glucose (BG) level exceeding 140 mg/dL – may develop in up to 60% of cases.^[5]

Various studies have demonstrated that perioperative hyperglycemia, whether in critically ill patients or those undergoing cardiac surgery, increases morbidity and mortality rates. Regardless of a prior diabetes diagnosis, patients with perioperative hyperglycemia are associated with higher rates of wound infections; development of acute kidney injury, prolonged hospital stays, and increased risk of perioperative mortality.^[6]

Stress hyperglycemia that develops in individuals without a diagnosis of diabetes, particularly those undergoing coronary artery bypass graft surgery or being monitored in the intensive care unit, is associated with worse clinical outcomes than in individuals with known diabetes. In these patients, the complication rate has been found to be four times higher, and the mortality rate twice as high, compared to normoglycemic patients.^[7]

The development of stress hyperglycemia involves several mechanisms, including stress hormones (cortisol, adrenaline), proinflammatory cytokines, and disruption of insulin secretion and action mediated by the central nervous system. This leads to increased glucose production in the liver and reduced glucose uptake in peripheral tissues.^[8]

The adverse outcomes of hyperglycemia are explained by mechanisms such as inflammation, oxidative stress, prothrombotic activity, and vascular dysfunction.^[9]

Long-term follow-up of patients who develop stress hyperglycemia is of great importance. It has been reported that approximately 60% of these individuals are diagnosed with

diabetes within 1 year.^[10]

The effects of different types of anesthesia on intraoperative glucose control were evaluated in a systematic review and meta-analysis conducted by Li et al.^[11] in 2017. According to this study published in *Medicine*, combined general-epidural anesthesia was found to be more effective in controlling intraoperative glucose levels compared to general anesthesia alone. However, no significant difference was observed between isolated epidural anesthesia and general anesthesia.

Pre-Operative Assessment

The pre-operative assessment of diabetic patients is critically important for the successful management of the surgical process (Fig. 1). The following steps constitute the core components of this evaluation:

- A detailed medical history and physical examination should be conducted. The type and duration of diabetes, current medications, and the presence of diabetes-related organ damage must be assessed^[12]
- Glycemic control status should be determined through tests such as hemoglobin A1c (HbA1c) and BG measurements. These tests play a significant role in shaping perioperative glycemic management strategies^[13]
- Liver and renal functions should be evaluated, as diabetic patients often experience impairments in kidney and liver function^[14]

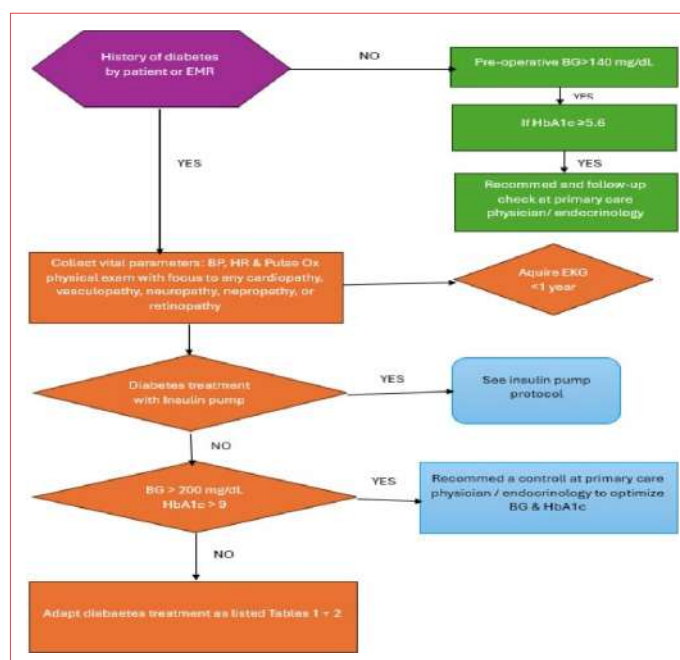


Figure 1. Pre-operative diabetes screening and management algorithm.

Table 1. Perioperative effects of oral antidiabetic agents

OAD class	Examples	Warnings/Precautions
Secretagogues (Sulfonylureas, etc.,)	Gliburide Glimepiride	Risk of hypoglycemia, prolonged drug effect, and challenges in dose titration.
Biguanides	Metformin	Risk of lactic acidosis; use with caution in renal and hepatic impairment
Thiazolidinediones	Rosiglitazone	Intravascular volume expansion, delayed onset of action, and challenges in dose titration

OAD: Oral Anti Diabetic.

- Electrolyte balance and ECG evaluations should be performed, especially considering the effects of hyperglycemia on cardiac rhythm.^[15]

ORAL ANTIDIABETICS

Oral antidiabetic therapy plays an important role in the management of diabetes and consists of various pharmacological classes (Table 1). These drugs aim to control BG by either enhancing insulin effects or inhibiting glucose production.

- Sulfonylureas** increase insulin secretion by blocking potassium channels in pancreatic beta cells. These drugs generally reduce HbA1c by approximately 1–2%.^[16] This group of drugs is commonly used in diabetes treatment and is particularly effective in patients with moderate hyperglycemia
- Metformin** increases insulin sensitivity in tissues and reduces hepatic gluconeogenesis. Metformin effectively lowers hyperglycemia by about 25% in 90% of patients.^[17] In addition, the cardiovascular benefits of metformin represent a significant advantage, making it the first-line therapy for most diabetic patients
- Thiazolidinediones** regulate glucose metabolism by increasing insulin sensitivity. These drugs are generally recommended for obese patients and those with developed insulin resistance^[18]
- Meglitinides** accelerate insulin release from pancreatic beta cells and are typically administered before meals. These drugs help prevent rapid post-prandial glucose spikes^[19]
- Alpha-glucosidase inhibitors** delay the absorption of carbohydrates in the intestines, thereby controlling post-pran-

dial hyperglycemia. These agents are particularly used in patients with rapid BG increases after meals^[20]

- Glucagon-like peptide-1 agonists** increase insulin secretion, inhibit glucagon release, and delay gastric emptying. Moreover, they reduce hunger sensation, supporting weight loss and weight management^[21]
- Sodium-glucose cotransporter 2 (SGLT2) inhibitors** inhibit glucose reabsorption in the kidneys, promoting excretion of excess glucose through urine. These drugs not only control hyperglycemia but also offer cardiovascular benefits.^[22]

In a randomized controlled trial, the hypothesis that continuation of oral antidiabetic drugs (OADs) before surgery would reduce perioperative BG levels was tested. The study compared two groups: one in which pre-operative OAD use was continued, and another in which OADs were discontinued. The group in which OADs were discontinued had an average BG level of 156 mg/dL (95% confidence interval: 146–167 mg/dL; $p<0.001$), while BG levels in the group continuing OADs were significantly lower (mean: 138 mg/dL; 95% confidence interval: 130–146 mg/dL).^[23]

This result demonstrates that continuation of OADs pre-operatively has a beneficial effect on perioperative BG management.

Furthermore, it is emphasized that in patients using insulin, home insulin regimens and fasting glucose measurements must be carefully reviewed. Optimization of insulin therapy plays an important role in achieving BG control during the perioperative period.

Preoperatively, long-acting insulins are less likely to result in hypoglycemia and should therefore not be withheld. Half the normal dose of intermediate insulin should be taken on the day of surgery. Rapid-acting insulin should be withheld in patients with a BG below 200 mg/dL and carefully titrated in patients with a BG exceeding 200 mg/dL. General guidelines for insulin are summarized in Table 2.^[24]

Management of Diabetic Patients in The Perioperative Period: Clinical Protocol Recommendations

To ensure the safe and effective management of surgical procedures in diabetic patients, each healthcare institution should establish its own clinical protocol. These protocols should cover the pre-operative and intraoperative periods to optimize patients' metabolic status.

In the pre-operative period, HbA1c and BG levels should be evaluated at least 3–4 days before the scheduled surgery. In elective surgeries, if BG exceeds 250 mg/dL, the procedure should be postponed.^[1,25] Surgeries should preferably be scheduled in the early morning hours, considering the patient

Table 2. Insulin treatment on the day of surgery

Insulin types	Regiment on the day of surgery
Lantus/toujeo, tresiba, levemir (long-acting insulins)	Half dose of normal in the morning of surgery
Nph insulin (intermediate insulin)	Half dose of normal in the morning of surgery
Insulin aspart protamine, insulin aspart, insulin lispro protamine, insulin lispro, insulin neutral protamine hagedorn, and insulin regular (all mixed insulin)	Depending to the blood glucose: if >200 mg/dL: Take half dose of normal in the morning. If <200 mg/dL: no insulin
All models of insulin pumps: Endocrinology consult recommended expect patient’s ambulatory	Basel rate until operation, continue with IV insulin during surgery

will not be able to eat breakfast. To prevent catabolic response and dehydration due to fasting, the use of carbohydrate-containing clear fluids or glucose gels is recommended.^[26]

During intraoperative evaluation, rapid sequence intubation should be performed in diabetic patients with a high risk of difficult airway, particularly those suspected of gastroparesis, to reduce the risk of aspiration. Electrolyte disturbances, which are frequently encountered, should be carefully monitored. The target intraoperative BG range is 120–180 mg/dL, and continuous glucose monitoring (CGM) is essential to prevent both hypo- and hyperglycemic episodes.^[1,26,27]

Use of CGM in The Perioperative Period

CGMs, which are minimally invasive and measure interstitial glucose levels every 1–5 minutes, are widely used in daily diabetes management. However, these devices have not yet been officially approved for use in the perioperative setting.^[28]

Physiological and technical factors during surgery, such as hypotension, hypothermia, hypoxia, and electrical interference, may compromise the accuracy of CGM readings. Therefore, CGM data should not be fully relied upon intraoperatively, and plasma glucose levels should be confirmed with standard methods when necessary.^[25,29]

According to the updated 2023 guideline titled “Guideline for Perioperative Care for People with Diabetes Mellitus Undergoing Elective and Emergency Surgery,” several key recommendations have been provided for perioperative diabetes management. The guideline emphasizes avoiding prolonged pre-operative fasting and scheduling diabetic patients for surgery in the early morning. The recommended target BG range is 6–10

mmol/L (108–180 mg/dL), with values up to 12 mmol/L (216 mg/dL) considered acceptable. If BG falls below 70 mg/dL, intravenous glucose administration is advised.^[30]

The new guideline offers detailed guidance on topics such as the management of patients using continuous subcutaneous insulin infusion (CSII), the risk of diabetic ketoacidosis with SGLT-2 inhibitors, and intervention protocols for impending hypoglycemia (4–6 mmol/L) and clinically significant hypoglycemia (<4 mmol/L). It also provides comprehensive recommendations for adjusting insulin and other antidiabetic medications in the pre- and post-operative periods. The 2023 edition is more detailed than its 2021 predecessor and aims to reduce surgical complications.^[30]

Perioperative Hyperglycemia and Insulin Management

Perioperative BG levels exceeding 180 mg/dL are associated with increased morbidity, particularly infection risk, and higher mortality. Therefore, insulin therapy should be initiated, aiming to maintain BG within the range of 140–180 mg/dL. Tight glycemic control targeting normoglycemia increases the risk of severe hypoglycemia and has not demonstrated additional benefit. In patients with Type 1 or Type 2 diabetes, or those with stress-induced hyperglycemia, transition to continuous intravenous insulin infusion (IVCSII) is recommended when a personal insulin pump is discontinued. This strategy is particularly preferred for prolonged surgeries and in critically ill patients.^[31]

For nausea and vomiting prophylaxis, the use of 4 mg dexamethasone in combination with another antiemetic is recommended, and doses of 8 mg should be avoided. Regional anesthesia should be preferred whenever possible, as it facilitates post-operative pain control and reduces insulin resistance. Patients with poor glycemic control often require increased analgesic support. Preventing hypothermia, encouraging early mobilization, using minimally invasive surgical techniques, and minimizing blood loss are also beneficial in reducing insulin resistance-related perioperative complications.^[31]

Perioperative Hypoglycemia

Symptoms of perioperative hypoglycemia may be masked under general anesthesia; thus, glucose levels must be closely monitored. Hypoglycemia is classified as follows:

- **Level 1:** <70 mg/dL
- **Level 2:** <54 mg/dL
- **Level 3:** <40 mg/dL

Hypoglycemia is particularly common in patients with Type 1 diabetes using insulin and in elderly patients on sulfonylureas. For treatment, administration of 25–50 mL of 50% dextrose solution or 500 mL of 5% dextrose is recommended.^[31]

Approach to Hypoglycemia Risk in Perioperative Glycemic Management and Clinical Implications

The article titled “Near Miss Hypoglycemia Reflections on Perioperative Glucose Management Guidelines in Diabetics” highlights the weak points in clinical practice by examining cases in which hypoglycemia was narrowly avoided. Attempting to maintain glucose levels within a narrow range (e.g., 4–6 mmol/L) increases the risk of hypoglycemia. Prolonged pre-operative fasting and improper adjustment of antidiabetic agents – particularly insulin and sulfonylureas – can lead to perioperative hypoglycemia.

According to recent recommendations, it is advised that certain oral antidiabetic drugs (such as sulfonylureas) be withheld on the morning of surgery, and that doses of long-acting insulin be reduced by approximately 70–80%. It has been emphasized that variable rate intra-venous insulin infusions may cause abrupt glucose drops if glucose and caloric intake are not carefully managed. Furthermore, most hypoglycemic events have been linked to incomplete handovers of insulin administration times or BG information during staff transitions.^[32]

According to the most recent *Standards of Care in Diabetes – 2025* published by the American Diabetes Association, perioperative BG levels should be maintained between 80 and 180 mg/dL. Metformin and other oral glucose-lowering agents should be discontinued on the day of surgery. SGLT2 inhibitors should be stopped 3–4 days before surgery. Doses of NPH and long-acting insulins (e.g., glargine) should be reduced by 20–25% the day before surgery, and by approximately 50% on the morning of the procedure.^[33]

Patients Using CSII

- In planned and short-duration surgeries, the insulin pump may be continued; basal infusion should be maintained, and glucose levels monitored hourly
- In emergency surgeries or procedures lasting longer than 3 h, the pump should be discontinued and transitioned to intravenous insulin infusion. BG should be maintained within a target range of 140–180 mg/dL (7.7–10 mmol/L).^[34]

CONCLUSION

In light of all this information, we at Bilkent City Hospital implement these protocols in our perioperative glucose management strategies and believe they will also serve as valuable guidance for other anesthesiologists.

DECLARATIONS

Informed Consent: All patients included in the study gave their verbal and written consent.

Conflict of Interest: The authors declare they have no conflict of interest with regard to the results of this study.

Funding: The authors declare they have received no funding during or after this study.

Use of AI for Writing Assistance: Artificial intelligence (ChatGPT, OpenAI) was used solely for grammar correction and language editing purposes. No AI was involved in data analysis, interpretation, or content generation.

Authorship Contributions: Concept – MŞ; Design – HG, MŞ; Supervision – HG; Fundings – MŞ; Materials – BNÇ; Data collection &/or processing – MŞ; Analysis and/or interpretation – MŞ; Literature search – BNÇ; Writing – EE; Critical review – EE, IEA, BNÇ.


Peer-review: Externally peer-reviewed.

REFERENCES

1. Türkiye Endokrinoloji ve Metabolizma Derneği. Diabetes mellitus ve komplikasyonlarının tanı, tedavi ve izlem kılavuzu. Ankara: Türkiye Endokrinoloji ve Metabolizma Derneği; 2024.
2. Satman I, Yilmaz T, Sengül A, Salman S, Salman F, Uygur S, et al. Population-based study of diabetes and risk characteristics in Turkey: Results of the Turkish diabetes epidemiology study (TURDEP). *Diabetes Care* 2002;25:1551–6.
3. Satman I, Omer B, Tutuncu Y, Kalaca S, Gedik S, Dincçag N, et al. Twelve-year trends in the prevalence and risk factors of diabetes and prediabetes in Turkish adults. *Eur J Epidemiol* 2013;28:169–80.
4. Centers for Disease Control and Prevention (CDC). National diabetes statistics report 2023. Atlanta (GA): US Department of Health and Human Services; 2023.
5. Lazar HL, McDonnell M, Chipkin SR, Furnary AP, Engelman RM, Sadhu AR, et al. The Society of Thoracic Surgeons practice guideline series: Blood glucose management during adult cardiac surgery. *Ann Thorac Surg* 2009;87:663–9.
6. Dungan KM, Braithwaite SS, Preiser JC. Stress hyperglycaemia. *Lancet* 2009;373:1798–807.
7. Umpierrez GE, Isaacs SD, Bazargan N, You X, Thaler LM, Kitabchi AE. Hyperglycemia: An independent marker of in-hospital mortality in patients with undiagnosed diabetes. *J Clin Endocrinol Metab* 2002;87:978–82.
8. Marik PE, Bellomo R. Stress hyperglycemia: An essential survival response! *Crit Care* 2013;17:305.
9. NICE-SUGAR Study Investigators; Finfer S, Chittock DR, Su SY, Blair D, Foster D, et al. Intensive versus conventional glucose control in critically ill patients. *N Engl J Med* 2009;360:1283–97.
10. Godinjak A, Iglica A, Burekovic A, Jusufovic S, Ajanovic A, Tancica I, et al. Hyperglycemia in critically ill patients: Management and prognosis. *Med Arch* 2015;69:157–60.

11. Li X, Wang J, Chen K, Li Y, Wang H, Mu Y, et al. Effect of different types of anesthesia on intraoperative blood glucose of diabetic patients: A PRISMA-compliant systematic review and meta-analysis. *Medicine (Baltimore)* 2017;96:e6451.
12. Zhang X, Hou A, Cao J, Liu Y, Lou J, Li H, et al. Association of diabetes mellitus with postoperative complications and mortality after non-cardiac surgery: A meta-analysis and systematic review. *Front Endocrinol (Lausanne)* 2022;13:841256.
13. American Diabetes Association. Standards of medical care in diabetes—2018. *Diabetes Care* 2018;41:S1–S9.
14. Sudhakaran S, Surani SR. Guidelines for perioperative management of the diabetic patient. *Surg Res Pract* 2015;2015:284063.
15. Dilworth L, Facey A, Omoruyi F. Diabetes mellitus and its metabolic complications: The role of adipose tissues. *Int J Mol Sci* 2021;22:7644.
16. Bailey CJ, Turner RC. Metformin. *N Engl J Med* 1996;334:574–9.
17. Rena G, Hardie DG, Pearson ER. The mechanisms of action of metformin. *Diabetologia* 2017;60:1577–85.
18. Petersen MC, Shulman GI. Mechanisms of insulin action and insulin resistance. *Physiol Rev* 2018;98:2133–23.
19. Adams JD, Egan AM, Laurenti MC, Schembri Wismayer D, Bailey KR, Cobelli C, et al. Insulin secretion and action and the response of endogenous glucose production to a lack of glucagon suppression in nondiabetic subjects. *Am J Physiol Endocrinol Metab* 2021;321:E728–36.
20. Hanefeld M, Josse RG, Chiasson JL. Alpha-glucosidase inhibitors for patients with type 2 diabetes: Response to van de Laar et al. *Diabetes Care* 2005;28:1841.
21. Drucker DJ. The biology of incretin hormones. *Cell Metab* 2006;3:153–65.
22. Zelniker TA, Wiviott SD, Raz I, Im K, Goodrich EL, Bonaca MP, et al. SGLT2 inhibitors for primary and secondary prevention of cardiovascular and renal outcomes in type 2 diabetes: A systematic review and meta-analysis of cardiovascular outcome trials. *Lancet* 2019;393:31–9.
23. Gasanova I, Meng J, Minhajuddin A, Melikman E, Alexander JC, Joshi GP. Pre-operative continuation versus interruption of oral hypoglycemics in type 2 diabetic patients undergoing ambulatory surgery: A randomized controlled trial. *Anesth Analg* 2018;127:e54–6.
24. Galway U, Chahar P, Schmidt MT, Araujo-Duran JA, Shivakumar J, Turan A, et al. Perioperative challenges in management of diabetic patients undergoing non-cardiac surgery. *World J Diabetes* 2021;12:1255–66.
25. American Diabetes Association. Standards of care in diabetes—2024. *Diabetes Care* 2024;47:S1–S300.
26. Rizvi AA, Chillag SA, Chillag KJ. Perioperative management of diabetes and hyperglycemia in patients undergoing orthopaedic surgery. *J Am Acad Orthop Surg* 2010;18:426–35.
27. Joshi GP, Chung F, Vann MA, Ahmad S, Gan TJ, Goulson DT, et al. Society for Ambulatory Anesthesia consensus statement on perioperative blood glucose management in diabetic patients undergoing ambulatory surgery. *Anesth Analg* 2010;111:1378–87.
28. Spanakis EK, Levitt DL, Siddiqui T, Singh LG, Pinault L, Sorokin J, et al. The effect of continuous glucose monitoring in preventing inpatient hypoglycemia in general wards: The glucose telemetry system. *J Diabetes Sci Technol* 2018;12:20–5.
29. Aleppo G, Laffel LM, Ahmann AJ, Hirsch IB, Kruger DF, Peters A, et al. A practical approach to using trend arrows on the Dexcom G5 CGM system for the management of adults with diabetes. *J Endocr Soc* 2017;1:1445–60.
30. Centre for Perioperative Care. Guideline for perioperative care for people with diabetes mellitus undergoing elective and emergency surgery. London: CPOC; 2023.
31. Rajan N, Duggan EW, Abdelmalak BB, Butz S, Rodriguez LV, Vann MA, et al. Society for ambulatory anesthesia updated consensus statement on perioperative blood glucose management in adult patients with diabetes mellitus undergoing ambulatory surgery. *Anesth Analg* 2024;139:459–77.
32. Ahmad R, Naftalovich R, Tewfik G, Eloy JD, Rodriguez-Correa DT. Near-miss hypoglycemia-reflections on perioperative glucose management guidelines in diabetes. *BMC Anesthesiol* 2023;23:190.
33. American Diabetes Association. Standards of care in diabetes—2025. *Diabetes Care* 2025;48:S1–S291.
34. Sreedharan R, Khanna S, Shaw A. Perioperative glycemic management in adults presenting for elective cardiac and non-cardiac surgery. *Perioper Med (Lond)* 2023;12:13.

The Relationship between the Dietary Inflammatory Index and Colorectal Cancer

 Noyan Kafaoglu,¹  Engin Olcucuoglu,²  Ismail Oskay Kaya²

¹Department of General Surgery, Ministry of Health, Tirebolu State Hospital, Giresun, Türkiye

²Department of General Surgery, Ankara Etlik City Hospital, Health Sciences University, Ankara, Türkiye

ABSTRACT

Objective: Colorectal cancer is the third most common type of cancer worldwide and one of the leading causes of cancer-related deaths. Chronic inflammation is known to be associated with colorectal cancer. This study aimed to evaluate the relationship between the Dietary Inflammatory Index (DII) and colorectal cancer.

Materials and Methods: 149 patients over the age of 18 who underwent surgery with the diagnosis of colorectal cancer and 120 control patients in the same age group who were hospitalized for a non-cancer reason were included in the study. DII scores were calculated from the patients' 3-day 24-h food consumption records. The level of relationship between DII and colorectal cancer was analyzed with regression analysis.

Results: A total of 269 patients were included in the study, 149 in the study group and 120 in the control group. The mean age of the study group was 64.45 ± 11.36 , and that of the control group was 65.90 ± 10.36 , and the difference was not significant ($p=0.280$). A significant association was found between high DII score and colorectal cancer (odds ratio [OR]: 2.62, $p<0.001$). When adjusted for age and gender, high DII score was also found to be a risk factor for colorectal cancer (OR: 2.72, $p<0.001$).

Conclusion: There is a significant association between an inflammatory diet and high DII scores, which are a measure of it, and the development of colorectal cancer. High DII scores are a significant risk factor for colorectal cancer regardless of age and gender. This risk does not vary according to the location of the cancer and is similar for colon and rectum cancers.

Keywords: Colorectal cancer, Cytokines, Dietary habits, Nutrition

Cite this article as: Kafaoglu N, Olcucuoglu E, Oskay Kaya I. The Relationship between the Dietary Inflammatory Index and Colorectal Cancer. Eur Arch Med Res 2025;41(3):131–137.

INTRODUCTION

Colorectal cancer is the third most common type of cancer globally and a leading cause of cancer-related mortality.^[1] Incidence and mortality rates of colorectal cancer are higher in developed countries, whereas they are lower in less developed regions such as Asia, Africa, and most of Latin America.^[2]

Inflammation typically occurs as a natural response of the body to tissue injury or damage.^[3] An acute inflammatory response plays a crucial role in the healing and regeneration process, usually leading to recovery within a few days.^[4] Chronic inflammation, however, represents a persistent condition where tissue destruction and repair occur simultaneously due to the sustained presence of pro-inflammatory cytokines,

Address for correspondence: Engin Olcucuoglu, Department of General Surgery, Ankara Etlik City Hospital, Health Sciences University, Ankara, Türkiye

E-mail: drengin@gmail.com **ORCID ID:** 0000-0003-0756-3247

Submitted: 28.04.2025 **Revised:** 01.05.2025 **Accepted:** 20.05.2025 **Available Online:** 12.09.2025

European Archives of Medical Research – Available online at www.eurarchmedres.org

OPEN ACCESS This work is licensed under a Creative Commons Attribution-NonCommercial 4.0 International License.



often resulting from increased blood flow to the injured area mediated by mast cell-derived histamine.^[5] Elevated levels of these cytokines are also believed to be associated with colorectal cancer.^[6] Chronic inflammation is widely recognized to be associated with epithelial cancers, particularly colorectal cancer, which remains the most studied.^[7,8]

Several studies have indicated a direct link between specific dietary components and inflammation.^[9,10] There is growing evidence that these dietary elements influence both inflammation and colorectal cancer risk.^[9,11]

The 2012 Continuous Update Project by the American Institute for Cancer Research/World Cancer Research Fund reported that consumption of pro-inflammatory foods such as red and processed meats is associated with an increased risk of colorectal cancer. Conversely, consumption of anti-inflammatory dietary fiber has an inverse relationship with colorectal cancer risk.^[12] Additional dietary components known for their anti-inflammatory properties, such as tea and coffee, have also demonstrated various health benefits, including lower cancer incidence and mortality.^[13,14] Comprehensive studies on dietary patterns have shown that unhealthy diets are linked to higher risks of colorectal cancer and adenomas, whereas healthy diets are associated with reduced risks.^[15]

Research on the role of diet in inflammation and colorectal cancer suggests that dietary patterns represent a complex array of exposures involving cumulative and frequent interactions that affect inflammatory responses and outcomes. Although several dietary indices exist to evaluate diet quality, most lack the capacity to assess the inflammatory potential of a diet. In 2009, researchers at the University of South Carolina developed the first Dietary Inflammatory Index (DII), based on literature published until 2007, as a tool to summarize the inflammatory impact of dietary intake.^[16] This index was later revised and updated in 2014.^[17] The DII categorizes individuals' diets on a continuum from maximally pro-inflammatory to maximally anti-inflammatory. Higher DII scores indicate more pro-inflammatory diets, while lower scores reflect more anti-inflammatory dietary patterns.^[17]

The aim of this study was to evaluate the relationship between DII scores and colorectal cancer.

MATERIALS AND METHODS

This study was conducted prospectively as a single-center study at the University of Health Sciences, Dışkapı Yıldırım Beyazıt Health Practice and Research Center, following the approval of the local ethics committee. Informed consent was obtained from all participating volunteers. This study was conducted in accordance with the Declaration of Helsinki.

The study included 149 patients (study group) diagnosed histopathologically with colorectal cancer and who underwent

surgery at the General Surgery Department of the Dışkapı Yıldırım Beyazıt Training and Research Hospital between July 2020 and November 2021, as well as 120 patients (control group) who were followed and treated for non-cancer diagnoses during the same period. Patients included were over 18 years of age, volunteered to participate, and had complete data available. All patients in the study group had a histopathological diagnosis of colorectal cancer.

Exclusion criteria included: those unwilling to participate, individuals with inflammatory bowel disease, those with a first-degree family history of colorectal cancer, patients with genetic syndromes associated with colorectal cancer, those diagnosed with other cancers or metastases, individuals with alcohol or substance abuse, patients receiving hormone therapy or medical nutrition therapy for other conditions, individuals with incomplete data, and those with communication impairments rendering them unable to complete the questionnaire.

Data Collection Tools

Demographic data, such as age, gender, family history of cancer, smoking status, weight loss, physical activity levels, and history of rectal bleeding were collected. Biochemical parameters, including carcinoembryonic antigen (CEA), cancer antigen (CA) 19-9, and hemoglobin levels, as well as the frequency of consumption of alcohol, coffee, tea, garlic, turmeric, and saffron, were recorded. For colorectal cancer patients, tumor location and pathological diagnosis were also documented.

Each patient completed a 3-day 24-h dietary recall form (including 2 weekdays and 1 weekend day) for the week before surgery. For 10 additional food items not included in the BeBIS® 8.2 (Nutrition Information System) software but necessary for DII calculation, a food frequency questionnaire was completed according to the Turkish Dietary Guidelines (TÜBER). Physical activity levels were classified according to the World Health Organization guidelines.

DII Calculation

The DII was calculated using data from 24-h dietary recall forms analyzed with BeBIS® 8.2, based on 36 nutritional components (including alcohol, Vitamins B12, B6, cholesterol, energy, total fat, fiber, folic acid, carbohydrates, iron, magnesium, polyunsaturated and monounsaturated fatty acids, beta-carotene, caffeine, niacin, omega-3 and 6, protein, riboflavin, saturated fats, selenium, thiamine, trans fats, Vitamins A, C, D, and E, zinc, and total flavonoids), as well as the consumption frequencies of 10 additional items (ginger, saffron, turmeric, pepper, thyme, rosemary, coffee, tea, onion, and garlic).

Statistical Analysis

Data were analyzed using the Statistical Package for the Social Sciences (SPSS) version 22.0 (SPSS, Chicago, IL, USA). Continuous variables are expressed as mean±standard deviation and median (minimum–maximum), and categorical variables as

number and percentage. The Shapiro–Wilk test was used to evaluate the normality of data distribution. For comparisons, the independent t-test was applied to normally distributed variables, and the Mann–Whitney U test for non-normally distributed variables. Categorical variables were compared using the Chi-square test. The relationship between DII scores and colorectal cancer was assessed using regression analysis. Adjustments were made for age and sex. A $p < 0.05$ was considered statistically significant.

RESULTS

A total of 269 patients were included in the study: 149 in the study group and 120 in the control group. The mean age was 64.45 ± 11.36 years in the study group and 65.90 ± 10.36 years in the control group, with no statistically significant difference between the two ($p = 0.280$). Of the patients in the study group, 103 (69.1%) were male and 46 (30.9%) were female. In the control group, 90 (75.0%) were male and 30 (25.0%) were female.

Gender distribution was similar between groups ($p = 0.288$).

A family history of cancer was reported in 46 patients (30.9%) in the study group and in 34 patients (28.3%) in the control group ($p = 0.651$). The proportion of smokers was 47.7% in the study group and 46.7% in the control group, with no significant difference ($p = 0.872$). Physical activity levels were also comparable between groups ($p = 0.259$). Weight loss was observed in 63 patients (42.3%) in the study group and 19 patients (15.8%) in the control group, a statistically significant difference ($p < 0.001$). Rectal bleeding was reported in 34 patients (22.8%) in the study group and 10 patients (8.3%) in the control group ($p = 0.001$).

Fecal occult blood test positivity was observed in 13.4% of the study group and 0.8% of the control group. Among patients diagnosed with colorectal cancer, the median CEA level was 3 $\mu\text{g/L}$ (range: 2–7 $\mu\text{g/L}$), and the median CA 19-9 level was 16 U/mL (range: 10–31 U/mL). Hemoglobin levels were similar in both groups ($p = 0.097$). Table 1 summarizes the demographic characteristics.

Table 1. Demographic characteristics

Variable	Study group (n=149) (%)	Control group (n=120) (%)	p
Age (years)	64.45 ± 11.36	65.90 ± 10.36	0.280*
Gender			0.288**
Male	103 (69.1)	90 (75.0)	
Female	46 (30.9)	30 (25.0)	
Family history of cancer			0.651**
Yes	46 (30.9)	34 (28.3)	
No	103 (69.1)	86 (71.7)	
Smoking			0.872**
Yes	71 (47.7)	56 (46.7)	
No	78 (52.3)	64 (53.3)	
Physical activity			0.259**
Inactive (<150 min/week)	39 (26.2)	38 (31.7)	
Active (150–299 min/week)	72 (48.3)	46 (38.3)	
Very active (>300 min/week)	38 (25.5)	36 (30.0)	
Weight loss			<0.001**
Yes	63 (42.3)	19 (15.8)	
No	86 (57.7)	101 (84.2)	
Rectal bleeding			0.001**
Yes	34 (22.8)	10 (8.3)	
No	115 (77.2)	110 (92.7)	
FOBT positive	20 (13.4)	1 (0.8)	<0.001**
CEA ($\mu\text{g/L}$)	3 (2–7)	–	–
CA 19-9 (U/mL)	16 (10–31)	–	–
Hemoglobin (g/dL)	13.6 (11.0–14.8)	14.2 (8.7–19.0)	0.097***

*Independent samples t-test, **Chi-square test, ***Mann–Whitney U test. CEA: Carcinoembryonic antigen, CA: Cancer antigen, Hb: Hemoglobin, FOBT: Fecal occult blood test. Values are presented as mean \pm standard deviation, n (%), and median (min–max).

Tumor Location and Pathology

Among patients with colorectal cancer, tumors were located in the sigmoid colon in 42 patients (28.4%), right colon in 38 (25.7%), left colon in 27 (18.2%), rectum in 16 (5.9%), rectosigmoid junction in 14 (9.5%), and transverse colon in 11 (7.4%). The pathological diagnosis was adenocarcinoma in 132 patients (88.6%) and mucinous adenocarcinoma in 17 patients (11.4%). Table 2 summarizes the tumor location and pathology.

Regression Analysis

Table 3 summarizes regression analysis revealed a significant association between higher DII scores and colorectal cancer (odds ratio [OR]: 2.62, $p<0.001$). This association remained significant after adjusting for age and sex (adjusted OR: 2.72, $p<0.001$). When stratified by tumor location:

- High DII scores were significantly associated with colon cancer (OR: 2.37, $p<0.001$; adjusted OR: 2.51, $p<0.001$).
- When the colon was subdivided into proximal and distal regions:
 - Proximal colon cancer showed a strong association (OR: 3.07, $p<0.001$; adjusted OR: 3.15, $p<0.001$).

Table 2. Tumor location and pathology	
Tumor location	n (%)
Sigmoid colon	42 (28.4)
Right colon	38 (25.7)
Left colon	27 (18.2)
Rectum	16 (5.9)
Rectosigmoid	14 (9.5)
Transverse colon	11 (7.4)
Tumor pathology	n (%)
Adenocarcinoma	132 (88.6)
Mucinous adenocarcinoma	17 (11.4)

- Distal colon cancer also showed a significant relationship (OR: 2.14, $p=0.003$; adjusted OR: 2.39, $p<0.001$).

High DII scores were similarly associated with rectal cancer (OR: 2.52, $p=0.003$; adjusted OR: 2.59, $p=0.003$).

DII Scores

The mean DII score in the study group was -3.86 ± 1.04 . In the control group, the mean DII score was -4.37 ± 0.35 . The distribution of DII scores in each group is shown in Figures 1 and 2, respectively. The average DII score was significantly higher in the study group than in the control group ($p=0.008$) (Fig. 3).

DISCUSSION

The results of our study demonstrate that higher DII scores are associated with an increased risk of colorectal cancer. Even after adjusting for age and sex, our findings show a positive correlation between DII scores and colorectal cancer, including both colon (proximal and distal) and rectal cancers. Considering that high DII scores indicate a pro-inflammatory dietary pattern, our results support the hypothesis that such diets are associated with increased colorectal cancer risk.

The association between dietary habits and colorectal cancer has been well documented in numerous studies.^[18-20] A recent meta-analysis found that healthy dietary patterns are associated with reduced colorectal cancer risk, whereas Western-style diets and alcohol consumption increase risk.^[21] The World Cancer Research Fund and the American Institute for Cancer Research conducted a systematic review of the evidence on food, beverages, and colorectal cancer, reporting that processed meats and alcoholic beverages elevate the risk. Conversely, dairy products, whole grains, and foods rich in dietary fiber were shown to reduce the risk of colorectal cancer, colorectal adenomas, and chronic colonic inflammation.^[7]

Previous studies have examined the impact of specific foods such as red meat and nutrients, such as folate and zinc on colorectal cancer risk.^[18,22,23] However, these foods and nutrients are typically consumed in combination with others, potentially confounding their individual effects. High intercorrelation

Table 3. Association between DII scores and colorectal cancers				
Cancer type	Control/Case	OR (95% CI)	Adjusted OR* (95% CI)	p
Colorectal cancer	120/149	2.62 (1.69–4.05)	2.72 (1.74–4.27)	<0.001
Colon cancer	120/118	2.37 (1.56–3.60)	2.51 (1.63–3.86)	<0.001
Proximal colon cancer	120/49	3.07 (1.82–5.15)	3.15 (1.83–5.41)	<0.001
Distal colon cancer	120/69	2.14 (1.34–3.42)	2.39 (1.46–3.91)	0.003/<0.001
Rectal cancer	120/30	2.52 (1.37–4.66)	2.59 (1.38–4.89)	3
*Adjusted for age and sex. OR: Odds ratio; CI: Confidence interval; DII: Dietary inflammatory index.				

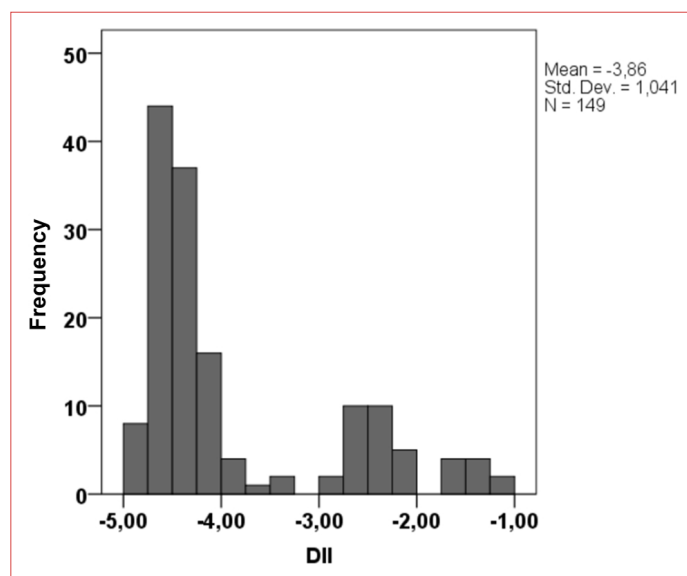


Figure 1. Distribution of dietary inflammatory index scores in the study group.

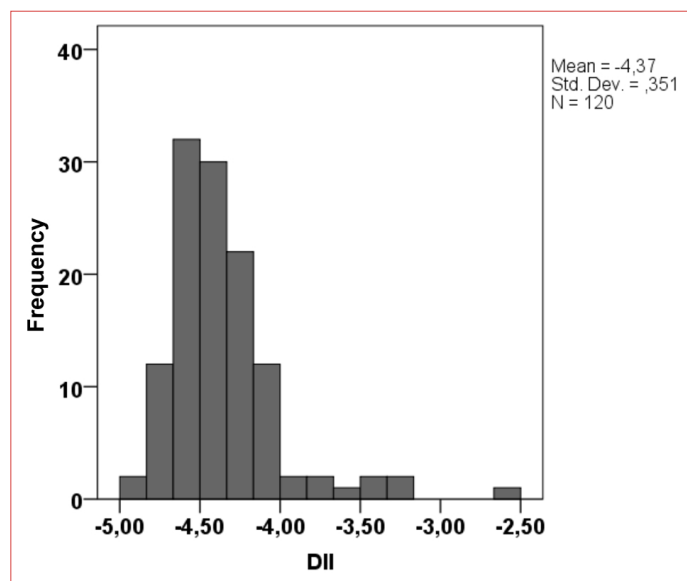


Figure 2. Distribution of dietary inflammatory index scores in the control group.

among food items and the resulting loss of statistical power make it difficult to isolate the risk associated with any single nutrient. Unlike such approaches, the DII was developed by focusing on the functional impacts of dietary components on inflammation. The DII score is based on a systematic review and scoring of the literature regarding inflammation and diet. It also standardizes the intake of pro- and anti-inflammatory dietary components across populations using reference values, allowing for cross-cultural comparisons.^[24,25]

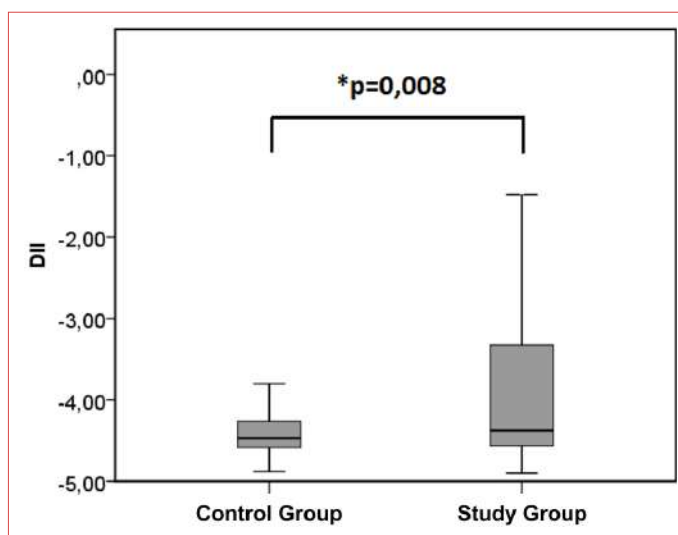


Figure 3. Comparison of dietary inflammatory index (DII) scores between study and control groups. (Mann–Whitney U test, $p=0.008$ – indicating significantly higher DII scores in the study group).

Therefore, in our study, we investigated the association between colorectal cancer development and DII scores calculated from patients' overall dietary patterns, rather than the intake of specific foods. Shivappa et al.^[18] calculated DII scores based on a questionnaire involving 121 food items among 34,703 women aged 55–69 and reported that increased DII scores were associated with higher colorectal cancer incidence. Park et al.^[26] found a similar association in a study involving 923 colorectal cancer cases and 1,846 controls using a 106-item semi-quantitative food frequency questionnaire. Harmon et al.^[19] conducted a multiethnic cohort study of 190,963 individuals aged 45–75 from various ethnic backgrounds, followed for over 20 years, and found that increased DII scores were linked to greater colorectal cancer risk. Our study supports these findings and confirms the significant association between DII scores and colorectal cancer risk in our population.

The greatest and non-modifiable risk factor for sporadic colorectal cancer is age. The incidence of both colorectal polyps and cancer increases significantly after age 50.^[27] Many environmental factors have also been implicated in colorectal cancer development, with dietary patterns being among the most significant. Diet plays a critical role not only in cancer onset but also in the formation and recurrence of polyps.

There are multiple pathways by which pro-inflammatory diets may increase colorectal cancer risk. Such diets can elevate systemic inflammation, potentially inducing insulin resistance, which in turn raises levels of insulin, triacylglycerol, and non-esterified fatty acids. These metabolic disturbances

can promote excessive proliferation of colonic epithelial cells and increase their exposure to reactive oxygen species.^[28] Diets rich in red and processed meats are high in N-nitroso compounds, which can damage DNA. In contrast, fruits and vegetables contain micronutrients with antioxidant and anti-tumor properties, as well as fibers that reduce intestinal transit time.

The DII score reflects the collective impact of various foods, nutrients, and flavonoids known to influence inflammation.^[29,30] The most potent anti-inflammatory dietary components include polyphenols and antioxidants, which produce localized anti-inflammatory effects, especially through modulation of the gut microbiota. These compounds can also reduce levels of reactive oxygen species and prevent cancer initiation and progression. Phytochemicals found in the diet can inhibit colorectal cancer cell proliferation and interrupt the cell cycle.^[31]

The DII is a robust indicator of a person's overall dietary inflammatory potential. High scores reflect a diet with strong pro-inflammatory capacity. It is well established that inflammation increases susceptibility to colorectal cancer.^[32-34] Inflammatory cytokines, such as tumor necrosis factor- α have been shown to induce insulin resistance by inhibiting insulin receptors. Insulin resistance may contribute to cancer development through elevated insulin, glucose, or triglyceride levels. Furthermore, activation of the cyclooxygenase-2 pathway may promote local proliferation, angiogenesis, and mutagenesis – all of which can be stimulated by cytokines such as interleukin-6. These mechanisms clarify how an inflammatory diet, as defined by high DII scores, contributes to colorectal cancer development. Our findings support these mechanisms by demonstrating their clinical implications.

Dietary habits are shaped by culture and socioeconomic factors and often change over a person's lifetime. People rarely maintain the same diet throughout life, and it is still unclear which nutrients, in what amounts and frequency, and during which life stages exert the greatest influence on cancer development. In our study, DII scores were calculated based on recent dietary intake. However, because cancer develops over extended periods and the timing of its onset is often unclear, more accurate results would require long-term data. Therefore, prospective cohort studies with long-term follow-up are needed for more definitive conclusions.

CONCLUSION

There is a significant association between inflammatory diets, as measured by higher DII scores, and the development of colorectal cancer. Elevated DII scores represent a dietary pattern with high pro-inflammatory potential and were found to be a meaningful risk factor for colorectal cancer, independent of age and sex.

This risk does not vary based on tumor location; the association between high DII scores and cancer is consistent for both colon and rectal cancers. These findings suggest that reducing the inflammatory potential of the diet may be an important preventive strategy against colorectal cancer. Further prospective studies involving long-term dietary monitoring and larger populations are recommended to establish more robust evidence and inform public health interventions.

DECLARATIONS

Ethics Committee Approval: The study was approved by University of Health Sciences, Dışkapı Yıldırım Beyazıt Health Practice and Research Center Ethics Committee (No: 91/01, Date: 06/07/2020).

Informed Consent: Informed consent was obtained from the patients.

Conflict of Interest: The authors declare that there is no conflict of interest.

Funding: The authors received no financial support for the research and/or authorship of this article.

Use of AI for Writing Assistance: Artificial intelligence programs were not used in the study.

Authorship Contributions: Concept – NK, EÖ; Design – İOK, NK; Supervision – İOK; Fundings – İOK; Materials – NK; Data collection &/or processing – NK, EÖ; Analysis and/or interpretation – NK; Literature search – NK; Writing – NK; Critical review – EÖ, İOK.







Peer-review: Externally peer-reviewed.

REFERENCES

1. Smith RE, Renaud RC, Hoffman E. Colorectal cancer market. *Nat Rev Drug Discov* 2004;3:471–2.
2. Vogel VG, McPherson RS. Dietary epidemiology of colon cancer. *Hematol Oncol Clin North Am* 1989;3:35–63.
3. Keibel A, Singh V, Sharma MC. Inflammation, microenvironment, and the immune system in cancer progression. *Curr Pharm Des* 2009;15:1949–55.
4. Thun MJ, Henley SJ, Gansler T. Inflammation and cancer: An epidemiological perspective. *Novartis Found Symp* 2004;256:6–21.
5. Coussens LM, Werb Z. Inflammation and cancer. *Nature* 2002;420:860–7.
6. Chung YC, Chang YF. Serum interleukin-6 levels reflect the disease status of colorectal cancer. *J Surg Oncol* 2003;83:222–6.
7. World Cancer Research Fund/American Institute for Cancer Research. Continuous update project report: Food, nutrition, physical activity, and the prevention of colorectal cancer. Washington (DC): American Institute for Cancer Research; 2011.

8. Godos J, Bella F, Torrisi A, Sciacca S, Galvano F, Grosso G. Dietary patterns and risk of colorectal adenoma: A systematic review and meta-analysis of observational studies. *J Hum Nutr Diet* 2016;29:757–67.
9. Cavicchia PP, Steck SE, Hurley TG, Hussey JR, Ma Y, Ockene IS, et al. A new dietary inflammatory index predicts interval changes in serum high-sensitivity C-reactive protein. *J Nutr* 2009;139:2365–72.
10. Shivappa N, Steck SE, Hurley TG, Hussey JR, Hébert JR. Designing and developing a literature-derived, population-based dietary inflammatory index. *Public Health Nutr* 2014;17:1689–96.
11. Galano Urgellés R, Rodríguez Fernández Z, Casás Prieto A. Cáncer de colon: Seguimiento posoperatorio. *Rev Cubana Cir* 1997;36:59–63. [Article in Spanish]
12. Granados-Romero JJ, Valderrama-Treviño AI, Contreras-Flores EH, Barrera-Mera B, Herrera Enríquez M, Uriarte-Ruiz K, et al. Colorectal cancer: A review. *Int J Res Med Sci* 2017;5:4667–76.
13. Arcos MC, Tirado MTA. Revisión y actualización general en cáncer colorrectal. *An Radiol Mex* 2009;8:99–115. [Article in Spanish]
14. Cappell MS. From colonic polyps to colon cancer: Pathophysiology, clinical presentation, and diagnosis. *Clin Lab Med* 2005;25:135–77.
15. DeVita VT Jr, Lawrence TS, Rosenberg SA, editors. *Cancer: Principles and practice of oncology*. 9th ed. Philadelphia: Lippincott Williams & Wilkins; 2011.
16. Silva AC, Hara AK, Leighton JA, Heppell JP. CT colonography with intravenous contrast material: Varied appearances of colorectal carcinoma. *Radiographics* 2005;25:1321–34.
17. Ulualp K. Kolon tümörleri. In: Andican AA, editor. *Abdominal operasyonlar*. 1st ed. İstanbul: Nobel Kitabevi; 2008. p. 625–60.
18. Shivappa N, Prizment AE, Blair CK, Jacobs DR Jr, Steck SE, Hébert JR. Dietary inflammatory index and risk of colorectal cancer in the Iowa Women's Health Study. *Cancer Epidemiol Biomarkers Prev* 2014;23:2383–92.
19. Harmon BE, Wirth MD, Boushey CJ, Wilkens LR, Draluck E, Shivappa N, et al. The dietary inflammatory index is associated with colorectal cancer risk in the multiethnic cohort. *J Nutr* 2017;147:430–8.
20. Wu CW, Wang SR, Chao MF, Wu TC, Lui WY, P'eng FK, et al. Serum interleukin-6 levels reflect disease status of gastric cancer. *Am J Gastroenterol* 1996;9:1417–22.
21. Feng YL, Shu L, Zheng PF, Zhang XY, Si CJ, Yu XL, et al. Dietary patterns and colorectal cancer risk: A meta-analysis. *Eur J Cancer Prev* 2017;26:201–11.
22. Tabung FK, Steck SE, Ma Y, Liese AD, Zhang J, Lane DS, et al. Changes in the inflammatory potential of diet over time and risk of colorectal cancer in postmenopausal women. *Am J Epidemiol* 2017;186:514–23.
23. Syed Soffian SS, Mohammed Nawi A, Hod R, Ja'afar MH, Isa ZM, Chan HK, et al. Meta-analysis of the association between dietary inflammatory index (DII) and colorectal cancer. *Nutrients* 2022;14:1555.
24. Groblewska M, Mroczko B, Sosnowska D, Szmitkowski M. Interleukin 6 and C-reactive protein in esophageal cancer. *Clin Chim Acta* 2012;413:1583–90.
25. Santos S, Oliveira A, Lopes C. Systematic review of saturated fatty acids on inflammation and circulating levels of adipokines. *Nutr Res* 2013;33:687–95.
26. Park Y, Lee J, Oh JH, Shin A, Kim J. Dietary patterns and colorectal cancer risk in a Korean population: A case-control study. *Medicine (Baltimore)* 2016;95:e3759.
27. Cho YA, Lee J, Oh JH, Shin A, Kim J. Dietary inflammatory index and risk of colorectal cancer: A case-control study in Korea. *Nutrients* 2016 J;8:469.
28. Attlee A, Saravanan C, Shivappa N, Wirth MD, Aljaberi M, Alkaabi R, et al. Higher dietary inflammatory index scores are associated with stress and anxiety in dormitory-residing female university students in the United Arab Emirates. *Front Nutr* 2022;9:814409.
29. Mármol I, Sánchez-de-Diego C, Pradilla Dieste A, Cerrada E, Rodríguez Yoldi MJ. Colorectal carcinoma: A general overview and future perspectives in colorectal cancer. *Int J Mol Sc.* 2017;18:197.
30. Bruce WR, Wolever TM, Giacca A. Mechanisms linking diet and colorectal cancer: The possible role of insulin resistance. *Nutr Cancer* 2000;37:19–26.
31. Shivappa N, Steck SE, Hurley TG, Hussey JR, Hébert JR. Designing and developing a literature-derived, population-based dietary inflammatory index. *Public Health Nutr* 2014;17:1689–96.
32. Shin D, Lee KW, Brann L, Shivappa N, Hébert JR. Dietary inflammatory index is positively associated with serum high-sensitivity C-reactive protein in a Korean adult population. *Nutrition* 2019;64:155–61.
33. Jaganathan SK, Vellayappan MV, Narasimhan G, Supriyanto E, Octorina Dewi DE, Narayanan AL, et al. Chemopreventive effect of apple and berry fruits against colon cancer. *World J Gastroenterol* 2014;20:17029–36.
34. Santos S, Oliveira A, Lopes C. Saturated fatty acids intake in relation to C-reactive protein, adiponectin, and leptin: A population-based study. *Nutrition* 2013;29:892–7.

Neutrophil-Lymphocyte Ratio and C-Reactive Protein-Albumin Ratio as Predictors of Union Complications in Proximal Humerus Fractures

 Nazim Erkurt,¹  Murat Cakar,¹  Ali Yuce,¹  Abdulhamit Misir,²  Tahsin Olgun Bayraktar,¹  Serdar Aki¹

¹Department of Orthopedics and Traumatology, Prof. Dr. Cemil Taşcıoğlu City Hospital, Istanbul, Türkiye

²Department of Orthopedics and Traumatology, Bahçeşehir University Göztepe Medical Park Hospital, Istanbul, Türkiye

ABSTRACT

Objective: Classification systems play a crucial role not only in determining diagnostic and therapeutic strategies but also in predicting patient prognosis. As the severity of trauma increases, the complexity of fractures and the classification level also tend to rise accordingly. In this study, we aimed to investigate how inflammatory markers that reflect trauma severity – such as the neutrophil-to-lymphocyte ratio (NLR) and the C-reactive protein-to-albumin ratio (CAR) – vary according to the NEER classification of proximal humerus fractures, and whether these markers can predict complications related to fracture healing.

Materials and Methods: This retrospective study reviewed patients with proximal humerus fractures treated with plate-screw osteosynthesis between January 2016 and January 2022 at a single medical center. 171 patients were grouped by bone union status and NEER classification. Non-union (5.4%) was defined as the absence of radiographic healing signs up to 6 months post-operatively. Blood samples for routine full blood count and biochemical analysis were collected within the first 24 h of emergency department admission for surgical evaluation. The correlation between the number of Neer fragments and inflammatory biomarkers was assessed. In addition, the association between inflammatory biomarkers and fracture healing was analyzed.

Results: The non-union rates of 3-part and 4-part fractures were higher than those of 2-part fractures. ($p=0.047$, $p=0.048$). However, there was no significant difference in blood parameters between the two groups. No statistically significant differences in C-reactive protein, Albumin, CAR, or NLR levels were found among Neer fracture types.

Conclusion: Inflammatory status may not have been affected by union or Neer classification, but integrating these classifications into multivariate union models for proximal humerus fractures might yield more scientifically rigorous and precise outcomes.

Keywords: C-reactive protein-to-albumin ratio, Neutrophil-lymphocyte ratio, Proximal humerus non-union

Cite this article as: Erkurt N, Cakar M, Yuce A, Misir A, Bayraktar TO, Aki S. Neutrophil-Lymphocyte Ratio and C-Reactive Protein-Albumin Ratio as Predictors of Union Complications in Proximal Humerus Fractures. Eur Arch Med Res 2025;41(3):138–145.

Address for correspondence: Nazim Erkurt, Department of Orthopedics and Traumatology, Prof. Dr. Cemil Taşcıoğlu City Hospital, Istanbul, Türkiye

E-mail: nzmkrkt@gmail.com **ORCID ID:** 0000-0003-4329-1437

Submitted: 13.03.2025 **Revised:** 07.05.2025 **Accepted:** 26.05.2025 **Available Online:** 12.09.2025

European Archives of Medical Research – Available online at www.eurarchmedres.org

OPEN ACCESS This work is licensed under a Creative Commons Attribution-NonCommercial 4.0 International License.



INTRODUCTION

Fracture healing is a complex biological process influenced by a variety of clinical factors. Age, sex, osteoporosis, and chronic comorbidities have traditionally been utilized to predict fracture prognosis.^[1] Despite this, the role of systemic inflammatory status – particularly outside the context of overt infection – remains underexplored in present fracture healing models. Following a traumatic fracture, neutrophils are rapidly mobilized into circulation and, by the end of the 1st week, differentiate into tissue macrophages. These macrophages secrete cytokines that activate lymphocytes, thereby initiating and supporting tissue regeneration. However, excessive cytokine induction may disrupt this balance and impair bone union.^[2] Among inflammatory markers, the neutrophil-to-lymphocyte ratio (NLR) has shown a strong correlation with various post-fracture outcomes, including delirium, thromboembolic events, and mortality.^[3,4]

In addition, C-reactive protein-to-albumin ratio (CAR), a marker reflecting both nutritional and inflammatory status, has been associated with the prognosis of various malignancies and with post-operative minor and major complications.^[5,6] Given this background, both NLR and CAR have emerged as promising markers for evaluating the severity of trauma and the extent of systemic inflammatory response. Their potential utility in predicting fracture healing outcomes remains a compelling subject for further investigation.

Fracture radiological classification systems are developed to establish diagnostic and treatment strategies and to predict prognosis.^[7] Consequently, some fracture classifications have demonstrated a relationship between fracture severity and these biomarkers indicating an inflammatory response.^[8–10] It remains unclear whether the Neer classification system, the most commonly used system for proximal humerus fractures, is influenced by the severity of inflammation.

Non-union following surgery for proximal humerus fractures represents significant morbidity and necessitates secondary surgical interventions.^[11,12] There is a paucity of studies investigating the relationship between these complications and pre-operative blood tests. This study aims to elucidate the relationship between CAR and NLR ratios and the Neer fracture classification. In addition, it seeks to examine the association between these biomarkers and post-operative union complications. We hypothesize that higher pre-operative CAR and NLR are significantly associated with higher Neer fracture classification grades, and that elevated CAR and NLR are independent risk factors for post-operative union complication.

MATERIALS AND METHODS

After receiving approval from the study ethics committee (Approval Number: 2025/115), the medical records of patients with proximal humerus fractures treated with plate-screw osteosynthesis between January 2016 and January 2022 were retrospectively reviewed at a single center. The study was conducted in accordance with the Declaration of Helsinki. Patients aged 18 and older who presented to the emergency orthopedic clinic with shoulder trauma, were diagnosed with proximal humerus fractures, and underwent plate-screw osteosynthesis as treatment and had a minimum of 6 months of radiological follow-up after surgery were included in the study. Exclusion criteria included inaccessible medical records, pathological fractures, ongoing oncological treatment, multiple traumas, additional infection findings during hospitalization, albumin replacement within the first 24 h of hospitalization due to rheumatologic disease, and the use of non-steroidal anti-inflammatory drugs (NSAIDs) or bisphosphonates before the fracture. Specifically, three patients with pathological fractures, fourteen with multiple fractures, two with bilateral proximal humerus fractures, seven with upper respiratory tract infections, one with rheumatoid arthritis, one with ankylosing spondylitis, three using NSAIDs, and two with inaccessible medical records were excluded from the study. Ultimately, 171 patients were included in the study out of the initial 204 patients (Fig. 1).

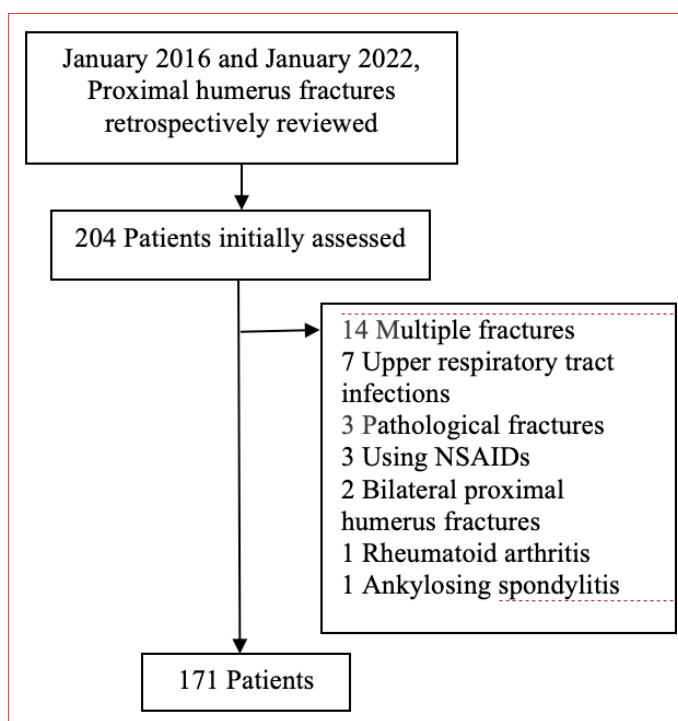


Figure 1. The patient flow chart in our study.

Neer fracture classification images, including standard AP axillary radiographs and computed tomography, were obtained from the hospital image archiving unit. Evaluations were independently conducted by two experienced orthopedic surgeons, and any discrepancies were resolved through joint re-evaluation. Patients were classified according to the Neer system based on the number of fragments.

Non-union was defined as the absence of radiographic evidence of fracture healing within 6 months post-operatively, characterized by distinct sclerotic borders between fracture fragments and the absence of trabecular bone formation.^[13] At 6 months, compared to early post-operative imaging, the occurrence of significant displacement between fracture fragments accompanied by broken screws was classified as a non-union complication (Figs 2 and 3). Union complications were subsequently confirmed through tomographic evaluation.^[5,13] Furthermore, post-operative screw cut-out or screw cut-through was categorized as union complications.^[13]

Routine hemogram and biochemistry blood samples for anesthesia preparation were collected from each patient within the first 24 h of emergency room admission. Laboratory tests previously evaluated as prognostic factors were analyzed from these blood samples, including hemoglobin (Hb) (g/dL), white blood cell count (K/ μ L), neutrophil count (mg/dL), lymphocyte count (mg/dL), platelet count (mg/dL), albumin (g/dL), C-reactive protein (CRP) (mg/dL), NLR, platelet/lymphocyte



Figure 2. Displacement with screw cut through at 6 months was defined as non-union.



Figure 3. At the 9-month follow-up, reduction loss and a sclerotic border on the medial side.

ratio, and CAR.^[3-5,14] The patients were divided into two groups: Those with complete fracture healing and those with non-union complications. The relationship between the number of Neer fragments and blood parameters was analyzed in these patients.

All patients were treated using a deltopectoral approach in the semi-chaise longue position under general anesthesia. Blood samples were collected within 24 h of the trauma. Surgeries were performed by two experienced trauma surgeons (each with over 10 years of experience). Proximal humerus locking plates and screws produced by Response Medical were used in all operations. Antibiotic prophylaxis was administered for 48 h post-surgery. Post-operative follow-up included a control visit 2 weeks later, with outpatient clinic records maintained.

Statistical Analysis

SPSS 21.0 for Windows was used for statistical analysis. Descriptive statistics were provided as numbers and percentages for categorical variables and as means, standard deviations, minimums, maximums, and medians for numerical variables. Due to the non-normal distribution of numerical variables, independent two-group comparisons were made using the Mann–Whitney U test, and independent multiple-group comparisons were made using the Kruskal–Wallis test. Group proportions were compared using the Chi-Square Test. Cohen's D test was performed for effect analysis. Relationships between numerical and ordinal variables were examined using Spearman Correlation Analysis. A binary logistic regression analysis was used to examine the risk factors associated with non-union complications. A multivariate analysis was performed using age, Hb level, albumin level, NLR, CAR, charlson comorbidity index (CCI) score, Neer fracture type, time to surgery, and sex. The statistical alpha significance level was set at $p < 0.05$.

RESULTS

The age and gender demographics of the patients are shown in Table 1. Non-union was observed in 5.8% of the patients (n=10). There was no gender difference between patients who had complications and those with complete union ($p=0.516$). A statistically significant difference was found in the Neer fracture types of patients with union complications ($p=0.046$). Among these patients, the incidence of Neer 3-part and 4-part fractures was high, while no Neer 2-part fractures were observed (Table 1). Post hoc comparisons revealed statistically significant differences in healing between 2- and 3-part fractures ($p=0.047$) as well as between 2- and 4-part fractures ($p=0.048$). Multivariate regression analysis revealed a statistically significant association between Neer fracture type and the risk of non-union (Table 2).

The mean time to surgery was 6.1 days. There was no significant relationship between union complications and the time to surgery ($p=0.737$). In addition, no significant difference was found in the age-adjusted CCI, nor in the present blood parameters between the two groups (Table 3). There was no statistically significant difference between the number of Neer fragments and CRP, Albumin, CAR, and NLR levels (Table 4). There was no correlation between the number of Neer fragments and CRP, Albumin, CAR, and NLR (Table 5).

Table 1. Comparison of Neer fracture type, side, and gender between two groups

	Non-union		Total n (%)	p*
	No n (%)	Yes n (%)		
Sex	161 (94.2)	10 (5.8)	171 (100)	0.516
Male	89 (55.3)	7 (70.0)	96 (56.1)	
Female	72 (44.7)	3 (30.0)	75 (43.9)	
Side	69 (42.9)	6 (60.0)	75 (43.9)	0.416
Left	92 (57.1)	4 (40.0)	96 (56.1)	
Neer	49 (30.4)	0 (0.0)	49 (28.7)	0.046
3	97 (60.2)	8 (80.0)	105 (61.4)	
4	15 (9.3)	2 (20.0)	17 (9.9)	

*Chi-square test.

Table 2. Multivariate analysis parameters associated with fracture healing

	Multivariate	
	Hazard ratio (95% confidence interval)	p
Age (year)	0.089	0.405
CCI*	−0.203	0.079
Neer classification	0.176	0.028
Side	−0.049	0.528
Sex	0.072	0.382
Time to surgery	0.096	0.223
Albumin (g/dL)	−0.049	0.537
Hemoglobin (g/dL)	−0.041	0.632
NLR*	0.053	0.505
CAR*	0.043	0.627

*CCI: Carlson index; NLR: Neutrophil/lymphocyte ratio; CAR: C-Reactive protein/albumin ratio.

DISCUSSION

The pre-operative inflammatory markers of the patients included in our study were not affected by the type of fracture and the number of fragments. The number of fragments may be a risk factor for non-union complication ($p=0.046$). However, there seems to be no relationship between union problems and pre-operative inflammatory status ($p=0.747$, $p=0.87$).

CRP is a key biomarker of acute inflammation and increases in response to various conditions, such as trauma and infection. However, the inflammatory response triggered by trauma or surgical intervention is generally more limited and resolves more rapidly compared to infection.^[15] Therefore, dynamic monitoring of CRP levels and the CAR in the post-operative period may provide more clinically meaningful insights for the early prediction of potential complications. In a study by Swarnkar et al.^[16] involving patients who underwent abdominal surgery, post-operative CRP and CAR levels were found to be effective predictors of complications. In the orthopedic surgery literature, particularly after prosthetic procedures, persistent elevation or further increase in CAR has been identified as a significant risk factor for periprosthetic joint infection. After total knee arthroplasty, failure of CRP and CAR levels to decline, or a secondary rise in these markers, raises clinical suspicion of infection.^[17,18] In our own patient cohort, pre-operative CAR values assessed after trauma were above the reference ranges reported in the lit-

Table 3. Comparison of age, Carlson index, and blood test result between two groups

	Non-union			95% confidence interval of the difference Lower- upper	Cohen's D	p*
	No Mean±SD (Min-Maks) (Median)	Yes Mean±SD Min-Maks (Median)	Total Mean±SD (Min-Maks)			
Age	54.5±14.6 18–90 (56)	55.5±11.2 35–68 (57)	54.5±14.4 (18–90)	(–10.33)–(8.26)	0.07	0.800
Carlson index	1.5±2.1 0–12 (1)	0.8±1.0 0–3 (0.5)	1.4±2.1 (0–12)	(–0.67)–(2)	0.47	0.476
Hemoglobin	11.2±1.9 1.4–16.5 (11.1)	11.0±1.6 7.4–12.9 (11.15)	11.2±1.9 (1.4–16.5)	(–1.04)–(1.44)	5.75	0.887
White blood cell	11.2±3.8 2.68–21.86 (10.8)	10.5±3.0 5.3–15.81 (10.6)	11.2±3.7 (2.68–21.86)	(–1.68)–(3.09)	0.25	0.662
Monocyte	0.88±1.50 0.11–13.6 (0.66)	0.69±0.34 0.25–1.2 (0.675)	0.87±1.46 (0.11–13.6)	(–0.74)–(1.13)	0.72	0.948
Neutrophil	9.50±7.10 0.83–86.8 (8.39)	8.44±2.68 4.2–12.7 (8.36)	9.44±6.92 (0.83–86.8)	(–3.40)–(5.51)	3.8	0.720
Lymphocyte	1.62±1.45 0.39–13.7 (1.35)	1.35±0.80 0.36–3.12 (1.06)	1.60±1.42 (0.36–13.7)	(–0.64)–(1.18)	0.26	0.576
Albumin	3.87±2.22 2.2–31 (3.7)	3.66±0.33 3.1–4 (3.805)	3.86±2.16 (2.2–31)	(–1.18)–(1.6)	0.13	0.777
CRPμ	56.0±70.4 0.43–364 (27)	52.8±55.4 5–141 (32.5)	55.8±69.4 (0.43–364)	(–41.66)–(47.97)	0.74	0.801
NLRμ	8.81±13.50 0.4–163.8 (6.5)	8.80±7.06 2.5–25.9 (6.7)	8.81±13.20 (0.4–163.8)	(–1.93)–(0.83)	1.56	0.818
PLRμ	218.0±150.3 21.8–1096.7 (178.1)	255.1±144.2 51.3–550 (225.4)	220.1±149.8 (21.8–1096.7)	(–144.61)–(59.41)	1.58	0.252
LMRμ	2.50±2.19 0–20.8 (2.1)	2.11±0.97 0.9–3.8 (1.9)	2.48±2.14 (0.0–20.8)	(–0.98)–(1.76)	1.1	0.808
CARμ	0.234±0.184 0.025–1.578 (0.195)	0.225±0.057 0.152–0.336 (0.201)	0.233±0.179 (0.025–1.578)	(–0.10)–(0.12)	0.06	0.282

*Mann–Whitney U test. μ CRP: C-reactive protein; NLR: Neutrophil/lymphocyte ratio; PLR: Platelet/lymphocyte ratio; LMR: Lymphocyte/monocyte ratio; CAR: C-reactive protein/albumin ratio.

erature; however, these values did not appear to be reliable predictors of post-operative bone healing complications. This finding is also statistically supported by a small effect size (Cohen's $d=0.06$). In contrast, CRP and CAR levels measured and monitored over time in the post-operative period appear to provide more reliable results in the early detection of complications.^[19]

Most studies in the literature have focused on mortality rather than post-operative fracture complications. There is limited literature investigating the relationship between pre-opera-

tive CAR and post-fracture complications.^[8,9] Although studies investigating the association between aseptic non-union and inflammatory status exist in the literature, to the best of our knowledge, there are no publications specifically examining the relationship between pre-operative inflammatory status and aseptic non-union in patients with proximal humerus fractures.

Another parameter indicating systemic inflammatory status is NLR. The NLR ratio, similar to the CAR ratio, has been used to predict the severity of cardiovascular disease after hip frac-

Table 4. Association between Neer type and inflammation markers

	NEER			p
	2	3	4	
	Ort.±SD Min-Maks (Median)	Ort.±SD Min-Maks (Median)	Ort.±SD Min-Maks (Median)	
CRP*	45.5±55.5 0.43–235 (22)	59.6±71.7 0.59–333 (29)	61.3±89.5 2.9–364 (23)	0.642
Albumin	3.83±0.57 2.7–4.8 (3.9)	3.66±0.55 2.2–4.8 (3.7)	5.18±6.66 3.1–31 (3.6)	0.193
CAR*	0.24±0.22 0.11–1.58 (0.2)	0.22±0.14 0.09–1.19 (0.19)	0.26±0.24 0.03–1.14 (0.21)	0.870
NLR*	11.39±22.97 1.41–163.77 (6.62)	7.59±5.13 0.40–25.92 (6.47)	8.94±8.14 2.52–31.36 (5.99)	0.747

*CRP: C-reactive protein, NLR: Neutrophil/lymphocyte ratio, CAR: C-reactive protein/albumin ratio.

Table 5. Correlation between neer type and inflammation markers

	NEER	
	r	p
CRP*	0.061	0.431
Albumin	–0.138	0.072
CAR*	0.029	0.706
NLO*	–0.034	0.657

*CRP: C-reactive protein; NLR: Neutrophil/lymphocyte ratio; CAR: C-reactive protein/albumin ratio.

ture in some types of cancer.^[3,20,21] Johan et al.^[22] reported that pre-operative NLR is associated with tissue healing in patients with type 3 open fractures. Increased NLR may affect tissue healing and fracture healing. However, there are limited studies in the literature showing the relationship between aseptic non-union patients and NLR. In this study, conducted with proximal humerus fractures, the fact that no significant relationship was found between CAR and NLR may be due to the limited number of patients.

Fracture classification systems are performed to group fractures with similar fracture patterns to predict complications and guide the surgeon.^[8,23] Therefore, there is a relationship between some accepted fracture classifications and systemic inflammatory status.^[8,9] Wang et al.^[8] stated that the Schatzker classification reflected the severity of trauma and was related to inflammation markers. The generally accepted and most

commonly used classification system for proximal humerus fractures is the Neer classification. In our study, there was no relationship between pre-operative NLR and CAR after proximal humerus fractures and the Neer classification system. Therefore, the Neer classification may not reflect the systemic inflammatory status.

The primary limitation of our study is its retrospective design. Patient selection bias is inevitable among the proximal humerus fracture patients included in the study. Another limitation is the fact that avascular necrosis and non-union, despite being distinct entities, were not evaluated separately. Humeral head collapse and screw penetration may occur secondary to avascular necrosis.^[24] Changes in fracture reduction and plate-screw osteosynthesis during the post-operative period were considered as a non-union complication. Another notable limitation of the study is the potential variation of NLR and CRP levels in postmenopausal osteoporotic patients.^[25] Due to the retrospective nature of the study, sufficient data regarding osteoporosis status and bone mineral density were unavailable. However, patients with a history of bisphosphonate use were excluded based on their medical records. Our sample size may have limited our ability to detect significant differences; however, the effect size suggests a potential association with the NLR ratio (Cohen's $d=1.56$). In contrast, for the CAR ratio, neither the p-value nor the effect size indicated a meaningful difference between the groups (Cohen's $d=0.06$). These findings suggest that CAR may not have a substantial effect in this context; however, definitive conclusions are constrained by the limited sample size.

CONCLUSION

Proximal humerus fractures are among the most common intra-articular fractures and are frequently associated with significant shoulder mobility impairments. The complexity of the fracture, including the number of fragments, serves as a critical predictor for potential complications in fracture union. Systematic monitoring of the body's inflammatory response, alongside an analysis of its progression patterns, provides valuable insights for establishing evidence-based and effective clinical judgments.

DECLARATIONS

Ethics Committee Approval: The study was approved by Istanbul Prof. Dr. Cemil Taşcıoğlu City Hospital Ethics Committee (No: 2025/115, Date: 26/03/2025).

Conflict of Interest: The authors declare that there is no conflict of interest.

Funding: The authors received no financial support for the research and/or authorship of this article.

Use of AI for Writing Assistance: Not declared.

Authorship Contributions: Concept – NE, MÇ, AY, AM, SA, TOB; Design – NE, MÇ, AY, AM, SA, TOB; Supervision – NE, MÇ, AY, AM, SA, TOB; Fundings – SA, MÇ, TOB; Materials – MÇ, AY, TOB; Data collection &/or processing – SA, NE, AM; Analysis and/or interpretation – NE, SA, TOB; Literature search – NE, MÇ; Writing – NE, AY; Critical review – AY, AM.








Peer-review: Externally peer-reviewed.

REFERENCES

- Yeritsyan D, Momenzadeh K, Mohamadi A, Mortensen SJ, Beeram IR, Caro D, et al. Sociodemographic and lifestyle risk factors associated with fragility hip fractures: A systematic review and meta-analysis. *Osteology* 2024;4:64–87
- Long J, Xian H, Li Z, Liu C, Zhang Y. Predictive value of the neutrophil-to-lymphocyte ratio for clinical outcome of fractures: A systematic review and meta-analysis. *Curr Probl Surg* 2025;67:101774. Erratum in: *Curr Probl Surg* 2025;69:101831.
- Igde N, Yerli M, Yuce A, Ayaz MB, Gurbuz H. The role of neutrophil-lymphocyte ratio, platelet-lymphocyte ratio, CRP and albumin to predict postoperative one-year mortality in patients with hip fractures. *Medicine Science* 2022;11:729–33.
- Yüce A, Yerli M, Erkurt N, Gürbüz S, Çakar M, Adaş M. Neutrophil-lymphocyte and C-reactive protein-albumin ratios as predictors of re-surgery in adult native knee septic arthritis. *J Clin Invest Surg* 2022;7:191–8.
- Errani C, Cosentino M, Ciani G, Ferra L, Alfaro PA, Bordini B, et al. C-reactive protein and tumour diagnosis predict survival in patients treated surgically for long bone metastases. *Int Orthop* 2021;45:1337–46.
- Gupta A, Upadhyaya S, Cha T, Schwab J, Bono C, Hershman S. Serum albumin levels predict which patients are at increased risk for complications following surgical management of acute osteoporotic vertebral compression fractures. *Spine J* 2019;19:1796–802.
- Audigé L, Bhandari M, Hanson B, Kellam J. A concept for the validation of fracture classifications. *J Orthop Trauma* 2005;19:401–6.
- Wang Z, Tian S, Zhao K, Zhang R, Yin Y, Zhu Y, et al. Neutrophil to lymphocyte ratio and fracture severity in young and middle-aged patients with tibial plateau fractures. *Int Orthop* 2020;44:2769–77.
- Song Q, Hu H, Deng X, Xing X, Chen W, Zhang Y. The predictive role of platelet-to-lymphocyte ratio and systemic immune-inflammation index in young and middle-aged patients with tibial plateau fractures. *Res Square* 2021;Pre-print.
- Fisher ND, Barger JM, Driesman AS, Belayneh R, Konda SR, Egol KA. Fracture severity based on classification does not predict outcome following proximal humerus fracture. *Orthopedics* 2017;40:368–74.
- Clement ND, Duckworth AD, McQueen MM, Court-Brown CM. The outcome of proximal humeral fractures in the elderly: Predictors of mortality and function. *Bone Joint J* 2014;96:970–7.
- Jost B, Spross C, Grehn H, Gerber C. Locking plate fixation of fractures of the proximal humerus: Analysis of complications, revision strategies and outcome. *J Shoulder Elbow Surg* 2013;22:542–9.
- Boesmueller S, Wech M, Gregori M, Domaszewski F, Bukaty A, Fialka C, et al. Risk factors for humeral head necrosis and non-union after plating in proximal humeral fractures. *Injury* 2016;47:350–5.
- Meinberg EG, Agel J, Roberts CS, Karam MD, Kellam JF. Fracture and dislocation classification compendium-2018. *J Orthop Trauma* 2018;32:S1–170.
- Battistelli S, Fortina M, Carta S, Guerranti R, Nobile F, Ferrata P. Serum C-reactive protein and procalcitonin kinetics in patients undergoing elective total hip arthroplasty. *Biomed Res Int* 2014;2014:565080.
- Swarnkar M, Pendkar R. Diagnostic accuracy of the postoperative C - reactive protein to albumin ratio in prediction of complications after major abdominal surgery. *J Family Med Prim Care* 2020;9:5944–7.
- Shetty S, Ethiraj P, Shanthappa AH. C-reactive protein is a diagnostic tool for postoperative infection in orthopaedics.

- Cureus 2022;14:e22270.
18. Yigit Ş, Akar MS, Şahin MA, Arslan H. Periprosthetic infection risks and predictive value of C-reactive protein / albumin ratio for total joint arthroplasty. *Acta Biomed* 2021;92:e2021324.
19. Straatman J, Cuesta MA, Tuynman JB, Veenhof AAFA, Berman WA, van der Peet DL. C-reactive protein in predicting major postoperative complications are there differences in open and minimally invasive colorectal surgery? Substudy from a randomized clinical trial. *Surg Endosc* 2018;32:2877–85.
20. Alexandru L, Haragus H, Deleanu B, Timar B, Poenaru DV, Vlad DC. Haematology panel biomarkers for humeral, femoral, and tibial diaphyseal fractures. *Int Orthop* 2019;43:1567–72.
21. Afari ME, Bhat T. Neutrophil to lymphocyte ratio (NLR) and cardiovascular diseases: An update. *Expert Rev Cardiovasc Ther* 2016;14:573–7.
22. Johan MP, Putra LT, Yurianto H, Usman MA, Arifin J, Abidin MA, et al. The role of neutrophil to lymphocyte ratio with wound healing in open tibial fracture grade IIIA. *Int J Surg Open* 2024;62:51–6.
23. Brøchner AC, Toft P. Pathophysiology of the systemic inflammatory response after major accidental trauma. *Scand J Trauma Resusc Emerg Med* 2009;17:43.
24. Cancio-Bello AM, Barlow JD. Avascular necrosis and post-traumatic arthritis after proximal humerus fracture internal fixation: Evaluation and management. *Curr Rev Musculoskelet Med* 2023;16:66–74.
25. Yilmaz H, Uyfun M, Yilmaz TS, Namuslu M, Inan O, Taskin A, et al. Neutrophil-lymphocyte ratio may be superior to C-reactive protein for predicting the occurrence of postmenopausal osteoporosis. *Endocr Regul* 2014;48:25–33.

Temporal Evolution of Large Language Models For Response Evaluation Criteria in Solid Tumors-Based Response Evaluation After Locoregional Therapy

 Esat Kaba,¹  Davide Giardino,²  Arvin Naeimi,³  Merve Solak,¹  Mehmet Beyazal,¹  Fatma Beyazal Çeliker,¹
 Thomas Vogl⁴

¹Department of Radiology, Recep Tayyip Erdogan University, Training and Research Hospital, Rize, Türkiye

²Department of Radiology, Università degli Studi di Udine, Udine, Italy

³School of Medicine, Guilan University of Medical Sciences, Rasht, Gilan, Iran

⁴Department of Diagnostic and Interventional Radiology, Frankfurt University Hospital, Frankfurt, Germany

ABSTRACT

Objective: This study aimed to evaluate the response evaluation criteria in solid tumors (RECIST) using tumor measurements from computed tomography (CT) reports of hepatocellular carcinoma (HCC) patients before and after transcatheter arterial chemoembolization with various large language models (LLMs).

Materials and Methods: Ninety-three patients were included after the exclusion criteria were applied. RECIST assessments were performed using Bard, Bing, and ChatGPT-4 in 2023, and their updated versions—ChatGPT-4, Gemini, and Copilot—in 2025. Evaluations were based on RECIST categories determined by baseline and follow-up measurements of the longest tumor diameters from contrast-enhanced CT scans. A zero-shot prompting was used for the LLM inputs. LLM-generated RECIST classifications were compared with radiologist reports. Model performance was assessed in both years, and changes over time were analyzed.

Results: ChatGPT-4 (both 2023 and 2025) and Copilot (2025) achieved perfect scores across accuracy, precision, recall, and F1 (all 1.000). Gemini improved significantly, with accuracy rising from 0.581 in 2023 (as Bard) to 0.989 in 2025. Bing's accuracy also increased from 0.839 to 1.000 after being updated to Copilot. Cohen's Kappa showed moderate agreement between ChatGPT-4 and Bing in 2023 ($\kappa=0.612$, $p<0.001$) and perfect agreement between ChatGPT-4 and Copilot in 2025 ($\kappa=1.000$). McNemar's test showed no significant change for ChatGPT-4 between 2023 and 2025 ($p=1.000$), while Gemini and Copilot improved significantly ($p<0.0001$ and $p=0.0003$).

Conclusion: LLMs demonstrate strong potential in RECIST evaluation from CT reports in HCC patients, and ongoing improvements suggest they may increasingly aid radiological assessments in the future.

Keywords: Baseline, Follow-up, Hepatocellular carcinoma, Large language model, Response evaluation criteria in solid tumors

Cite this article as: Kaba E, Giardino D, Naeimi A, Solak M, Beyazal M, Beyazal Çeliker F, et al. Temporal Evolution of Large Language Models For Response Evaluation Criteria in Solid Tumors-Based Response Evaluation After Locoregional Therapy. Eur Arch Med Res 2025;41(3):146–153.

Address for correspondence: Esat Kaba, Department of Radiology, Recep Tayyip Erdogan University, Training and Research Hospital, Rize, Türkiye

E-mail: esatkaba04@gmail.com **ORCID ID:** 0000-0001-7464-988X

Submitted: 27.04.2025 **Revised:** 13.05.2025 **Accepted:** 02.06.2025 **Available Online:** 12.09.2025

European Archives of Medical Research – Available online at www.eurarchmedres.org

OPEN ACCESS This work is licensed under a Creative Commons Attribution-NonCommercial 4.0 International License.



INTRODUCTION

Artificial intelligence (AI) has advanced significantly in recent years and has acquired a significant role in many areas of diagnostic and interventional radiology.^[1] Numerous studies on AI applications have been published, covering a broad spectrum of topics from image reconstruction to diagnostic support, report writing, and dose optimization.^[2] Large language models (LLMs), a type of generative AI, have gained widespread attention in the past year, sparking discussions about their role in radiology.^[3] These discussions have primarily centered on report generation, text mining in radiology reports, and report optimization.^[4,5] Beyond diagnostic radiology, their use in interventional radiology is also under investigation.^[6] Over the last few years, several notable LLMs have been released, including ChatGPT-3.5 and 4 by OpenAI, Bard by Google, and Bing by Microsoft. Studies have examined the knowledge levels of these models in radiology and their potential applications across various areas. For instance, a study by Bhayana et al.^[7] evaluated ChatGPT's performance on the radiology board exam and found that it answered 69% of the questions correctly.

In another study, the high text analysis capabilities of these models were leveraged to investigate the success of detecting incidental findings in radiology reports using a single-shot learning prompt technique, yielding highly satisfactory results.^[8] In addition, Schmidt et al.^[9] focused on the ability of LLMs to detect speech errors in radiology reports. In this study, ChatGPT-4 demonstrated high accuracy in detecting both clinically significant errors (precision, 76.9%; recall, 100%; F1 score, 86.9%) and clinically insignificant errors (precision, 93.9%; recall, 94.7%; F1 score, 94.3%). Based on such studies, the capacity of LLMs to analyze data in radiology reports appears quite noteworthy.

We designed this study to determine the level of knowledge of LLMs about response evaluation criteria in solid tumors (RECIST), which is a critical component of diagnostic and interventional radiology in the follow-up of malignancy after treatment, and to reveal the potential use and reliability of LLMs in this regard in the future. In this study, we evaluated and compared the performance of Bard, Bing, and ChatGPT-4 in the RECIST assessment. In addition, we conducted the same evaluation using the latest versions of these LLMs to demonstrate their progress in this domain over time.

MATERIALS AND METHODS

Study Cohort

A publicly available dataset comprising hepatocellular carcinoma (HCC) patients was utilized in the present study.^[10,11] The dataset contained 105 HCC patients who were monitored with contrast-enhanced computed tomography (CT) both before and after the transcatheter arterial chemoembolization (TACE)

procedure. The specific CT technique employed in the dataset was described in a previous study.^[11] The mean baseline examination time in the dataset was 3 weeks before TACE, and the mean follow-up time was 9 weeks after the procedure. The dataset also contained reports from three radiologists, including measurements of the longest diameter of lesions and the RECIST assessment. For this study, we utilized the measurements and RECIST assessments from Radiologist 1, which included evaluations for 93 out of 105 patients. In other words, baseline and follow-up measurements for 93 HCC patients were included in our study. All measurements were taken at the longest diameter of the tumor, and the radiologist conducted a RECIST assessment based on the tumor's growth and shrinkage rates. According to the radiologist's assessment, this data set included 19 patients with complete response (CR), 40 patients with partial response (PR), 28 patients with stable disease (SD), and 6 patients with progressive disease (PD). These assessments were validated by an experienced interventional radiologist (T.J.V.) with over 25 years of experience. This study was conducted following the Helsinki Declaration. Ethics committee approval and patient informed consent were not required since a publicly available dataset was used for this retrospective study.

LLMs

This study aimed to evaluate and compare the classification performance of LLMs in assessing treatment response based on the RECIST criteria. Six LLMs were included: ChatGPT4 (2023), Bard (2023), Bing (2023), and their respective updated versions in 2025: ChatGPT4 (2025) (<https://chatgpt.com/>), Gemini (2025) (<https://gemini.google.com/app?hl=tr>), and Copilot (2025) (<https://copilot.microsoft.com/>). Baseline and follow-up tumor measurements were provided to LLM's chatbots by entering the following initial prompt.

Prompt

"In an interventional radiology unit where TACE for HCC is frequently performed, we need a RECIST classification to evaluate the response of lesions to treatment. Can you use the pre-treatment (baseline) and post-treatment (follow-up) values of the longest diameter of the patient's tumors to determine the percentage of tumor growth and shrinkage and perform RECIST assessment of each tumor?" This prompt provided default hyperparameters to three different models and their updated versions in November 2023 and March 2025, respectively.

Moreover, no explanation or information was provided to the models during the RECIST assessment. In other words, the zero-shot learning technique was used for prompting. RECIST assessment responses of all models were then compared with the radiologist's report as the gold standard label.

Statistical Analysis

To assess the classification performance of LLMs across different versions and RECIST categories (CR, PR, SD, PD), standard evaluation metrics, including accuracy, macro precision, macro recall, and macro F1 score, were calculated. Confusion matrices were generated to visualize the distribution of correct and incorrect predictions across classes. To evaluate the agreement between models, Cohen’s Kappa coefficient was computed. Cohen’s Kappa analysis is interpreted as shown in Table 1.^[12] Performance differences between model versions from 2023 to 2025 were analyzed using McNemar’s test. This test was applied both globally and within each RECIST category (PR, SD, PD) to determine whether the changes in classification performance were statistically significant across time. In addition, McNemar’s test was used for pairwise comparisons between different models within the same RECIST class to evaluate relative classification differences. The Wilcoxon signed-rank test was also used to compare model rankings based on accuracy and F1 score. $P<0.05$ was considered indicative of statistical significance. All statistical analyses and visualizations were performed using IBM Statistical Package for the Social Sciences Statistics version 23 (IBM Corp., Armonk, NY, USA) and the Python programming language (scikit-learn, matplotlib, and seaborn libraries).

RESULTS

Of the 93 patients in the study, 59 were male and 34 were female. The mean age of patients was 68.8 ± 10.53 . The mean baseline diameter of the lesions was 79.97 mm (15.6–243.9), and the mean follow-up diameter was 45.6 mm (0–173.9 mm).

All LLMs defined it as CR if the lesion had completely disappeared, PR if there was more than 30% shrinkage, SD if there was between 20% growth and 30% shrinkage, and PD if there was more than 20% growth. As a result, all models automatically considered the RECIST version 1.1 criteria without any RECIST definition. In addition, all chatbots calculated the percentage of change according to the following formula without any information from us.

Table 1. Interpretation of Cohen’s Kappa statistic

Kappa value (κ)	Level of agreement
κ<0	Poor agreement (less than chance)
0.00–0.20	Slight agreement
0.21–0.40	Fair agreement
0.41–0.60	Moderate agreement
0.61–0.80	Substantial agreement
0.81–1.00	Almost perfect agreement

Overall Performance

Among all models, ChatGPT 4 (2023 and 2025) and Copilot (2025) yielded optimal classification performance, achieving maximum values across all evaluated metrics (Accuracy, Precision, Recall, and F1 Score=1.00). Gemini (2025) demonstrated high overall performance (Accuracy=0.989, F1 Score=0.973), indicating a substantial improvement compared to its 2023 version (Bard), which exhibited the lowest performance across all metrics (Accuracy=0.581, F1 Score=0.437). Bing (2023) showed intermediate performance (Accuracy=0.839, F1 Score=0.776). A detailed analysis is presented in Table 2, and confusion matrices for all models are shown in Figure 1.

Model Agreement and Evolution

Cohen’s Kappa analysis revealed moderate to substantial agreement among models in 2023, with the highest agreement between ChatGPT4 and Bing ($\kappa=0.612$, $p<0.001$) (Table 3). In contrast, 2025 models showed almost perfect agreement, particularly between ChatGPT4 and Copilot ($\kappa=1.000$) (Table 4).

McNemar’s tests were performed to evaluate performance differences between model versions over time. No significant difference was found between ChatGPT4 (2023 vs. 2025) ($p=1.000$), suggesting temporal consistency. In contrast, both Gemini and Copilot exhibited statistically significant improvements between 2023 and 2025 ($p<0.0001$ and $p=0.0003$, respectively) (Table 5). Gemini misclassified only one patient by labeling the case as SD, although it was actually PD. Similarly, Bard and Bing also misclassified this same patient in 2023, incorrectly identifying it as a PR.

Class-level Analysis

The accuracies of the models in all groups are shown in Figure 2. Class-based comparisons showed that Gemini (2025) demonstrated statistically significant improvements in both PR and SD categories ($p<0.001$), while the difference in PD did not reach statistical significance ($p=0.0736$). Similarly, Copilot

Table 2. Performance metrics of the large language models in 2023 and 2025

Model	Accuracy	Precision	Recall	F1 score
ChatGPT4 (2023)	1.0	1.0	1.0	1.0
Bard (2023)	0.581	0.429	0.544	0.437
Bing (2023)	0.839	0.921	0.738	0.776
ChatGPT4 (2025)	1.0	1.0	1.0	1.0
Gemini (2025)	0.989	0.991	0.958	0.973
Copilot (2025)	1.0	1.0	1.0	1.0

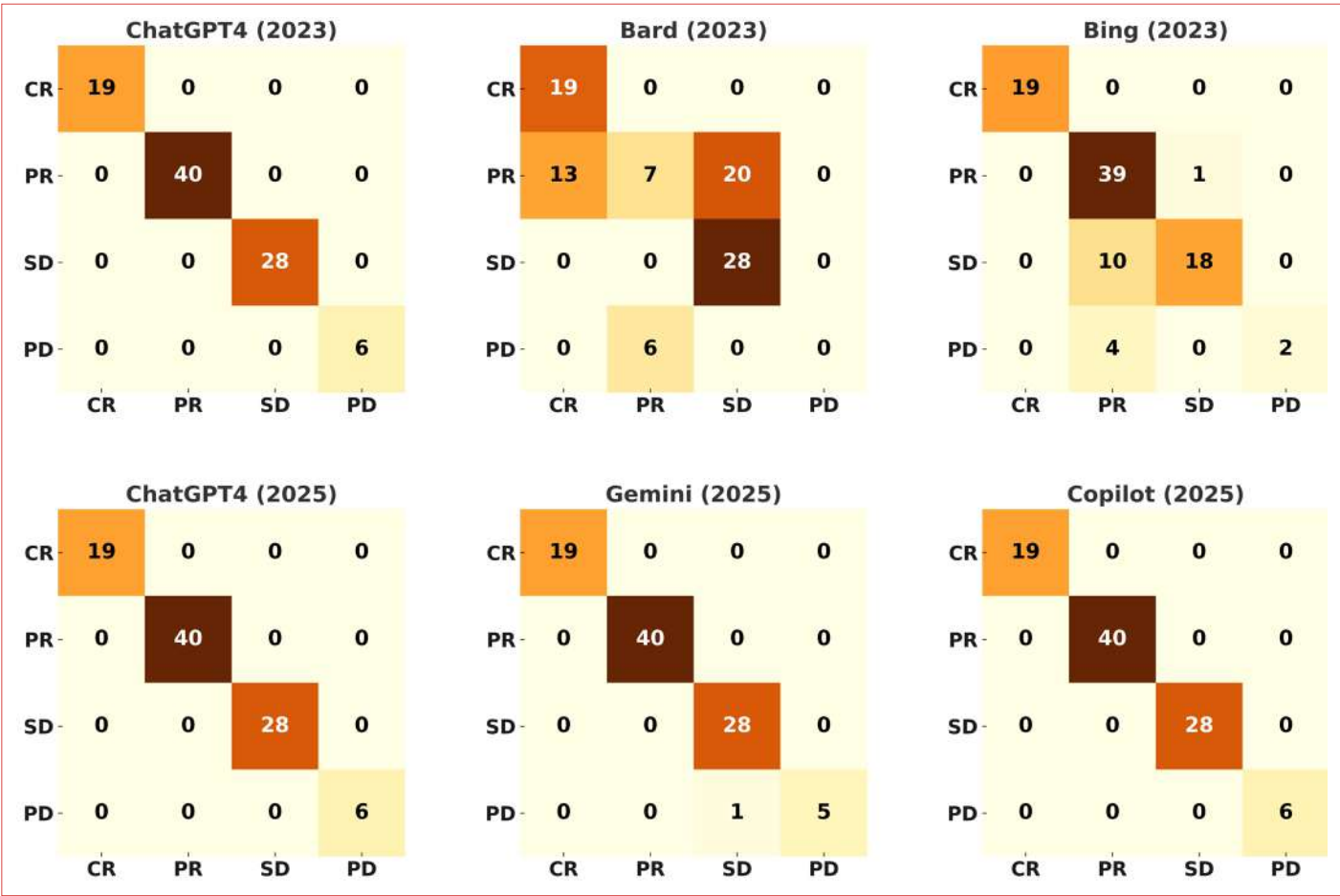


Figure 1. Confusion matrices for all models.

Table 3. In 2023, the agreement analysis between the large language models		
Models (2023)	Cohen’s kappa	p*
ChatGPT4 versus bard	0.418	<0.001
ChatGPT4 versus bing	0.612	<0.001
Bard versus bing	0.349	<0.001
*Wilcoxon signed-rank test.		

(2025) significantly improved in the SD category ($p=0.004$) but not in the PR or PD classes (Table 6). All models demonstrated 100% accuracy in identifying cases within the CR group.

DISCUSSION

This study investigated the accuracy of Bard, Bing, and ChatGPT-4 in 2023 and their updated versions in 2025 in the assessment of response to locoregional therapy in patients with HCC. We provided the models with the baseline and follow-up

Table 4. In 2025, the agreement analysis between the LLMs. The Wilcoxon signed-rank test could not be computed for the comparison between ChatGPT4 and Copilot, as all paired predictions were identical, resulting in zero differences across the answers		
Models (2025)	Cohen’s kappa	p*
ChatGPT4 versus Gemini	0.978	0.317
ChatGPT4 versus Copilot	1.000	-
Gemini versus Copilot	0.978	0.317
*Wilcoxon signed-rank test. LLMs: Large language models.		

longest tumor diameters as input. Afterward, the models were prompted to calculate tumor growth/shrinkage percentages and then perform a RECIST evaluation. No information other than baseline and follow-up values was provided during the LLM evaluation. The results were obtained without manipulating the models in any direction (zero-shot learning). As a result,

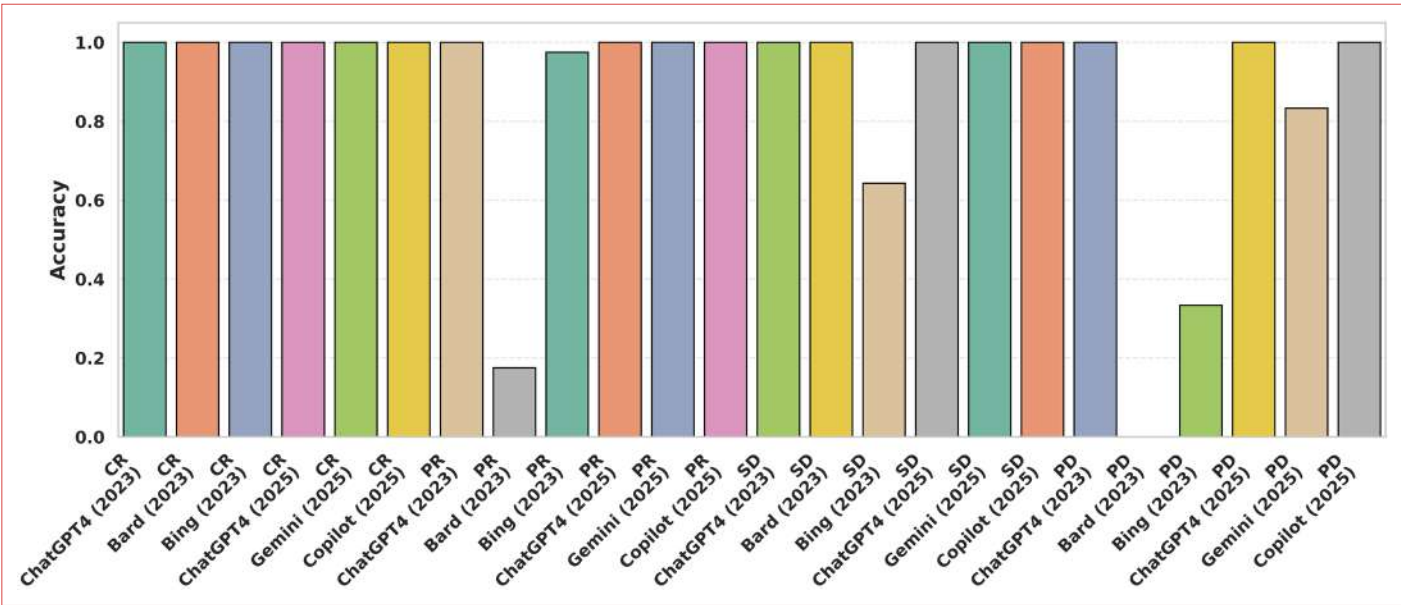


Figure 2. The accuracies of the large language models in all response evaluation criteria in solid tumors groups.

Table 5. Accuracy analysis of answers across years. The number of patients for which the models answered correctly in 2023 and incorrectly in 2025, and the number of patients for which the models answered incorrectly in 2023 and correctly in 2025 are indicated, and statistical analysis is presented

Model evolution	2023 correct/ 2025 incorrect	2023 incorrect/ 2025 correct	McNemar p-value
ChatGPT4 (2023 → 2025)	0	0	0.000
Bard → Gemini	0	38	<0.0001
Bing → Copilot	0	15	0.0003

while minor variations existed between the models, all LLMs demonstrated high accuracy in calculating the percentage of tumor diameter change. In the RECIST assessment based on these calculations, both ChatGPT-4 versions achieved 100% accuracy. Bard and Bing, on the other hand, significantly improved their accuracy from their 2023 version to the 2025 version.

LLMs have rapidly influenced millions worldwide. In medicine, researchers are actively exploring their potential to transform the field, particularly through their capacity to process vast medical texts using natural language processing. This ability holds promise for analyzing reports, identifying patient data patterns, and supporting clinical decisions. Their applications in medicine fall into three domains: Research, education, and

Table 6. Accuracy analysis of class-based answers across years. The number of patients for which the models answered correctly in 2023 and incorrectly in 2025, and the number of patients for which the models answered incorrectly in 2023 and correctly in 2025 are indicated, and statistical analysis is presented

Class	Models	2023 correct / 2025 incorrect	2023 incorrect / 2025 correct	McNemar p-value
PR	Bing (2023) → Copilot (2025)	0	1	1.000
SD	Bing (2023) → Copilot (2025)	0	10	0.004
PD	Bing (2023) → Copilot (2025)	0	4	0.134
PR	Bard (2023) → Gemini (2025)	0	33	<0.001
SD	Bard (2023) → Gemini (2025)	0	32	<0.001
PD	Bard (2023) → Gemini (2025)	0	5	0.0736

PR: Partial response; SD: Stable disease; PD: Progressive disease.

patient care.^[13] In research, they assist with data analysis, literature review, and coding. In education, both medical and patient education are being explored, with studies assessing LLMs' success in medical examinations and their role in producing patient education materials.^[14,15] For instance, Gilson et al.^[14] evaluated ChatGPT's performance on the United States Medical Licensing Examination, finding it achieved over 60% accuracy, comparable to a 3rd-year medical student's basic competency. In patient care, LLMs may summarize histories, analyze images, and interpret clinical data, underscoring their versatility and broad applicability in clinical settings.^[16]

Potential applications of LLM in radiology also cover a wide range of topics.^[17] Given the advanced text analysis capabilities of LLMs, the simplification of radiology reports and the extraction of some analytics from them are one of the main topics of research. In this regard, Fink et al.^[18] compared GPT-4 and ChatGPT to extract lesion parameters from CT reports and identify metastatic status and label oncological progression. The authors report that GPT-4 achieved 98.6% accuracy in extracting lesion parameters, 98.1% accuracy in identification of metastatic status, and an F1 score of 0.96 in labeling oncological progression. In all tasks, GPT-4 showed superior performance in their study.

In our study, we tested and compared the accuracy of four different LLMs in calculating the growth and shrinkage rate of lesions and subsequent RECIST assessment, which are very important in diagnostic and interventional radiology. The findings of our study reveal that LLMs, especially updated versions, correctly classify patients, providing the most important hope for the future. Several studies in the literature have evaluated the performance of LLMs at different time points, highlighting their potential for continued improvement over time. A study evaluated the performance of LLMs (GPT-4, GPT-3.5, Claude, and Google Bard) on radiology exam questions over 3 months, focusing on accuracy, subspecialty performance, and internal consistency.^[19] Among the models, GPT-4 achieved the highest overall accuracy, although a slight downward trend was observed over time, while Claude demonstrated gradual improvement. The observed reduction in intra-model discordance across all models suggests increasing internal consistency, yet persistent variability across subspecialties and difficulty with fact-based questions highlight the current limitations of LLMs in domain-specific medical reasoning. Our study also found that while ChatGPT-4 was the most accurate model among the 2023 versions, both Bard and Bing showed a marked improvement in their 2025 versions.

Considering that LLMs can potentially be integrated into hospital image archiving and communication systems in the future, treatment response assessment applications can be created quickly and effectively by accessing patients' reports

and using baseline and follow-up measurement results.^[20] Evaluating our findings with other studies in the literature, we conclude that in the future, LLMs, particularly advanced models like ChatGPT-4, will not only support physicians in their demanding daily routines but will also enable them to perform certain analyses of patients' radiology reports. These models can also support the patient-physician interview by offering high accuracy in assessing treatment responses based on radiology reports. This capability is crucial in oncology, where accurate assessment of treatment responses, such as in HCC, directly influences clinical decision-making. In addition, LLMs could enhance patient understanding by converting complex medical information into clear, accessible language, aiding patients and their families in comprehending diagnoses, treatment options, and expected outcomes. This improved communication can lead to better patient engagement and adherence to treatment plans. Ultimately, integrating LLMs into clinical workflows can promote a more efficient and patient-centered approach in healthcare, leading to improved outcomes for both physicians and patients.

The rapid development and strong performance of LLMs offer significant promise for healthcare innovation. However, their deployment brings several limitations and ethical concerns. A major issue is the inheritance of biases from training data, whose sources and quality are often uncertain, making bias correction challenging.^[20,21] In addition, LLMs cannot verify the accuracy of their outputs, leading to potential misinformation or "hallucinations," which may cause serious harm in medical contexts. Complex architectures also limit interpretability and hinder transparency and accountability.^[22] While techniques such as the Chain of thought may help address some issues, robust solutions remain necessary. Patient privacy is another critical consideration; although anonymized data can be used, complete anonymization cannot always be guaranteed and increases ethical risks. Therefore, LLMs must be strictly secured against unauthorized access in healthcare settings.^[20,22,23]

The current study has some limitations. First, the number of patients was limited. Studies investigating the RECIST assessment of LLMs using much larger datasets are needed. Second, the present study only reported the baseline and follow-up longest diameters instead of providing the complete radiology reports. In addition, the RECIST assessment is not only based on the longest diameter but also includes many other criteria. Hence, more studies with complete reports and larger sample sizes that include all the criteria used in the RECIST assessment are recommended. However, in our study, we have demonstrated the capabilities of LLM in the field of radiology for exploratory purposes. As more comprehensive reports become available, a comprehensive assessment of RECIST with LLMs can be conducted in the future.

CONCLUSION

This study has demonstrated the evolution of LLMs over the years in terms of some medical knowledge and as an effective tool in RECIST assessment and revealed their potential advantages in various medical and radiological contexts. LLMs can efficiently assess treatment responses in radiology reports and offer valuable support in managing the increasing workload of radiologists. Integrating LLMs into clinical workflows can support radiologists in current challenges and improve the overall quality of care, ultimately contributing to better outcomes for both physicians and patients.

DECLARATIONS

Ethics Committee Approval: Not required.

Informed Consent: Not required.

Conflict of Interest: The authors declare that there is no conflict of interest.

Funding: The authors received no financial support for the research and/or authorship of this article.

Use of AI for Writing Assistance: The authors used ChatGPT to correct grammar and English translations. The content of the publication is entirely the responsibility of the authors, and the authors reviewed it and made the necessary corrections.

Authorship Contributions: Concept – None; Design – EK, DG, AN, MS, MB, FBÇ, TV; Supervision – None; Fundings – None; Materials – EK, DG, AN, MS, MB, FBÇ, TV; Data collection &/or processing – EK, DG, AN, MS, MB, FBÇ, TV; Analysis and/or interpretation – EK, DG, AN, MS, MB, FBÇ, TV; Literature search – EK; Writing – EK, DG, AN, MS, MB, FBÇ, TV; Critical review – EK, DG, AN, MS, MB, FBÇ, TV.

Peer-review: Externally peer-reviewed.

REFERENCES

- Boeken T, Feydy J, Lecler A, Soyer P, Feydy A, Barat M, et al. Artificial intelligence in diagnostic and interventional radiology: Where are we now? *Diagn Interv Imaging* 2023;104:1–5.
- Barreiro-Ares A, Morales-Santiago A, Sendra-Portero F, Souto-Bayarri M. Impact of the rise of artificial intelligence in radiology: What do students think? *Int J Environ Res Public Health* 2023;20:1589.
- Bajaj S, Gandhi D, Nayar D. Potential applications and impact of ChatGPT in radiology. *Acad Radiol* 2024;31:125–61.
- Elkassam AA, Smith AD. Potential use cases for ChatGPT in radiology reporting. *AJR Am J Roentgenol* 2023;221:373–6.
- Amin KS, Davis MA, Doshi R, Haims AH, Khosla P, Forman HP. Accuracy of ChatGPT, Google Bard, and Microsoft Bing for simplifying radiology reports. *Radiology* 2023;309:e232561.
- Scheschenja M, Viniol S, Bastian MB, Wessendorf J, König AM, Mahnken AH. Feasibility of GPT-3 and GPT-4 for in-depth patient education prior to interventional radiological procedures: A comparative analysis. *Cardiovasc Intervent Radiol* 2024;47:245–50.
- Bhayana R, Krishna S, Bleakney RR. Performance of ChatGPT on a radiology board-style examination: Insights into current strengths and limitations. *Radiology* 2023;307:e230582.
- Bhayana R, Elias G, Datta D, Bhambra N, Deng Y, Krishna S. Use of GPT-4 with single-shot learning to identify incidental findings in radiology reports. *AJR Am J Roentgenol* 2024;222:e2330651.
- Schmidt RA, Seah JCY, Cao K, Lim L, Lim W, Yeung J. Generative large language models for detection of speech recognition errors in radiology reports. *Radiol Artif Intell* 2024;6:e230205.
- Moawad AW, Fuentes D, Morshid A, Khalaf AM, Elmohr MM, Abusaif A, et al. Multimodality annotated HCC cases with and without advanced imaging segmentation [dataset]. *Cancer Imaging Arch*; 2021.
- Morshid A, Elsayes KM, Khalaf AM, Elmohr MM, Yu J, Kaseb AO, et al. A machine learning model to predict hepatocellular carcinoma response to transcatheter arterial chemoembolization. *Radiol Artif Intell* 2019;1:e180021.
- McHugh ML. Interrater reliability: The kappa statistic. *Biochem Med (Zagreb)* 2012;22:276–82.
- Clusmann J, Kolbinger FR, Muti HS, Carrero ZI, Eckardt JN, Laleh NG, et al. The future landscape of large language models in medicine. *Commun Med (Lond)* 2023;3:141.
- Gilson A, Safranek CW, Huang T, Socrates V, Chi L, Taylor RA, et al. How does ChatGPT perform on the United States Medical Licensing Examination (USMLE)? The implications of large language models for medical education and knowledge assessment. *JMIR Med Educ* 2023;9:e45312. Erratum in: *JMIR Med Educ* 2024;10:e57594.
- Kuckelman IJ, Yi PH, Bui M, Onuh I, Anderson JA, Ross AB. Assessing AI-powered patient education: A case study in radiology. *Acad Radiol* 2024;31:338–42.
- Qiu J, Yuan W, Lam K. The application of multimodal large language models in medicine. *Lancet Reg Health West Pac* 2024;45:101048.
- Kim K, Cho K, Jang R, Kyung S, Lee S, Ham S, et al. Updated primer on generative artificial intelligence and large language models in medical imaging for medical professionals. *Korean J Radiol* 2024;25:224–42.
- Fink MA, Bischoff A, Fink CA, Moll M, Kroschke J, Dulz L, et al. Potential of ChatGPT and GPT-4 for data mining of free-text

- CT reports on lung cancer. *Radiology* 2023;308:e231362.
19. Gupta M, Virostko J, Kaufmann C. Large language models in radiology: Fluctuating performance and decreasing discordance over time. *Eur J Radiol* 2025;182:111842.
20. Akinci D'Antonoli T, Stanzione A, Bluethgen C, Vernuccio F, Ugga L, Klontzas ME, et al. Large language models in radiology: Fundamentals, applications, ethical considerations, risks, and future directions. *Diagn Interv Radiol* 2024;30:80–90.
21. Meskó B, Topol EJ. The imperative for regulatory oversight of large language models (or generative AI) in healthcare. *NPJ Digit Med* 2023;6:120.
22. Li H, Moon JT, Purkayastha S, Celi LA, Trivedi H, Gichoya JW. Ethics of large language models in medicine and medical research. *Lancet Digit Health* 2023;5:e333–5.
23. Stahl BC, Eke D. The ethics of ChatGPT – exploring the ethical issues of an emerging technology. *Int J Inf Manag* 2024;74:102700.

The Impact of ASXL1 Gene Mutations on Clinical Course and Prognosis in Myeloproliferative Neoplasms

 Neslihan Uslu,¹  Veysel Sabri Hancer,²  Reyhan Diz Kucukkaya³

¹Division of Endocrinology and Metabolic Diseases, Department of Internal Medicine, Istanbul Medeniyet University, Goztepe Prof. Dr. Suleyman Yalcin City Hospital, Istanbul, Türkiye

²Department of Medical Biology, Istanbul University, Faculty of Medicine, Istanbul, Türkiye

³Department of Hematology and Internal Medicine, Private Practice, Istanbul, Türkiye

ABSTRACT

Objective: Chronic myeloproliferative neoplasms (MPNs) form a group of diseases characterized by clonal proliferation in all three cell lines of the bone marrow. “Philadelphia chromosome”-negative (Ph-) MPNs are primarily categorized into essential thrombocythemia (ET), polycythemia vera (PV), and primary myelofibrosis (PMF). The JAK-2 V617F mutation was found in 95–98% of PV patients and 50% of ET and PMF patients. Later, JAK2 exon-12 mutations in PV, MPL W515L/K and calreticulin mutations in PMF and ET were identified. Another mutation observed in MPN patients is the additional sex combs like 1 (ASXL1) gene mutation. This study investigated the frequency of ASXL1 gene mutations in 103 Ph- MPN patients and examined their impact on the disease's clinical course and prognosis.

Materials and Methods: A total of 103 Ph- MPN patients were included in the study. DNA sequence analysis was used to screen for ASXL1 gene mutations using blood count samples.

Results: ASXL1 gene mutations were detected in 6 patients (5.8%) in our cohort. Screening of the 12th exon of the ASXL1 gene revealed the most common mutation as c.1934dupG (p.g646TrpfsX12) and the second most frequent as c.1954G.a (p.G652S). The group with ASXL1 gene mutations showed higher rates of thrombosis. In our MPN group with an average follow-up duration of 4.1 years, non-hematologic cancer rates (solid tumors) were found to be considerably high (14.5%). 80% of these patients had the JAK-2 V617F mutation. Two patients with the JAK-2 V617F mutation also had the ASXL1 c.1954G.a (p.G652S) gene mutation.

Conclusion: In our cohort, the diagnosis of non-hematologic cancer following the use of hydroxyurea in five patients initially diagnosed with MPN suggests that hydroxyurea use might contribute to the development of non-hematologic cancer. On the other hand, the development of secondary cancer in two patients without hydroxyurea use post-MPN diagnosis indicates that factors other than hydroxyurea may also influence the development of non-hematologic cancers.

Keywords: Additional sex combs like 1, Chronic myeloproliferative neoplasms, Essential thrombocythemia, Myeloproliferative neoplasms, Polycythemia vera, Primary myelofibrosis

Cite this article as: Uslu N, Hancer VS, Diz Kucukkaya R. The Impact of ASXL1 Gene Mutations on Clinical Course and Prognosis in Myeloproliferative Neoplasms. Eur Arch Med Res 2025;41(3):154–162.

Address for correspondence: Neslihan Uslu, Division of Endocrinology and Metabolic Diseases, Department of Internal Medicine, Istanbul Medeniyet University, Goztepe Prof. Dr. Suleyman Yalcin City Hospital, Istanbul, Türkiye

E-mail: neslihan.uslu@hotmail.com **ORCID ID:** 0000-0001-5688-7008

Submitted: 14.03.2025 **Revised:** 30.05.2025 **Accepted:** 17.06.2025 **Available Online:** 12.09.2025

European Archives of Medical Research – Available online at www.eurarchmedres.org

OPEN ACCESS This work is licensed under a Creative Commons Attribution-NonCommercial 4.0 International License.



INTRODUCTION

Myeloproliferative neoplasms (MPNs) are a group of diseases resulting from mutations in pluripotent hematopoietic stem or progenitor cells, leading to persistent and progressive increases in all three cell lines of the bone marrow. Chronic myeloid leukemia (CML) in this group is characterized by the presence of the “Philadelphia chromosome” and its oncogene BCR-ABL. Ph-negative (Ph–) MPNs are categorized into essential thrombocythemia (ET), polycythemia vera (PV), and primary myelofibrosis (PMF). The discovery of the JAK-2 V617F mutation in 2005 revealed its presence in 95–98% of PV patients and 50% of ET and PMF patients.^[1] It is crucial to exclude reactive erythrocytosis and thrombocytosis in the diagnosis of these diseases.^[2,3]

The additional sex combs like 1 (ASXL1) gene is the human homolog of the “Additional sex combs (Asx)” gene found in *Drosophila* located at 20q11, ASXL1 encodes a 1084 amino acid nuclear protein. The exact function of the ASXL1 protein is not fully understood, but it is believed to control epigenetic changes through histone modification. ASXL1 gene mutations are predominantly frameshift mutations located in the 12th exon, typically resulting in the loss of the carboxy-terminal plant homeofinger domain. ASXL1 gene mutations are observed in PV at a rate of 2–7%, in ET at 0–10%, and in PMF at 13–32%. Studies suggest that ASXL1 influences gene transcription by binding to chromatin, activating certain regions while repressing others, thus potentially contributing to the development of myeloid neoplasms.^[4–6] ASXL1 gene mutations have also been demonstrated in different hematologic malignancies, including MDS, AML, and CMML.^[7]

In this study, conducted at the Hematology Clinic of Istanbul Bilim University Faculty of Medicine, the frequency of ASXL1 gene mutations was investigated in 103 Ph– MPN patients, along with their impact on the clinical course and prognosis of the disease. ASXL1 gene mutations were screened using DNA sequence analysis of blood count samples taken during routine clinic visits, and their effects on clinical progression and prognosis were examined.

MATERIALS AND METHODS

This study included 103 patients (48 ET, 46 PV, 9 PMF) diagnosed with Ph– MPN meeting the criteria of the World Health Organization.^[8] The study received approval from the Ethics Committee of Istanbul Bilim University (Date: 17.02.2015, Number: 44140529/2015-30) and was conducted with informed consent from the patients. The study was supported by the Istanbul Bilim University Research Fund. All procedures were followed in accordance with the ethical standards of the Responsible Human Experimentation Committee (institutional and national) and with the 1964 Helsinki Declaration and its later versions.

Demographic and clinical data of the included patients, in-

cluding the onset of the disease, initial hemoglobin, leukocyte, platelet levels, presence of initial splenomegaly, thrombosis and bleeding complications, malignancy, and cytogenetic examinations (JAK-2 V617F, JAK-2 EXON 12, MPL W515L/K, calreticulin [CALR]), and administered drugs were reviewed.

Venous blood samples from the included patients were collected and processed at the Molecular Hematology and Oncology Laboratory of Istanbul Bilim University, where DNA isolation was performed, followed by sequencing analysis to screen for ASXL1 gene mutations.

Genomic DNA isolation was performed from 103 patients (48 ET, 46 PV, 9 PMF) diagnosed with Ph– MPN using a DNA isolation kit (HibriGen Biotechnology, Istanbul, Türkiye). The liquid containing genomic DNA was stored at +4°C until analysis time. For mutation analysis, the 12th exon of the ASXL1 gene was amplified using polymerase chain reaction (PCR) with a designed primer pair (Table 1).

ASXL1 gene mutations were analyzed using a device operating on the principle of Sanger’s dideoxy method (Applied Biosystems ABI 310xl Genetic Analyzer). The target region for examination was amplified using the PCR program outlined in Table 1. The success of amplification in PCR was verified by loading 5 µL of the product on a 2.5% (w/v) agarose gel. DNA sequencing was then performed in four stages. PCR products were purified using a column-based kit (PCR purification kit, HibriGen Biotechnology, Istanbul, Türkiye) and checked on a 2% (w/v) agarose gel. Samples not visible on the gel underwent PCR again. The purified samples were subjected to cycle sequencing on the same day. The cycle sequencing protocol was carried out according to the protocol below using the “ready reaction mix” from the kit (BigDye Terminator v3.1 Cycle Sequencing Kit, Applied Biosystems) containing fluorescently labeled four different dideoxy nucleotides.

Table 1. PCR mixture used for amplification of exons

PCR components	µL/Tube	Final concentration
Sterile ultra-pure water	16.7	-
10× PCR buffer	2.0	1X
MgCl2 (25 mM)	1.0	0.25 mM
dNTP mix (25 mM)	1.5	1.5 mM
Primer 1 (10 pmol/µL)	0.8	0.8 pmol
Primer 2 (10 pmol/µL)	0.8	0.8 pmol
Taq DNA polymerase (5U/µL)	0.2	1U
DNA	2	-
Total volume	25	-

PCR: Polymerase chain reaction.

Ready reaction mix: 8 µL Primer (3.2 pmol): 4 µL

DNA sample 2–5 µL dH2O: 3–6 µL

Total volume: 20 µL

Cycle sequencing was performed using the forward and reverse primers used in the PCR stage, and the sequencing mixture was prepared and applied according to the program below.

96°C for 10 s

50°C for 5 s 25 cycles

60°C for 4 min

4°C indefinitely

After cycle sequencing, a further purification step was conducted to clean the products from residuals. 2 µL of NaAc with pH 4.6 was added to the PCR product, followed by 50 µL of 95% (v/v) ethanol. The mixture was transferred to 1.5 mL tubes, gently mixed by tapping, and incubated on ice for 15 min. It was then centrifuged at 13,000 rpm for 20 min. The supernatant was removed, and 250 µL of 70% (v/v) ethanol was added, gently mixed, and centrifuged at 13,000 rpm for 5 min. After discarding the supernatant, the samples were left to dry at room temperature. The lyophilized DNA samples were either immediately loaded onto the analyzer (ABI Prism 310 Genetic Analyzer, Applied Biosystems) or stored at –20°C for up to 1 week for later analysis.

Statistical Analysis

Statistical analyses in this study were performed using Number Cruncher Statistical System 2007 Statistical Software (Utah, USA). Descriptive statistical methods (standard deviation, mean) were used for data evaluation, along with independent t-tests for comparing two groups, Chi-square, Fisher’s exact test, odds ratio (OR) values, and Tukey’s multiple comparison test for qualitative data comparisons. Results were considered significant at $p<0.05$.

RESULTS

In this study, a total of 103 patients with Ph– MPN, including 48 with ET, 46 with PV, and 9 with PMF, were examined. The gender distribution consisted of 58 female and 45 male patients. The average follow-up duration for our patient group was 4.21 years (standard deviation 3.83 years).

A statistically significant difference in gender distribution was observed among the ET, PV, and PMF groups ($p=0.0001$) (Table 2). There was no statistically significant difference in the average ages and diagnosis ages among the ET, PV, and PMF groups; however, PMF patients being of older age was noteworthy (respectively, $p=0.632$, $p=0.563$) (Table 2).

The presence of JAK-2 V617F was significantly higher in the PV group as expected ($p=0.041$). There was no statistically significant difference in the presence of CALR mutations between ET and PMF groups ($p=0.067$) (Table 3).

Table 2. Demographic characteristics of patients diagnosed with ET, PV, and PMF				
	ET n=48	PV n=46	PMF n=9	p
Age	52.75±19.87	55.33±15.72	58.11±16.81	0.632
Age of diagnosis	48.52±19.06	50.5±16.15	55.33±19.22	0.563
Gender, (%)				0.0001
Female	32 (66.67)	26 (56.52)	0 (0.00)	
Male	16 (33.33)	20 (43.48)	9 (100.00)	
ET: Essential thrombocythemia; PV: Polycythemia vera; PMF: Primary myelofibrosis.				

Table 3. Presence of genetic mutations in patients diagnosed with ET, PV, and PMF				
Mutation	ET n=48 (%)	PV n=46 (%)	PMF n=9 (%)	p
JAK-2 V617F	29 (60.42)	39 (84.78)	4 (44.4)	0.041
MPL W515L/K	0 (0.00)	0 (0.00)	1 (11.11)	0.004
CALR	6 (12.50)	0 (0.00)	1 (11.11)	0.067
ASXL1	3 (6.25)	2 (4.35)	1 (11.11)	0.720
c.1934dupG (p.g646TrpfsX12)	3 (6.25)	1 (2.17)	0 (0.00)	0.509
c.1954g.a (p.G652S)	0 (0.00)	1 (2.17)	1 (11.11)	0.061
ET: Essential thrombocythemia; PV: Polycythemia vera; PMF: Primary myelofibrosis.				

Among the 6 patients with ASXL1 gene mutations, 3 had ET (50%), 2 had PV (33.33%), and 1 had PMF (16.67%). Patients with ASXL1 gene mutations tended to be older in terms of age and diagnosis age compared to those without the mutations, but this difference was not statistically significant (Table 4).

When patients diagnosed with ET, PV, and PMF were grouped based on the presence of ASXL1 gene mutations, patients with these mutations tended to have higher initial platelet and hemoglobin averages. Their initial leukocyte and neutrophil averages were lower. However, due to the small number of patients, no statistically significant difference was found between the average values of initial hemoglobin, leukocyte, platelet, and neutrophil levels. There was no statistically significant difference

observed in the distribution of initial symptoms such as itching, plethora, fever, weight loss, and sweating between the two groups (respectively, $p=0.304$, 0.516 , 0.313 , 0.295 , 0.547). Constitutional symptoms were notably less in patients with ASXL1 gene mutations. Similarly, no statistically significant difference was observed in the presence of splenomegaly between the two groups ($p=0.286$), with a higher likelihood of splenomegaly in the group without ASXL1 gene mutations (Table 5).

An interesting observation in our study group was that non-hematologic (solid) cancers were more prevalent than expected. In our cohort of 103 patients, 15 (14.5%) had a total of 17 non-hematologic cancers. In 7 patients, cancer was known before the MPN diagnosis (1 sarcoma, 1 bladder cancer and renal cell cancer, 1 basal cell cancer, 1 colon cancer, 3 breast cancers), while 7 patients were diagnosed with non-hematologic cancer following an MPN diagnosis (1 basal cell cancer and parotid squamous cell cancer, 1 breast cancer, 1 pancreatic cancer, 1 cervical cancer, 1 lung cancer, 2 prostate cancers). In one patient, MPN and non-hematologic cancer were diagnosed simultaneously.

Molecular characteristics of patients with non-hematologic cancers revealed that 12 had the JAK-2 V617F mutation (12/15, 80%), and 1 had CALR mutations. Two patients had both JAK-2 V617F and ASXL1 c.1954g.a (p.G652S) mutations. Two patients were negative for all mutations, and the Ph– MPN diagnosis was made through bone marrow biopsy.

Patients were treated with hydroxyurea and interferon (IFN) for MPN. Ten patients had been diagnosed with non-hematologic cancer without having received any prior treatment. Five patients had a history of long-term hydroxyurea use. The average age of patients with non-hematologic cancer in Ph (–) MPN was 64.06, and the average age of diagnosis was 58.5.

Table 4. Comparison of demographic characteristics of patients diagnosed with ET, PV, and PMF based on the presence of ASXL1 gene mutations

Parameters	ASXL1 (+)	ASXL1 (–)	p
Age	54.51±17.82	52.17±18.49	0.756
Age of diagnosis	50.13±17.74	47.5±20.98	0.728
Gender, (%)			
Female	3 (50.00)	55 (56.70)	0.748
Male	3 (50.00)	42 (43.30)	
Diagnosis, (%)			
ET	3 (50.00)	45 (46.39)	0.720
PV	2 (33.33)	44 (45.36)	
PMF	1 (16.67)	8 (8.25)	

ASXL1: Additional sex combs like 1; ET: Essential thrombocythemia; PV: Polycythemia vera; PMF: Primary myelofibrosis.

Table 5. Comparison of clinical characteristics of patients diagnosed with ET, PV, and PMF based on the presence of ASXL1 gene mutations

Clinical feature	ASXL1 (+) n=6	ASXL1 (–) n=97	p
Initial hemoglobin (g/dL)	14.12±2.53	13.96±2.64	0.890
Initial platelets (mm ³)	733.83±559.84	629.56±392.63	0.540
Initial leukocytes (mm ³)	9486.67±3756.1	11249.37±5484.53	0.441
Initial neutrophils (mm ³)	4948±4105.79	7596.51±4302.93	0.186
Itching (%)	1 (0.9708)	39 (37.864)	0.304
Plethora (%)	1 (0.9708)	30 (29.126)	0.516
Fever (%)	0 (0.00)	15 (14.563)	0.313
Weight loss (%)	0 (0.00)	16 (15.533)	0.295
Sweating (%)	1 (0.9708)	29 (28.155)	0.547
Splenomegaly (%)	2 (1.941)	54 (52.427)	0.286

ASXL1: Additional sex combs like.

DISCUSSION

The gender distribution of the 103 included Ph(–) MPN patients showed 58 females and 45 males. In the largest study reported from Türkiye, involving 184 Ph(–) MPN patients, the female-to-male ratio was reported as 54.3% female and 45.7% male (58/49) in ET cases and 55.84% female, 44.16% male (43/34) in PMF cases.^[9] Due to the small number of PMF patients in our study, it is not possible to make a definitive comment on the difference in gender distribution.

The average diagnosis age of our ET patients was 48.52 ± 19.06 ; for PV patients, it was 50.5 ± 16.15 , and for PMF patients, it was 55.33 ± 19.22 . Although no statistically significant difference was found when comparing the average onset ages, our findings indicate that ET tends to occur in relatively younger individuals, whereas PMF is seen in an older patient group. The literature reports average ages of 50–57 for ET, 60 for PV, and 65 for PMF.^[10] The average diagnosis ages for Ph(–) MPN subgroups in our cohort were notably lower. This may be explained by the ability to screen all patients in our laboratory for the 3 mutations (JAK-2 V617F, CALR, MPL W515L/K) considered significant markers in the diagnosis of Ph(–) MPN. Routine use of molecular diagnostic methods can be considered as facilitating factor for earlier diagnosis in patients.

When initial hematologic parameters were considered, as expected, high platelet counts in ET, high erythrocyte counts in PV, and high leukocyte and neutrophil counts in PMF were observed. There was a statistically significant difference in the distribution of splenomegaly presence among ET, PV, and PMF groups; a lower incidence of splenomegaly was observed in the ET group, while a higher tendency for splenomegaly was noted in the PMF group.

In this study of Ph– MPN patients, when evaluated for commonly occurring clonal mutations, the JAK-2 V617F mutation was detected in 71.3% of patients (72/103). Examining the distribution across subgroups, this mutation was found in 84.78% of PV patients (39/46), 60.42% of ET patients (29/48), and 50% of PMF patients (4/8). One PV patient was found to have the JAK-2 exon 12 mutation, bringing our detection rate of mutant JAK-2 molecules in PV patients to 87%. Compared to the literature, the rate of JAK-2 mutations in our PV patient group was low.^[11] Several interpretations can be made for this. In some cases, the JAK-2 V617F mutation could not be demonstrated in peripheral blood cells but was positive in genetic examination from bone marrow. Unfortunately, not all patients with negative JAK-2 mutations underwent genetic examination from bone marrow, as some were diagnosed based on bone marrow biopsies performed at external centers and did not consent to a second marrow procedure.

CALR mutations were found in a total of 7 patients, with 6 in the ET group and one in the PMF group. The MPL W515L/K mutation was demonstrated in only one PMF patient.

In our study group, ASXL1 gene mutations were detected in 6 patients (5.8%). These mutations were present in 6.25% of ET patients (3/48), 4.35% of PV patients (2/46), and 11.11% of PMF patients (1/9). Looking at the distribution of these mutations by diagnosis in the literature, the frequencies are reported as 2–7% in PV, 0–10% in ET, and 13–32% in PMF.^[9,12–16] Although there are different results in studies concerning ASXL1 gene mutations, the frequency is generally given as approximately 10% in Ph(–) MPN patients.^[13] In a study published in 2011 by Stein et al.,^[15] 166 MPN patients were evaluated for ASXL1 gene mutations. ASXL1 gene mutations were found in 2% of PV patients, 32% of PMF patients, and none in ET patients. In another study conducted in 2012 by Brecqueville et al.,^[12] ASXL1 gene mutations were investigated in 149 MPN patients: found in 7% of 30 PV patients, 4% of 53 ET patients, 20% of 30 PMF patients, 50% of 4 post-PV PMF patients, and 10% of 10 post-ET PMF patients. In a study by Gelsi-Boyer et al.^[16] in 2009, the frequencies were determined as 2–5% in PV, 5–10% in ET, and 13–26% in PMF. In a study conducted in Türkiye by Yonal-Hindilerden et al.,^[9] the frequency of ASXL1 gene mutations in 184 MPN patients was investigated and found to be 8.4% in ET (9/107) and 24.7% in PMF (19/77).

In our Ph– MPNs cohort, the most common mutations found upon screening the 12th exon of the ASXL1 gene were c.1934dupG (p.g646TrpfsX12) in four patients, followed by c.1954G.a (p.G652S) in two patients. No other mutations were detected. Similar to another study conducted in Türkiye, only exon 12 of the ASXL1 gene was screened, identifying the same frequent mutations: c.1934dupG (p.g646TrpfsX12), c.1954G.a (p.G652S), and 1900_1922 del.^[9]

Internationally, the most commonly observed mutation is also c.1934dupG (p.g646TrpfsX12). In a study by Gelsi-Boyer et al.^[7] in 2012, this mutation was found in over 50% of patients with ASXL1 gene mutations. In a cohort study by Stein et al.,^[15] c.1934dupG (p.g646TrpfsX12) was the most frequent mutation found, followed by c.1900_1922del and c.1954G.a (p.G652S). Tefferi et al.'s^[17] study similarly highlighted the prevalence of the c.1934dupG (p.g646TrpfsX12) variant.

Due to the limited number of ASXL1 gene mutations (c.1934dupG p.g646TrpfsX12, c.1954G.a p.G652S) in our patient group, it was not possible to separately analyze these two ASXL1 variants. Statistical analysis was conducted by grouping patients based on the presence or absence of ASXL1 gene mutations. The relationship between ASXL1 gene mutations and epidemiological and clinical findings is not yet fully clarified in the literature, and there are conflicting interpretations. In

our patient group, the gender distribution among the six patients with ASXL1 gene mutations was equal (3 males and 3 females). The average age was 54.51 ± 17.82 , and the average age at diagnosis was 50.13 ± 17.74 . Although no statistically significant difference was found between patients with and without ASXL1 gene mutations in terms of average age and diagnosis age, it is notable that those with ASXL1 gene mutations tended to be older.

In a cohort study by Stein et al.^[15] involving 83 patients, those carrying ASXL1 gene mutations were found to have a lower average onset age and average age, though the difference was not statistically significant ($p=0.14$ and 0.67 , respectively). Vannuchi et al.'s^[18] study covering 879 Ph(–) MPN patients found ASXL1 gene mutations more frequently in older patients. In a 2012 study by Brecqueville et al.^[12] involving 127 Ph(–) MPN patients, the average age of patients with ASXL1 gene mutations was 74, significantly older than the 63 years in those without mutations ($p=0.008$). In a Turkish study involving 184 Ph(–) MPN patients, the diagnosis age and average age were higher in those with ASXL1 gene mutations compared to those without.^[9]

The distribution of ASXL1 gene mutations and their demographic characteristics in PV, ET, and PMF are contradictory in the literature. In our study, ASXL1 gene mutations were more common in women than in men in ET (66.7%), equally distributed in PV, and only found in male patients in PMF. Due to the small number of patients and the presence of only male patients in the PMF group in our study, it is not feasible to make a definitive comment on these observations.

In our study, we investigated the impact of ASXL1 gene mutations on the initial platelet and hemoglobin averages in patients with Ph– MPNs. It was observed that patients with ASXL1 gene mutations had higher initial hemoglobin and platelet averages, but lower initial leukocyte and neutrophil averages compared to those without mutations. Due to the small number of patients, these findings were not statistically significant. Although not statistically significant, the higher platelet counts in ASXL1-positive patients may be attributed to the higher proportion of ET patients (50%) in this group. This contrasts with another study conducted in Türkiye by Yonal-Hindilerden et al.,^[9] where patients with Ph(–) MPN and ASXL1 gene mutations had higher initial leukocyte values compared to the group without mutations, while the initial platelet and hemoglobin values were similar in both groups. In a cohort study by Stein et al.,^[15] initial leukocyte, hemoglobin, and platelet values were found to be similar in PMF patients with and without ASXL1 gene mutations. Brecqueville et al.^[12] found no difference in initial leukocyte and platelet counts between groups with and without ASXL1 gene mutations, although hemoglobin levels were lower in those with muta-

tions. Overall, results in the literature vary significantly.

In our study, the rate of splenomegaly in patients with ASXL1 gene mutations was lower (33.33% vs. 55.67%). The relationship between ASXL1 gene mutations and splenomegaly has been highlighted in a few studies. In a cohort study by Stein et al.,^[15] spleen sizes were compared in PMF patients with and without ASXL1 gene mutations, but no significant difference was found. Yonal-Hindilerden et al.'s^[9] study also found no significant difference in the presence of splenomegaly and spleen sizes between ET and PMF patients with and without ASXL1 gene mutations. Unfortunately, in our study, not all patients had ultrasound data for spleen sizes, so no conclusions could be drawn in this regard.

Our study found that the development of thrombosis was 1.66 times higher in patients with ASXL1 gene mutations compared to those without. The rate of arterial thrombosis was 66.7% and venous thrombosis was 33.3% in patients with ASXL1 gene mutations. In the mutation-negative group, the rates were 14.4% for arterial thrombosis and 20.6% for venous thrombosis. Few studies in the literature investigate the relationship between ASXL1 gene mutations and thrombosis. In a 2012 study by Brecqueville et al.,^[12] no significant difference was found in the development of thrombosis between patient groups with and without ASXL1 mutations. Similarly, in Yonal-Hindilerden et al.'s^[9] recent study, the rates of thrombosis development were similar between groups with and without ASXL1 mutations. In contrast, our study demonstrated higher rates of arterial thrombosis in the group with ASXL1 gene mutations.

The relationship between ASXL1 gene mutations and survival has been the subject of numerous studies. In a 2012 study by Brecqueville et al.,^[12] it was observed that in a group of 44 patients with PMF, those with ASXL1 gene mutations had a shorter 5-year survival rate compared to those without mutations (56% vs. 87%). A cohort study by Mayo Clinic involving 279 PMF patients found similar 5-year survival rates in groups with and without ASXL1 gene mutations.^[18] A 2012 study by Gelsi-Boyer et al.^[7] showed that patients with ASXL1 gene mutations had a worse prognosis. In an international study published in 2014 by Tefferi et al.,^[19] involving 570 PMF patients, the presence of ASXL1 gene mutations was identified as a poor prognostic factor. It was shown that patients with these mutations were older, had higher DIPSS-Plus scores, and significantly reduced survival. The same study also indicated that CALR type 1 mutations had a favorable prognostic impact. Based on these findings, Tefferi et al.^[19] suggested that ASXL1 and CALR gene mutations should be examined in all PMF patients and included in the DIPSS-Plus scoring. In a 2016 study by Alvarez Argote et al.,^[20] survival was also shorter in the presence of ASXL1 mutations in PMF. In our study, the av-

erage follow-up period for PMF patients is <5 years. All 9 PMF patients in our group are still under follow-up, with no cases of death or leukemic transformation. Therefore, it is not possible to comment on survival at this stage.

The association of ASXL1 gene mutations with hematologic malignancies other than MPN has been known since its first description in the literature. ASXL1 mutations in AML are predominantly associated with patients with secondary AML.^[20] A study of 40 patients with MDS/AML by Gelsi-Boyer et al.,^[16] conducted during genetic research, identified ASXL1 gene mutations. In this 2009 study, ASXL1 gene mutations were found in 4 out of 35 patients with MDS (11%) and 17 out of 39 patients with chronic myelomonocytic leukemia (43%). Another study by Carbuccioni reported ASXL1 gene mutations in 5 out of 64 patients with MPN (8%) and 11 out of 63 patients with AML (17%).^[13,21] In a 2010 study by Boulton et al.,^[22] ASXL1 gene mutations were detected in 5 out of 79 MDS patients (6%), 17 out of 55 patients with refractory anemia with excess blasts 1 (31%), and 17 out of 67 AML patients (25%).

It is known that in Ph(–) MPNs, conversion to acute leukemia may occur during follow-up in 1–5% of patients. However, the association between MPNs and non-hematologic cancers (solid tumors) is not well documented in the literature. None of the patients in our cohort transformed to acute leukemia, which could be attributed to the relatively short average follow-up time (4.66 years). On the other hand, in our cohort, 17 non-hematologic cancers (solid tumors) were identified in 15 patients (14.5%, 15/103), which is considerably higher than what might be expected in a normal population of the same age. The increased frequency of non-hematologic cancers can be explained by several hypotheses.

Firstly, it could be speculated that mutations associated with MPN might facilitate the development of other malignancies. When we examined the molecular characteristics of our patients who developed non-hematologic cancers, MPN mutations were found in all except two patients (12 with JAK-2 V617F mutations, one with a CALR mutation). Also in two patients, both JAK-2 V617F and ASXL1 c.1954G.a (p.G652S) mutations were detected. One of the patients with a diagnosis of non-hematologic cancer before the diagnosis of MPN had an ASXL1 c.1954G.a (p.G652S) mutation. These mutations are known to activate cell proliferation pathways, but current knowledge supports that they are somatic mutations occurring only in hematopoietic stem cells. Therefore, it seems unlikely that these mutations would induce malignant transformation in other cell lineages. There is no literature evidence that JAK-2 V617F and CALR mutations occur in non-hematologic cell lines. A study by Lee et al.^[23] that screened for JAK-2 V617F mutations in gastric cancers with activated JAK-STAT pathways found no positive cases.

The second possibility is the risk of developing secondary cancers due to drugs used in MPN treatment, particularly hydroxyurea. There is a significant amount of literature on the risk of secondary cancer development associated with hydroxyurea. One of the most significant studies in this regard is by Kissonva et al.,^[10] who investigated secondary cancer development in 172 Ph(–) MPN patients. In their study, 19.7% of the 66 patients treated with hydroxyurea developed secondary cancers, predominantly skin cancers (especially squamous cell carcinoma), which is a higher rate compared to those who used other cytoreductive treatments or did not use hydroxyurea. Another study by Hansen et al.,^[24] reported an increased risk of secondary malignancies in MPN patients treated with hydroxyurea compared with patients treated with IFN- α 2. In a study conducted by Mathur et al.^[25] in 2022, 10.2% of 324 MPN patients treated with hydroxyurea and 2% of 47 patients who did not receive hydroxyurea developed skin tumors during follow-up. In a 2020 study, Saliba et al.,^[26] was found that myelofibrosis is independently associated with an increased risk of non-hematologic malignancies. In our patient group, 7 patients had a history of malignancy before MPN diagnosis. Five patients developed non-hematologic cancers following MPN diagnosis and hydroxyurea treatment. Two patients developed secondary cancers after an MPN diagnosis without using hydroxyurea or another cytoreductive drug/IFN. These findings suggest that factors other than hydroxyurea may also contribute to the development of non-hematologic cancers in our patients. Further research involving larger patient groups is planned to continue exploring this issue.

Our finding of 14.5% non-hematologic cancer frequency is notably higher than the 6.6% secondary solid cancer rate reported by Hindilerden et al.^[27] in a recent multicenter Turkish study of 1013 Ph– MPN patients, though their study found similar associations with arterial thrombosis and potential protective effects of interferon-based therapy. Our finding that c.1934dupG (p.G646WfsX12) was the most common ASXL1 mutation (4/6 patients, 66.7%) is consistent with recent literature, as Yang et al.^[28] similarly identified G646WfsX12 as the most frequent amino acid change (47.06%) in their cohort of 34 ASXL1-mutated AML/MDS patients, and notably demonstrated that mutations in G646W were independently associated with worse prognosis (HR=4.302, 95% confidence interval: 1.150–16.097).

This study has several limitations that should be acknowledged. First, the small sample size, particularly in the PMF group (n=9) and overall ASXL1-positive cohort (n=6), limits statistical power and generalizability. Second, we screened only exon 12 of ASXL1, potentially missing mutations in other regions. Third, we did not assess ASXL1 mutation allele burden or perform tissue-specific analysis beyond peripheral blood. Fourth, potential confounding factors for non-hematologic

cancer development, including smoking history, environmental exposures, family history, and specific hydroxyurea dosing, were not collected. Finally, our follow-up period averaging 4.21 years may be insufficient to detect all long-term outcomes including leukemic transformation. Despite these limitations, our study provides valuable preliminary data on ASXL1 mutations in a Turkish MPN cohort and generates hypotheses for future research.

CONCLUSION

In this study focusing on Ph⁻ MPNs, ASXL1 gene mutations were screened, revealing several significant findings. ASXL1 gene mutations were detected in 6.25% of ET patients (3/48), 4.35% of PV patients (2/46), and 11.11% of PMF patients (1/9). The gender distribution among patients with these mutations was found to be equal, and patients with ASXL1 gene mutations tended to be older on average compared to those without. Furthermore, patients with ASXL1 gene mutations exhibited higher initial hemoglobin and platelet values but lower leukocyte and neutrophil values. Although not statistically significant splenomegaly rates were lower in patients with ASXL1 gene mutations, and the most common mutations identified were c.1934dupG (p.g646TrpfsX12) and c.1954G.a (p.G652S). Notably, thrombosis rates, particularly arterial thrombosis, were higher in the group with ASXL1 gene mutations.

In addition, a significant observation in our MPN cohort was the high rate of non-hematologic cancers (solid tumors), found in 14.5% of patients, with 80% of these patients carrying the JAK-2 V617F mutation. Intriguingly, two patients with JAK-2 V617F mutation also had ASXL1 gene mutations, both specifically the c.1954G.a (p.G652S) mutation. Similar to our study, a case report published by Liu et al.^[29] showed that JAK2 V617F mutation was associated with myeloproliferative, lymphoproliferative and solid neoplasms. The occurrence of non-hematologic cancers following hydroxyurea treatment in five patients initially diagnosed with MPN suggests a potential link between hydroxyurea use and the development of such cancers. However, the emergence of non-hematologic cancers in two patients who had not used hydroxyurea or other cytoreductive drugs post-MPN diagnosis indicates that factors other than hydroxyurea may also influence the development of non-hematologic cancers.

DECLARATIONS

Ethics Committee Approval: The study was approved by Istanbul Bilim University Ethics Committee (No: 44140529/2015-30, Date: 17/02/2015).

Informed Consent: Informed consent was obtained from the patients.

Conflict of Interest: The authors declare that there is no conflict of interest.

Funding: The study was supported by the Istanbul Bilim University Research Fund (Date: 25.03.2015, Number: 2015-01-17).

Use of AI for Writing Assistance: Not declared.

Authorship Contributions: Concept – NU; Design – VSH; Supervision – RDK; Fundings – RDK; Materials – VSH; Data collection &/or processing – NU; Analysis and/or interpretation – VSH; Literature search – NU; Writing – NU; Critical review – RDK.

Peer-review: Externally peer-reviewed.

REFERENCES

- Skoda RC, Duek A, Grisouard J. Pathogenesis of myeloproliferative neoplasms. *Exp Hematol* 2015;43:599–608.
- McMullin MF, Bareford D, Campbell P, Green AR, Harrison C, Hunt B, et al. Guidelines for the diagnosis, investigation and management of polycythaemia/erythrocytosis. *Br J Haematol* 2005;130:174–95.
- Can Turan. TET2 mutation in cases of essential thrombocythemia and primary myelofibrosis [specialization thesis]. Istanbul: Istanbul Science University; 2012.
- Fisher CL, Lee I, Bloyer S, Bozza S, Chevalier J, Dahl A, et al. Additional sex combs-like 1 belongs to the enhancer of trithorax and polycomb group and genetically interacts with Cbx2 in mice. *Dev Biol* 2010;337:9–15.
- Scheuermann JC, de Ayala Alonso AG, Oktaba K, Ly-Hartig N, McGinty RK, Fraterman S, et al. Histone H2A deubiquitinase activity of the Polycomb repressive complex PR-DUB. *Nature* 2010;465:24–7.
- Sauvageau M, Sauvageau G. Polycomb group proteins: Multi-faceted regulators of somatic stem cells and cancer. *Cell Stem Cell* 2010;7:299–313.
- Gelsi-Boyer V, Breckueville M, Devillier R, Murati A, Moziconacci MJ, Birnbaum D. Mutations in ASXL1 are associated with poor prognosis across the spectrum of malignant myeloid diseases. *J Hematol Oncol* 2012;5:12.
- Tefferi A, Vardiman JW. Classification and diagnosis of myeloproliferative neoplasms: The 2008 World Health Organization criteria and point-of-care diagnostic algorithms. *Leukemia* 2008;22:14–22.
- Yonal-Hindilerden I, Daglar-Aday A, Akadam-Teker B, Yilmaz C, Nalcaci M, Yavuz AS, et al. Prognostic significance of ASXL1, JAK2V617F mutations and JAK2V617F allele burden in Philadelphia-negative myeloproliferative neoplasms. *J Blood Med* 2015;6:157–75.
- Kissova J, Ovesna P, Penka M, Bulikova A, Kiss I. Second malignancies in philadelphia-negative myeloproliferative neoplasms-single-center experience. *Anticancer Res* 2014;34:2489–96.
- Passamonti F, Rumi E, Pietra D, Elena C, Boveri E, Arcaini L,

- et al. A prospective study of 338 patients with polycythemia vera: The impact of JAK2 (V617F) allele burden and leukocytosis on fibrotic or leukemic disease transformation and vascular complications. *Leukemia* 2010;24:1574–9.
12. Brecqueville M, Rey J, Bertucci F, Coppin E, Finetti P, Carbuccia N, et al. Mutation analysis of ASXL1, CBL, DNMT3A, IDH1, IDH2, JAK2, MPL, NF1, SF3B1, SUZ12, and TET2 in myeloproliferative neoplasms. *Genes Chromosomes Cancer* 2012;51:743–55.
13. Carbuccia N, Murati A, Trouplin V, Brecqueville M, Adélaïde J, Rey J, et al. Mutations of ASXL1 gene in myeloproliferative neoplasms. *Leukemia* 2009;23:2183–6.
14. Abdel-Wahab O, Pardanani A, Patel J, Wadleigh M, Lasho T, Heguy A, et al. Concomitant analysis of EZH2 and ASXL1 mutations in myelofibrosis, chronic myelomonocytic leukemia and blast-phase myeloproliferative neoplasms. *Leukemia* 2011;25:1200–2.
15. Stein BL, Williams DM, O’Keefe C, Rogers O, Ingersoll RG, Spivak JL, et al. Disruption of the ASXL1 gene is frequent in primary, post-essential thrombocythosis and post-polycythemia vera myelofibrosis, but not essential thrombocythosis or polycythemia vera: Analysis of molecular genetics and clinical phenotypes. *Haematologica* 2011;96:1462–9.
16. Gelsi-Boyer V, Trouplin V, Adélaïde J, Bonansea J, Cervera N, Carbuccia N, et al. Mutations of polycomb-associated gene ASXL1 in myelodysplastic syndromes and chronic myelomonocytic leukaemia. *Br J Haematol* 2009;145:788–800.
17. Tefferi A, Abdel-Wahab O, Cervantes F, Crispino JD, Finazzi G, Girodon F, et al. Mutations with epigenetic effects in myeloproliferative neoplasms and recent progress in treatment: Proceedings from the 5th International Post-ASH Symposium. *Blood Cancer J* 2011;1:e7.
18. Vannucchi AM, Lasho TL, Guglielmelli P, Biamonte F, Pardanani A, Pereira A, et al. Mutations and prognosis in primary myelofibrosis. *Leukemia* 2013;27:1861–9.
19. Tefferi A. Primary myelofibrosis: 2014 update on diagnosis, risk-stratification, and management. *Am J Hematol* 2014;89:915–25.
20. Alvarez Argote J, Dasanu CA. ASXL1 mutations in myeloid neoplasms: Pathogenetic considerations, impact on clinical outcomes and survival. *Curr Med Res Opin* 2018;34:757–63.
21. Carbuccia N, Trouplin V, Gelsi-Boyer V, Murati A, Rocquain J, Adélaïde J, et al. Mutual exclusion of ASXL1 and NPM1 mutations in a series of acute myeloid leukemias. *Leukemia* 2010;24:469–73.
22. Boultonwood J, Perry J, Pellagatti A, Fernandez-Mercado M, Fernandez-Santamaria C, Calasanz MJ, et al. Frequent mutation of the polycomb-associated gene ASXL1 in the myelodysplastic syndromes and in acute myeloid leukemia. *Leukemia* 2010;24:1062–5.
23. Lee IO, Kim JH, Choi YJ, Pillinger MH, Kim SY, Blaser MJ, et al. *Helicobacter pylori* CagA phosphorylation status determines the gp130-activated SHP2/ERK and JAK/STAT signal transduction pathways in gastric epithelial cells. *J Biol Chem* 2010;285:16042–50.
24. Hansen IO, Sørensen AL, Hasselbalch HC. Second malignancies in hydroxyurea and interferon-treated Philadelphia-negative myeloproliferative neoplasms. *Eur J Haematol* 2017;98:75–84.
25. Mathur A, Edman J, Liang L, Scott NW, Watson HG. Skin cancer in essential thrombocythemia and polycythemia vera patients treated with hydroxycarbamide. *EJHaem* 2022;3:1305–9.
26. Saliba W, Khudyakova M, Mishchenko E, Cohen S, Rennert G, Preis M. Association between myelofibrosis and risk of non-hematologic malignancies: A population-based retrospective cohort study. *Ann Hematol* 2020;99:1007–16.
27. Hindilerden F, Akay ÖN, Aksoy E, Dağlar-Aday A, Gültürk E, Nalçacı M, et al. Secondary solid cancers in patients with Philadelphia chromosome-negative myeloproliferative neoplasms: A multicenter study. *Turk J Haematol* 2024;41:246–55.
28. Yang L, Wei X, Gong Y. Prognosis and risk factors for ASXL1 mutations in patients with newly diagnosed acute myeloid leukemia and myelodysplastic syndrome. *Cancer Med* 2024;13:e6871.
29. Liu KG, Verma A, Derman O, Kornblum N, Janakiram M, Braunschweig I, Battini R. JAK2 V617F mutation, multiple hematologic and non-hematologic processes: An association? *Biomark Res* 2016;4:19.

Comparison of Titanium, Magnesium, and Polymer-based Cortical Screw Fixation for Fulkerson Tibial Tubercle Osteotomy: A Finite Element Analysis

Ali Levent,¹ Metin Yapti,² Huseyin Kursat Celik,³ Mehmet Baris Ertan,⁴ Ozkan Kose⁵

¹Department of Orthopedics and Traumatology, Metrolife Private Hospital, Şanlıurfa, Türkiye

²Department of Orthopedics and Traumatology, Health Sciences University Mehmet Akif İnan Education and Research Hospital, Şanlıurfa, Türkiye

³Department of Agricultural Machinery and Technology Engineering, Akdeniz University, Faculty of Agriculture, Antalya, Türkiye

⁴Department of Orthopedics and Traumatology, Private Medikum Hospital, Antalya, Türkiye

⁵Department of Orthopedics and Traumatology, Health Sciences University Antalya Training and Research Hospital, Antalya, Türkiye

ABSTRACT

Objective: To compare the biomechanical performance of titanium alloy (Titanium-Aluminum-Vanadium Alloy, Ti-6Al-4V), magnesium alloy (Magnesium-Yttrium-Rare Earth-Zirconium, MgYREZr), and polylactide (PLA) cortical screws in the fixation of Fulkerson tibial tubercle osteotomy (TTO) using finite element analysis (FEA).

Materials and Methods: A three-dimensional tibial model was created from computed tomography data of a 20-year-old male patient and simulated with a standardized Fulkerson osteotomy fixed using two bicortical screws. The screws were modeled using three different biomaterials. FEA simulations were performed under two loading conditions: 390 N (physiological gait) and 1654 N (worst-case scenario). Stress distribution (von Mises) and displacement were recorded for the osteotomy construct and screws.

Results: Under 390 N loading, Ti-6Al-4V screws demonstrated the highest mechanical resistance (max. stress: 123,830 MPa; displacement: 0.084 mm), followed by MgYREZr (95,172 MPa; 0.098 mm) and PLA (81,939 MPa; 0.219 mm). Under 1654 N loading, Ti-6Al-4V screws again showed superior performance (669,880 MPa; 0.333 mm), whereas MgYREZr (745,470 MPa; 0.407 mm) and PLA (339,720 MPa; 0.882 mm) showed increased stress and deformation, with PLA screws exhibiting the least mechanical stability.

Conclusion: Titanium screws demonstrated the highest mechanical reliability across both loading conditions, supporting their continued use in TTO, particularly in high-demand clinical scenarios. Although biodegradable materials, such as MgYREZr and PLA, offer theoretical advantages by eliminating the need for implant removal, their biomechanical performance remains inferior to titanium screws.

Keywords: Finite element analysis, Fulkerson osteotomy, Magnesium screw, Patellar instability, Polymer screw, Tibial tubercle osteotomy, Titanium screw

Cite this article as: Levent A, Yapti M, Celik HK, Ertan MB, Kose O. Comparison of Titanium, Magnesium, and Polymer-based Cortical Screw Fixation for Fulkerson Tibial Tubercle Osteotomy: A Finite Element Analysis. Eur Arch Med Res 2025;41(3):163–173.

Address for correspondence: Mehmet Baris Ertan, Department of Orthopedics and Traumatology, Private Medikum Hospital, Antalya, Türkiye

E-mail: mehmetbarisertan@gmail.com **ORCID ID:** 0000-0002-3783-7109

Submitted: 29.04.2025 **Revised:** 02.06.2025 **Accepted:** 17.06.2025 **Available Online:** 12.09.2025

European Archives of Medical Research – Available online at www.eurarchmedres.org

OPEN ACCESS This work is licensed under a Creative Commons Attribution-NonCommercial 4.0 International License.



INTRODUCTION

Anteromedialization of the tibial tubercle (TT), commonly referred to as the Fulkerson osteotomy (FO), is a well-established surgical technique for the management of recurrent patellofemoral instability (PFI), particularly in patients exhibiting increased lateralization of the TT.^[1,2] It is evident that reducing the quadriceps (Q) angle and improving patellar tracking within the trochlear groove (TG) effectively enhances joint biomechanics and patellofemoral congruity.^[3] A key indication for FO is an elevated TT–TG distance, typically assessed through axial imaging modalities, such as computed tomography (CT).^[4,5]

One of the major advantages of this technique is its ability to achieve simultaneous anteriorization and medialization of the TT, thereby allowing precise correction of patellar alignment and, when necessary, adjustment of patellar height. Despite these benefits, the procedure is associated with several potential complications, including tibial fracture, non-union, infection, limited post-operative range of motion, and implant-related irritation.^[6,7] Fixation is traditionally accomplished using metallic cortical screws, generally two or three, which provide compression and stability during the healing process.^[4] However, the limited soft tissue coverage over the TT often leads to hardware prominence and discomfort, particularly during kneeling. Such symptoms are a common reason for secondary implant removal, reported in a significant proportion of patients undergoing this procedure.^[5,8] Some authors have even advocated for routine screw removal regardless of the presence of symptoms, although this approach increases healthcare costs and exposes patients to additional surgical risks.^[8]

Bioabsorbable fixation systems have been investigated as alternatives to permanent metallic implants to address these issues. These materials gradually degrade and are replaced by native tissue, potentially eliminating the need for implant removal and avoiding complications, such as metal ion release and stress shielding.^[9–11] Magnesium alloys (Magnesium–Yttrium–Rare Earth–Zirconium, MgYREZr) and polymer-based materials have attracted particular attention due to their favorable biocompatibility and resorption characteristics among bioabsorbable options. Nonetheless, concerns remain regarding their mechanical integrity, especially in high-load environments, such as the extensor mechanism of the knee. Since the fixation construct must withstand substantial forces during the early post-operative period to allow safe mobilization and progressive weight-bearing, ensuring sufficient mechanical strength is critical for successful osteotomy healing.

Although the use of bioabsorbable screws is becoming more prevalent in various orthopedic applications, evidence regarding their performance in TT osteotomy (TTO) remains

limited. While previous studies have assessed the mechanical performance of various screw materials in orthopedic applications, none has directly compared titanium, magnesium, and polymer-based screws in the specific context of Fulkerson TTO using finite element modeling. The present study aims to address this gap by utilizing finite element modeling (FEM) to evaluate and compare the mechanical performance of these three screw types under simulated physiological loading conditions. This study uniquely provides a standardized finite element modeling approach to directly compare titanium, magnesium, and polymer-based screw fixation in TTO, allowing for objective assessment of their mechanical performance under both physiological and extreme loading conditions. We hypothesize that although biodegradable materials may offer clinical advantages by eliminating the need for hardware removal, their mechanical properties could be inferior to those of titanium screws, potentially limiting their effectiveness in high-demand fixation scenarios, such as TT osteotomies.

MATERIALS AND METHODS

Study Design

This study employed the finite element method (FEM) to investigate the behavior of screws composed of three distinct biomaterials when utilized to secure a FO under linear static loading conditions. The study pre-supposed that the materials used were homogeneous and isotropic, and it postulated that they would exhibit linear elastic behavior. Furthermore, the interactions among the various components within the model were regarded as non-linear. Within a standard FO model, screws manufactured from three materials (titanium, magnesium, and polymer) underwent testing under two distinct loading conditions. Ethical approval was not required because this finite element analysis (FEA) study was conducted virtually and involved no human or animal subjects.

Modeling of the FO

To create a realistic tibial model, we utilized a computerized tomography (CT) examination of a 20-year-old male with recurrent PFI. This individual had a height of 174 cm and weighed 76 kg. Notably, the patient exhibited excessive lateralization of the TT, with a TT–TG distance of 23 mm, indicating a potential need for a FO. The CT examination was conducted using a CT scanner (Siemens go. up, Siemens, Munich, Germany) at our university hospital. The specific scan parameters consisted of 232 axial slices captured at 120 kV, 30 mA, with a slice distance of 1.0 mm and a field of view spanning 218 mm, extending from the supracondylar femur to the proximal tibia. For modeling and simulating the FEA scenarios, we employed various software tools, including Materialise Mimics–Medical three-dimensional (3D) image-based engineering software (Materi-

alise NV, Belgium), SolidWorks parametric solid modeling software (Dassault Systems SolidWorks Corp, Waltham, USA), and Analysis System Software (FEA software) (ANSYS) Workbench FEA code (ANSYS, Ltd., Canonsburg, PA, USA).

The FO model was created based on previous descriptions.^[12] The osteotomy length was 72 mm, and the osteotomy plane was angled at 45° to the posterior condylar axis of the tibia. Both the upper and lower planes of the osteotomy were sloped. The fragment was shifted 10 mm toward the medial side. There was no gap between the fragments at the osteotomy plane. The model was secured using two 4.5 mm screws that were inserted parallel to each other in the sagittal plane and perpendicular to the posterior cortex of the tibia, as suggested in earlier studies. A bicortical fixation was performed (Fig. 1). Screws made of three different materials were used on the same model. The first screw model was made of titanium alloy (Titanium-Aluminum-Vanadium Alloy, Ti-6Al-4V), the second was a MgYREZr, and the third was polylactide (PLA) screws. The characteristics of the cortical screw (International Organization for Standardization/TC 150/SC 5, 1991) were as follows: A thread diameter of 4.5 mm, a thread pitch of 1.75 mm, a shaft diameter of 3.0 mm, and a head diameter of 8.0 mm. The upper screw was 48 mm in length, and the lower screw was 36 mm in length.

Boundary Conditions and Material Properties

The models were loaded with two different intensities of force. The first aimed to imitate ordinary walking, and the other aimed to imitate load to failure, which is the worst-case scenario. In previous studies, the typical maximal quadriceps force applied to the TT during the extension phase of the knee during walking is between 350 and 390 N. Davis et al.^[13] found that a TTO failure load fixed with two 4.5 mm cortical screws was 1654 N in a biomechanical study performed on fresh frozen cadavers. Thus, 390 N and 1654 N traction forces were applied to the patellar tendon footprint at the TT to each model, respectively (Fig. 2).

The proximal tibia was supported at the medial and lateral condyles, while the distal tibia was attached to the ground in an anatomical position. The force was applied to the patellar tendon footprint on the TT with a vectorial angle corresponding to the orientation of the patellar tendon fibers, which were analyzed and extracted from the CT data using the rendering technique. The 3D model specified the frictional contact (non-linear contact) between the screw-bone and bony fragment surfaces. In addition, bonded contact definitions were created between the cortical and trabecular bone. The screws were pre-loaded with 50 N, and prior studies found that the friction coefficients between bone and screw were 0.46 and 0.37, respectively (Table 1).^[14–18] The material characteristics

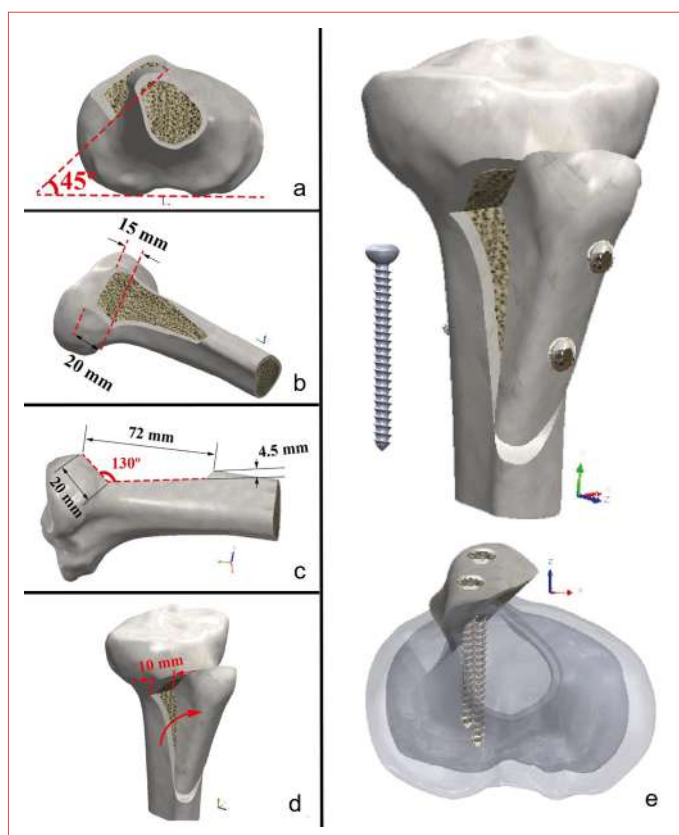


Figure 1. Three-dimensional finite element modeling of the Fulkerson tibial tubercle osteotomy. **(a)** Axial view showing the 45° osteotomy angle relative to the posterior condylar axis of the proximal tibia. **(b)** Sagittal view demonstrating the osteotomy dimensions: 15 mm anteriorization and 20 mm medialization. **(c)** Lateral view illustrating the osteotomy length (72 mm), cortical screw diameter (4.5 mm), and insertion angle (130° between screws). **(d)** Anteroposterior view showing the 10 mm medial translation of the osteotomized fragment. **(e)** Three-dimensional rendering of the final osteotomy model with two parallel bicortical screws inserted perpendicular to the posterior tibial cortex, used to simulate fixation with three different materials (titanium, magnesium alloy, and polymer).

for cortical and trabecular bone and the screws were allocated independently under the assumptions of the isotropic homogeneous linear elastic material model (Table 2).^[19–29]

Verification of Mesh Structure and Quality of the Models

The quality of a model's mesh structure has a significant impact on the accuracy of FEA simulations. One of the most important quality indicators for a mesh structure is the skewness metric, which indicates how closely a face or cell resembles an ideal one in a finite element model. The skewness values showed

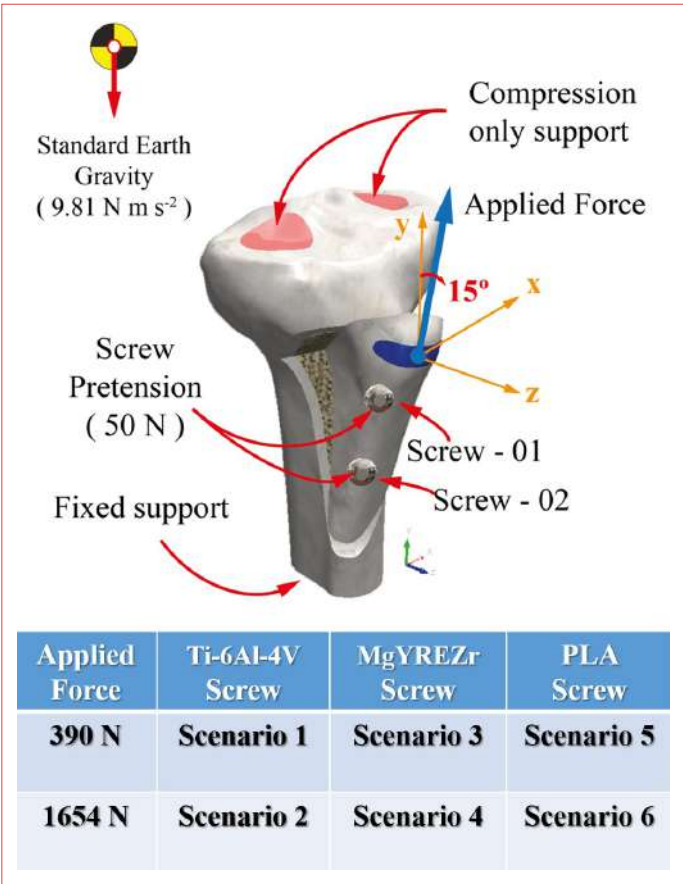


Figure 2. Boundary conditions and loading scenarios for finite element analysis. The tibial model was fixed distally and supported proximally to allow compression only. A 15° vectorial force simulating patellar tendon traction was applied to the tibial tubercle, with 50 N pretensions on both screws. Six simulation scenarios were created by combining two loading conditions (390 N and 1654 N) with three screw materials: Titanium alloy, magnesium alloy, and polylactide.

Table 1. Coefficients of friction and screw fixation pre-load assigned in the FEA setup

Coefficient of friction between	Bony parts and fixation screw	0.37
	Bony parts	0.46
Screw fixation pre-load (N)	50	

excellent mesh quality (average: 0.263) in all analyzed scenarios. The solid models’ final mesh structure was produced using a curvature-based meshing technique. An average of 1.4 million components and 2.1 million nodes were found for all solid models. A visual illustration of the models’ meshing is shown in Figure 3. Each simulation scenario was independently run with the same boundary conditions, and the resulting visual and numerical outputs were then recorded.

Assessment of Simulation Results

Calculations were made to determine the total deformation of the osteotomized fragment. The equivalent (von Mises) stress and total deformation distributions on the components were obtained using the simulation results.

RESULTS

All models have shown a similar displacement behavior. Loading of the models with patellar tendon traction force caused upward migration of the osteotomized TT fragment. Since the upper plane of the osteotomy was sloped, the TT fragment rested on the upper tibial surface. At this point, the top surface of the osteotomy fragment functioned as a fulcrum, and the distal portion of the TT fragment then started to separate from the tibia while the screws were resisting displacement. However, the screws underwent plastic deformation on the level of the lower plane of the osteotomy.

The finite element study compared the biomechanical performance of Ti-6Al-4V, MgYREZr, and PLA screws in the fixation of TTO under two loading conditions, 390 N and 1654 N. Under a

Table 2. Material properties assigned to the FEA model

Parameters	Unit	Model components				
		Cortical bone	Trabecular bone	Ti screws (Ti-6Al-4V)	Mg screw (MgYREZr)	Polymer screws (PLA)
Modulus of elasticity	(MPa)	19100	1000.61	115000	45000	3500
Poisson's ratio	(-)	0.30	0.30	0.33	0.29	0.36
Density	(kg m-3)	1980	830	4500	1840	1250

Ti-6Al-4V: Titanium alloy (Titanium-Aluminum-Vanadium Alloy); MgYREZr: Magnesium alloy (Magnesium-Yttrium-Rare Earth-Zirconium); PLA: Polylactide, FEA: Finite element analysis.

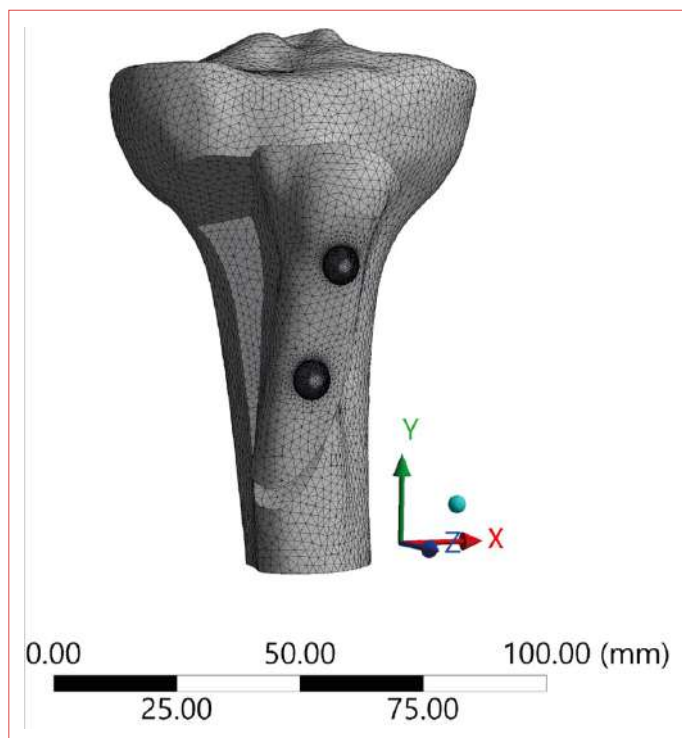


Figure 3. Mesh structure of the tibial tubercle osteotomy model. Curvature-based meshing generated a high-quality finite element mesh with excellent skewness metrics. The model includes approximately 1.4 million elements and 2.1 million nodes.

390 N loading, Ti-6Al-4V screws demonstrated the highest stress resistance, with a maximum equivalent stress of 123,830 Megapascal (MPa) in the screws and a resultant displacement of 0.084 mm in the entire model. MgYREZr screws exhibited a maximum stress of 95,172 MPa and a displacement of 0.098 mm, indicating less resistance compared to Ti-6Al-4V. PLA screws exhibited the lowest stress resistance, with a maximum stress of 81,939 MPa and the highest displacement of 0.219 mm, indicating that they may be the least suitable for high-load applications. Under 1654 N loading, Ti-6Al-4V screws still exhibited the highest stress resistance, with a maximum stress of 669,880 MPa and a displacement of 0.333 mm. MgYREZr screws had a max stress of 745,470 MPa and a displacement of 0.407 mm. PLA screws had a max stress of 339,720 MPa and the largest displacement of 0.882 mm. The data are presented in Table 3.

The visual outputs illustrate that all materials showed increased stress and displacement under higher loading, but the magnitude of change varied significantly across materials. Ti-6Al-4V screws remained the most robust, while PLA screws exhibited the greatest deformation, which may limit their clinical application in high-load-bearing situations (Figs 4 and 5).

DISCUSSION

This FEA revealed a distinct biomechanical stratification among titanium, magnesium, and polymer-based cortical screws utilized for fixation in Fulkerson TTO. Under moderate loading conditions (390 N), reflecting forces typically encountered during normal gait, titanium (Ti-6Al-4V) screws demonstrated superior mechanical behavior, characterized by minimal displacement and high stress resistance. This performance is likely attributable to the high yield strength and fatigue resistance of Ti-6Al-4V, which ensure reliable fixation during daily activities. The differences between materials became more pronounced under higher loading conditions (1654 N), simulating worst-case clinical scenarios, such as accidental falls or sudden high-impact events. While titanium screws maintained structural integrity across both loading conditions, MgYREZr screws exhibited intermediate mechanical performance, with greater deformation likely due to their lower elastic modulus. Polymer-based (PLA) screws, despite their favorable biocompatibility and biodegradability, showed the greatest displacement and lowest stress resistance, raising concerns about their suitability in settings requiring high mechanical stability. Interestingly, while titanium exhibited the highest stress resistance under physiological loading, magnesium showed higher peak stress under high-load conditions. This inversion likely reflects the distinct deformation behaviors and stress concentration points inherent to each material under increasing load, underscoring the non-linear response of MgYREZr in high-stress environments. These findings highlight the delicate balance between mechanical strength and biodegradability in implant selection, underscoring the continued use of titanium screws as the standard of care in patients with high functional demands following TTO.

These results are further supported by previous experimental and computational studies that have evaluated the mechanical performance of various implant materials in osteotomy fixation. In an *in vitro* biomechanical study, Partio et al.^[30] compared bioabsorbable and titanium screws for first tarsometatarsal joint arthrodesis and reported significantly higher yield and maximum failure loads for titanium screws, consistent with our findings that highlight the superior mechanical properties of titanium-based fixation systems. Despite demonstrating lower mechanical strength, the bioabsorbable screws were considered clinically sufficient in selected cases with lower mechanical demands, reflecting a similar trade-off observed in our analysis between strength and degradability. Complementary to these experimental results, Lee et al.^[31] utilized finite element modeling to compare titanium, MgYREZr, and polymer-based screws in sagittal split ramus osteotomy, concluding that titanium screws exhibited the highest stress resistance, while magnesium screws offered intermediate

Table 3. The finite element analysis outputs for stress distribution and displacement under two loading conditions (390 N and 1654 N)

Material	FEA outputs	Applied force: 390 N						
		Whole model	Proximal tibial fragment		Tibial tubercle fragment		Screws	
			Cortical	Trabecular	Cortical	Trabecular	Upper screw	Lower screw
Ti-6Al-4V	Max. eq. stress (MPa)	123,830	24,663	25,961	37,097	19,196	123,830	90,358
	Resultant displacement (mm)	0.084	-	-	-	-	0.067	0.054
MgYREZr	Max. eq. stress (MPa)	95,172	25,044	32,486	100,00	30,260	95,172	87,386
	Resultant displacement (mm)	0.098	-	-	-	-	0.082	0.064
PLA	Max. eq. stress (MPa)	81,939	23,114	74,473	56,138	60,778	81,939	59,977
	Resultant displacement (mm)	0.219	-	-	-	-	0.179	0.137
Material	FEA outputs	Applied force: 1654 N						
		Whole Model	Proximal tibial fragment		Tibial tubercle fragment		Screws	
			Cortical	Trabecular	Cortical	Trabecular	Upper screw	Lower screw
Ti-6Al-4V	Max. eq. stress (MPa)	669,880	102,860	149,290	124,550	104,600	669,880	539,520
	Resultant displacement (mm)	0,333	-	-	-	-	0.269	0.215
MgYREZr	Max. eq. stress (MPa)	745,470	101,350	186,510	158,180	162,360	745,470	353,970
	Resultant displacement (mm)	0.407	-	-	-	-	0.328	0.258
PLA	Max. eq. stress (MPa)	339,720	92,406	339,720	212,700	325,140	339,140	304,870
	Resultant displacement (mm)	0.882	-	-	-	-	0.728	0.562

Ti-6Al-4V: Titanium alloy (Titanium-Aluminum-Vanadium Alloy), MgYREZr: Magnesium alloy (Magnesium-Yttrium-Rare Earth-Zirconium), PLA: Polylactide, FEA: Finite element analysis.

stability superior to polymer screws. Their simulation results, which show minimal deformation of magnesium screws under functional loads and highlight the mechanical inferiority of polymer screws, align closely with the stratified performance outcomes identified in our study. Moreover, the work of Maninen et al.^[32] on PLA screw fixation in a high-strain olecranon osteotomy model demonstrated an increased failure rate for absorbable implants under high mechanical loads, reinforcing the observation that polymer-based fixation may not be suitable for load-bearing applications requiring substantial bio-mechanical stability. Together, these studies corroborate our FEA outcomes and strengthen the conclusion that titanium remains the most mechanically reliable material for TTO fixation. At the same time, biodegradable options, such as magnesium and polymer-based screws, require further optimization to meet the mechanical demands of high-stress clinical scenarios. Another important consideration is that bioabsorbable materials lose their mechanical strength gradually after im-

plantation. This progressive degradation poses a heightened risk of fixation failure, particularly in cases of delayed bone healing. In contrast, titanium screws maintain their initial bio-mechanical integrity over time, offering consistent mechanical support throughout the healing process.

To date, the available literature on the use of bioabsorbable screws in TTO remains limited, with only two clinical studies evaluating magnesium-based implants and a single cadaveric biomechanical study addressing PLA screws. Specifically, Ünal et al.^[8] and Delsmann et al.^[33] reported favorable clinical outcomes using magnesium screws for TT fixation, with successful union and no fixation failures observed during follow-up. However, in both studies, patients were managed with strict non-weight-bearing protocols for the first 6 weeks post-operatively, followed by gradual load progression. This suggests that reduced mechanical stress during the early healing phase may have contributed significantly to these positive outcomes. This approach contrasts with the me-

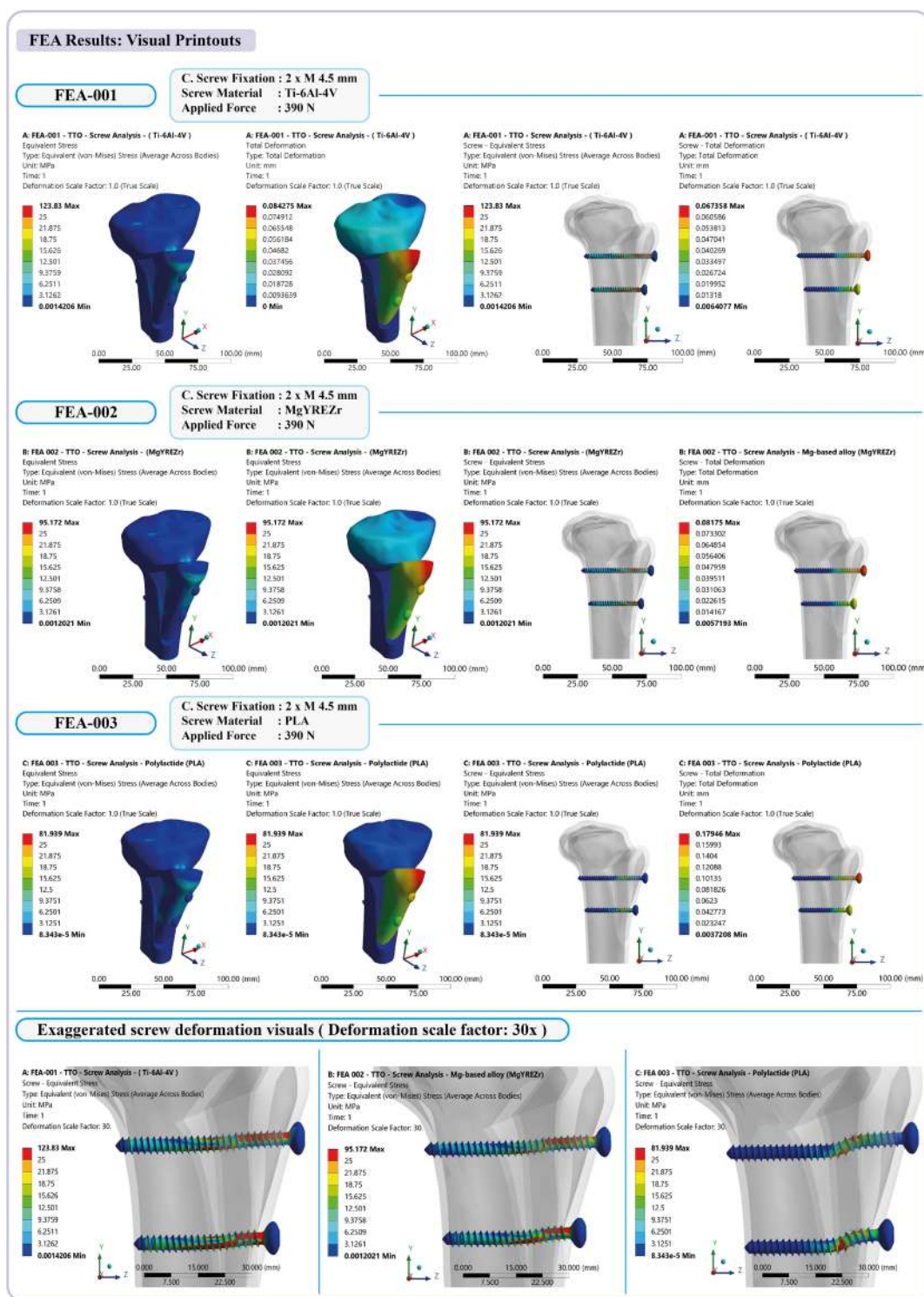


Figure 4. Finite element analysis results under physiological load (390 N). Stress distribution and deformation outputs for titanium alloy, magnesium alloy, and polylactide screws. The upper row shows von Mises stress, total deformation, and screw deformation (true scale), while the lower row presents screw deformation exaggerated 30x to visualize bending and displacement differences across materials

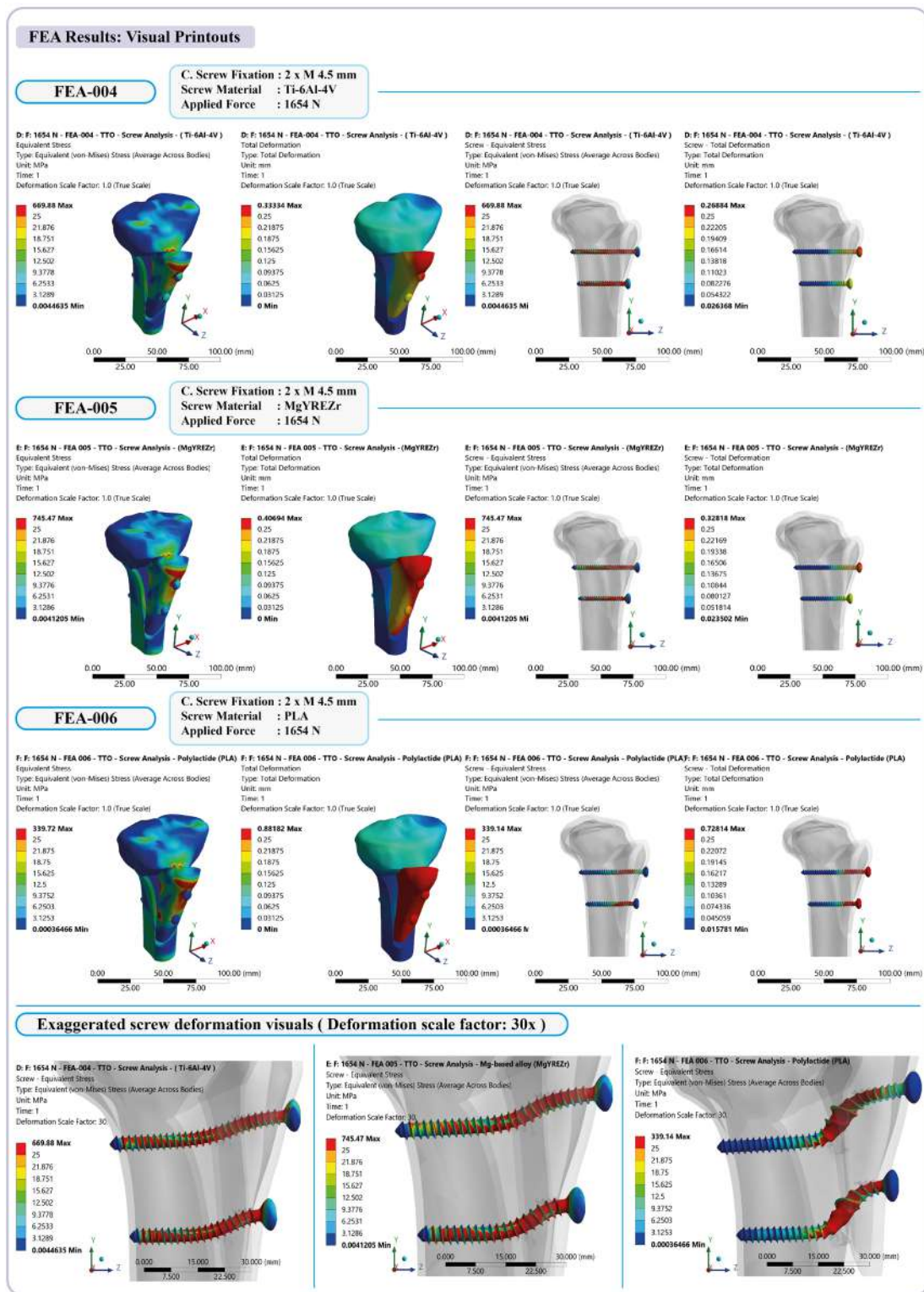


Figure 5. Finite element analysis results under high-load conditions (1654 N). Visual comparison of stress and deformation patterns for all three screw types under worst-case loading. As in Figure 4, top panels show actual stress and displacement fields, while bottom panels depict screw deformation at a 30x scale to highlight material behavior under elevated force.

chanical performance of titanium screws, which allow for earlier mobilization and weight-bearing due to their superior fixation strength. In addition to these clinical studies on magnesium, Nurmi et al.^[34] conducted the only biomechanical study on PLA screws in TT transfer, utilizing a cadaveric model without biological healing, where fixation strength was significantly lower for PLA screws compared to metallic screws (566 N vs. 984 N, respectively). It is essential to note that Nurmi et al.'s^[34] experimental design employed static loading in a single-screw configuration without proximal step-cut support, which limits the applicability of their findings to clinical practice, where two-screw fixation and dynamic biological processes are crucial. In contrast, the finite element modeling employed in the present study simulated both physiological loading and worst-case high-load scenarios, offering a more comprehensive assessment of implant behavior under varied mechanical demands. To the best of our knowledge, this study represents the first FEA evaluating bioabsorbable screw fixation in Fulkerson TTO, thereby filling a notable gap in the present literature. Given their reduced mechanical resistance, magnesium and polymer screws may be suitable for select patient populations, such as adolescents or individuals with low physical demands, or in scenarios that permit prolonged non-weight-bearing or partial weight-bearing rehabilitation protocols.

A key strength of this study is its standardized FEA-based methodology, which allows for a direct comparison of different biomaterials under consistent loading conditions. However, certain limitations should be acknowledged. As a computational model, the study does not replicate biological healing, bone remodeling, or soft tissue contributions, which are known to influence fixation stability in vivo. In addition, the assumption of isotropic, homogeneous, and linear elastic behavior for all materials, particularly for polymer-based materials, such as PLA, does not fully represent their real-world mechanical response. Moreover, the absence of cyclic or fatigue loading simulations limits the extrapolation of these results to long-term clinical behavior, particularly in scenarios where repetitive micro-loading could compromise fixation. Furthermore, although the direction of the patellar tendon force was derived from anatomical CT reconstruction, it was assumed to remain constant; however, in reality, this vector may vary with knee flexion angle, introducing additional clinical variability. Finally, although fixation with three screws is commonly used in clinical practice, only a two-screw model was analyzed in this study, limiting the exploration of potential reinforcement effects from additional screw fixation. Despite these limitations, the findings offer valuable biomechanical insight to support implant selection in TTO fixation.

CONCLUSION

This FEA demonstrated that titanium screws provide superior mechanical stability compared to magnesium alloy and polymer-based screws for TTO fixation. Although bioabsorbable screws offer the advantage of eliminating the need for secondary implant removal, their mechanical resistance remains inferior to that of titanium, particularly under high-load conditions where implant stability is crucial to prevent fixation failure. Although headless screw designs may help reduce implant-related symptoms and avoid hardware removal, this recommendation remains speculative, as such configurations were not included in the present FEA model. These findings support the continued use of titanium screws as the most reliable fixation option in scenarios where early weight-bearing and mechanical robustness are required, and highlight the need for future research to improve the performance of bioabsorbable implants for broader clinical applicability in TTO.

DECLARATIONS

Ethics Committee Approval: Ethical approval was not required because this finite element analysis (FEA) study was conducted virtually and involved no human or animal subjects.

Conflict of Interest: The authors declare that there is no conflict of interest.

Funding: The authors received no financial support for the research and/or authorship of this article.

Use of AI for Writing Assistance: Not declared.

Authorship Contributions: Concept – AL, OK, HKC, MY; Design – AL, OK, HKC, MY; Supervision – AL, OK; Data collection &/or processing – HKC, OK, MBE; Analysis and/or interpretation – OK, AL, MBE, HKC; Literature search – AL, OK, HKC, MY, MBE; Writing – AL, OK, HKC, MY, MBE; Critical review – AL, OK, HKC, MBE, MY.

Peer-review: Externally peer-reviewed.





REFERENCES

1. Lundeen A, Macalena J, Agel J, Arendt E. High incidence of complication following tibial tubercle surgery. *J ISAKOS* 2023;8:81–5.
2. Grimm NL, Lazarides AL, Amendola A. Tibial tubercle osteotomies: A review of a treatment for recurrent patellar instability. *Curr Rev Musculoskelet Med* 2018;11:266–71.
3. Luhmann SJ, Schoenecker PL, Dobbs MB, Gordon JE. Arthroscopic findings at the time of patellar realignment surgery in adolescents. *J Pediatr Orthop* 2007;27:493–8.
4. Ertan MB. Proximal migration of the femoral fixation anchor after medial patellofemoral ligament reconstruction in a skeletally immature patient: A case report. *Sports Traumatol Arthrosc* 2025;2:30–4.

5. Knapik DM, Kunze KN, Azua E, Vadhera A, Yanke AB, Chahla J. Radiographic and clinical outcomes after tibial tubercle osteotomy for the treatment of patella alta: A systematic review and meta-analysis. *Am J Sports Med* 2022;50:2042–51.
6. Yalcin S, Seals K, Joo P, Fulkerson JP, Farrow LD. Complications and radiographic outcomes of tibial tubercle osteotomy at minimum 5-year follow-up. *Orthop J Sports Med* 2024;12:23259671241278722.
7. Stokes DJ, Elrick BP, Carpenter ML, Raji Y, McQuivey KS, Sherman SL, et al. Tibial tubercle osteotomy: Indications, outcomes, and complications. *Curr Rev Musculoskelet Med* 2024;17:484–95.
8. Ünal M, Demirayak E, Ertan MB, Kilicaslan OF, Kose O. Bioabsorbable magnesium screw fixation for tibial tubercle osteotomy; a preliminary study. *Acta Biomed* 2022;92:e2021263.
9. Choo JT, Lai SHS, Tang CQY, Thevendran G. Magnesium-based bioabsorbable screw fixation for hallux valgus surgery - A suitable alternative to metallic implants. *Foot Ankle Surg* 2019;25:727–32.
10. Sahin A, Gulabi D, Buyukdogan H, Agar A, Kilic B, Mutlu I, et al. Is the magnesium screw as stable as the titanium screw in the fixation of first metatarsal distal chevron osteotomy? A comparative biomechanical study on sawbones models. *J Orthop Surg* 2021;29:23094990211056439.
11. Chang L, Luo Y, Li W, Liu F, Guo J, Dai B, et al. A comparative study on the effects of biodegradable high-purity magnesium screw and polymer screw for fixation in epiphyseal trabecular bone. *Regen Biomater* 2024;11:rbae095.
12. Fulkerson JP. Anteromedialization of the tibial tuberosity for patellofemoral malalignment. *Clin Orthop Relat Res* 1983;177:176–81.
13. Davis K, Caldwell P, Wayne J, Jiranek WA. Mechanical comparison of fixation techniques for the tibial tubercle osteotomy. *Clin Orthop Relat Res* 2000;380:241–9.
14. Gao X, Fraulob M, Haïat G. Biomechanical behaviours of the bone-implant interface: A review. *J R Soc Interface* 2019;16:20190259.
15. Hayes WC, Perren SM. Plate-bone friction in the compression fixation of fractures. *Clin Orthop Relat Res* 1972;89:236–40.
16. Eberle S, Gerber C, von Oldenburg G, Högel F, Augat P. A biomechanical evaluation of orthopaedic implants for hip fractures by finite element analysis and in-vitro tests. *Proc Inst Mech Eng H* 2010;224:1141–52.
17. Çelik T. Biomechanical evaluation of the screw preload values used in the plate placement for bone fractures. *Proc Inst Mech Eng H* 2021;235:141–7.
18. Zivic F, Mitrovic S, Grujovic N, Jovanovic Z, Dzunic D, Milenkovic S. Influence of 3D printing infill and printing direction on friction and wear of polylactic acid (PLA) under rotational sliding. *Trenie i Iznos* 2021;42:170–7. [Article in Russian]
19. Oldani C, Dominguez A. Titanium as a biomaterial for implants. In: Fokter SK, editor. *Recent advances in arthroplasty*. London: IntechOpen; 2012. p.149–62.
20. Alonso-Rasgado T, Jimenez-Cruz D, Karski M. 3-D computer modelling of malunited posterior malleolar fractures: Effect of fragment size and offset on ankle stability, contact pressure and pattern. *J Foot Ankle Res* 2017;10:13.
21. Dong XN, Acuna RL, Luo Q, Wang X. Orientation dependence of progressive post-yield behavior of human cortical bone in compression. *J Biomech* 2012;45:2829–34.
22. Wang X, Nyman J, Dong X, Leng H. *Fundamental biomechanics in bone tissue engineering*. San Rafael (CA): Morgan & Claypool Publishers; 2010.
23. Kim SH, Chang SH, Jung HJ. The finite element analysis of a fractured tibia applied by composite bone plates considering contact conditions and time-varying properties of curing tissues. *Compos Struct* 2010;92:2109–18.
24. Klekiel T, Będziński R. Finite element analysis of large deformation of articular cartilage in upper ankle joint of occupant in military vehicles during explosion. *Arch Metall Mater* 2015;60:2115–21.
25. Novitskaya E, Zin C, Chang N, Cory E, Chen P, D’Lima D, et al. Creep of trabecular bone from the human proximal tibia. *Mater Sci Eng C Mater Biol Appl* 2014;40:219–27.
26. Daniels AU, Chang MK, Andriano KP. Mechanical properties of biodegradable polymers and composites proposed for internal fixation of bone. *J Appl Biomater* 1990;1:57–78.
27. Antoniac I, Miculescu M, Mănescu Păltânea V, Stere A, Quan PH, Păltânea G, et al. Magnesium-based alloys used in orthopedic surgery. *Materials* 2022;15:1148.
28. Zhang P, Hu Z, Xie H, Lee GH, Lee CH. Friction and wear characteristics of polylactic acid (PLA) for 3D printing under reciprocating sliding condition. *Ind Lubr Tribol* 2020;72:533–9.
29. Farah S, Anderson DG, Langer R. Physical and mechanical properties of PLA, and their functions in widespread applications - A comprehensive review. *Adv Drug Deliv Rev* 2016;107:367–92.
30. Partio N, Mattila VM, Mäenpää H. Bioabsorbable vs. titanium screws for first tarsometatarsal joint arthrodesis: An in-vitro study. *J Clin Orthop Trauma* 2020;11:448–52.
31. Lee JH, Han HS, Kim YC, Lee JY, Lee BK. Stability of biodegradable metal (Mg-Ca-Zn alloy) screws compared with

- absorbable polymer and titanium screws for sagittal split ramus osteotomy of the mandible using the finite element analysis model. *J Craniomaxillofac Surg* 2017;45:1639–46.
32. Manninen MJ, Päiväranta U, Taurio R, Törmälä P, Suuronen R, Räihä J, et al. Polylactide screws in the fixation of olecranon osteotomies. A mechanical study in sheep. *Acta Orthop Scand* 1992;63:437–42.
33. Delsmann MM, Stürznickel J, Kertai M, Stücker R, Rolvien T, Rupprecht M. Radiolucent zones of biodegradable magnesium-based screws in children and adolescents-a radiographic analysis. *Arch Orthop Trauma Surg* 2023;143:2297–305.
34. Nurmi JT, Itälä A, Sihvonen R, Sillanpää P, Kannus P, Sievänen H, et al. Bioabsorbable versus metal screw in the fixation of tibial tubercle transfer: A cadaveric biomechanical study. *Orthop J Sports Med* 2017;5:2325967117714433.

Clinicopathological, Cytological, and Immunocytochemical Characteristics of 17 Schwannoma Cases Diagnosed by Fine-Needle Aspiration Cytology

 Burcu Ozcan,¹  Senay Erdogan Durmus,²  Zeynep Betul Erdem,³  Merve Cin¹

¹Department of Pathology, University of Health Sciences, Istanbul Training and Research Hospital, Istanbul, Türkiye

²Division of Cytopathology, Department of Pathology, University of Health Sciences, Izmir City Hospital, Izmir, Türkiye

³Department of Pathology, Leiden University Medical Center, Leiden, Netherlands

ABSTRACT

Objective: Schwannomas are benign tumors that originate from Schwann cells of the nerve sheath. Fine-needle aspiration cytology (FNAC) is a valuable tool for the pre-operative diagnosis of schwannomas, especially in locations where surgical resection is associated with significant morbidity. In this study, we aimed to identify the clinical, cytological, and immunohistochemical features of 17 schwannoma cases diagnosed by FNAC and to compare our findings with previously published case series in the literature.

Materials and Methods: We retrospectively reviewed 17 cytological specimens from patients with a cytological diagnosis of schwannoma between 2019 and 2024. The clinical data of the patients were retrieved from the hospital information management system. The cases were re-evaluated based on their cytological features.

Results: Of these patients, 10 were female and 7 were male. The patients' ages ranged from 36 to 78 years (mean 54 years). Four cases were hypercellular, seven showed moderate cellularity, and six were hypocellular. In all the cases, the cells formed cohesive fragments. All nuclei exhibited tapering ends and appeared wavy, hook-like, or comma-shaped. All cases displayed filamentous cytoplasmic extensions and syncytium-like clusters. Immunocytochemical evaluation was performed in all but two cases. S100 staining was strong in 14 cases and moderate in one. Sox10 was positive in five cases.

Conclusion: The diagnostic assessment of schwannomas integrates clinical evaluation, imaging, and cyto-histological analysis. FNAC facilitates preoperative planning by characterizing the lesion. Characteristic cytological findings include spindle cell clusters, nuclear palisading, Verocay bodies, and a fibrillary background.

Keywords: Cytological features, Fine-needle aspiration cytology, Schwannoma

Cite this article as: Ozcan B, Erdogan Durmus S, Erdem ZB, Cin M. Clinicopathological, Cytological, and Immunocytochemical Characteristics of 17 Schwannoma Cases Diagnosed by Fine-Needle Aspiration Cytology. Eur Arch Med Res 2025;41(3):174–182.

INTRODUCTION

Schwannomas, also known as neurilemmomas, are benign, typically slow-growing tumors that originate from Schwann cells of the nerve sheath.^[1,2] These tumors are typically benign,

solitary, slow-growing, and well-encapsulated.^[2-5] Schwannomas can occur throughout the body but are commonly found in the head-and-neck region.^[1] They may arise from cranial nerves, spinal nerve roots, or peripheral nerves.^[2,3,6,7] The pre-

Address for correspondence: Burcu Ozcan, Department of Pathology, University of Health Sciences, Istanbul Training and Research Hospital, Istanbul, Türkiye

E-mail: drburcuozcan@yahoo.com **ORCID ID:** 0000-0002-7662-3306

Submitted: 23.05.2025 **Revised:** 19.06.2025 **Accepted:** 07.07.2025 **Available Online:** 12.09.2025

European Archives of Medical Research – Available online at www.eurarchmedres.org

OPEN ACCESS This work is licensed under a Creative Commons Attribution-NonCommercial 4.0 International License.



cise etiology of schwannomas remains unclear, although some cases are associated with genetic syndromes such as neurofibromatosis type 2 (NF2).^[6] In the early phase, schwannomas generally lack pathognomonic symptoms, with the majority of cases presenting as painless, palpable, solitary masses. In advanced stages, clinical manifestations may include neurological deficits and symptoms related to compression or obstruction.^[5]

Fine-needle aspiration cytology (FNAC) is a valuable tool for the preoperative assessment of schwannomas,^[5,8] especially in locations where surgical resection is associated with significant morbidity.^[9,10] FNAC can help differentiate schwannomas from other lesions, guiding clinical management and surgical planning.^[8,9] However, it is essential to recognize the limitations of FNAC, as the cytomorphological features of schwannomas can overlap with those of other spindle cell tumors, potentially leading to diagnostic challenges.^[11] In some instances, FNAC may be inconclusive, necessitating further investigation, such as trucut biopsy or imaging studies.^[12]

Histologically, schwannomas exhibit two distinct patterns. Antoni A areas consist of compact, elongated cells with cytoplasmic extensions arranged in interlacing fascicles and contain Verocay bodies, typically found in regions of high cellularity with a minimal stromal matrix. The Antoni B areas, on the other hand, are hypocellular, featuring loosely distributed nuclei. Cystic degeneration and localized necrosis may also be encountered.^[13]

The cytological features of schwannomas typically reflect their histological architecture, which is characterized by alternating areas of high and low cellularity known as Antoni A and Antoni B areas, respectively.^[14] In cytological smears, these areas manifest as fragments of tightly cohesive fascicles with variable cellularity, corresponding to Antoni A areas, and scattered spindle cells against a myxoid background, representing Antoni B areas.^[14,15] The presence of fibrillary stroma, consisting of delicate, wispy strands of collagen, is also a common finding,^[11,16] contributing to the overall cytomorphological picture. Tumor cells usually have fusiform nuclei, fine chromatin, and an indistinct cytoplasm.^[17] Nuclear palisading, a characteristic arrangement of nuclei in parallel rows, can be observed in some cases.^[16,17] Verocay bodies, which are acellular areas surrounded by palisaded nuclei, are considered a hallmark of schwannomas but are not always present in cytological specimens. The absence of Verocay bodies does not exclude the diagnosis of schwannoma, especially in certain variants, such as ancient schwannomas.^[16]

However, the cytological diagnosis of schwannoma is not always straightforward.^[11] Several factors can contribute to diagnostic challenges, including cystic degeneration, hyaline

changes, and degenerative atypia.^[4,18] Cystic degeneration can result in poor cellularity of the aspirate, making it difficult to identify the characteristic cytomorphological features,^[4] whereas degenerative atypia, seen in ancient schwannomas, can mimic malignancy.^[18]

To improve the accuracy of cytological diagnosis, ancillary techniques such as immunohistochemistry can be employed. Schwannomas typically show strong and diffuse positivity for the S100 protein, a marker of neural crest origin.^[6,19] This immunohistochemical feature can help differentiate schwannomas from other spindle cell lesions that are negative for the S100 protein.^[20]

In this study, we aimed to identify the clinical, cytological, and immunohistochemical features of 17 schwannoma cases diagnosed by FNAC and to compare our findings with previously published case series in the literature.

MATERIALS AND METHODS

A retrospective search of the pathology report information system using the keywords “spindle cell” between 2019 and 2025 identified 59 cases diagnosed with “spindle cell proliferation,” “proliferating spindle cells,” “spindle cell tumorous lesion,” and “spindle cell mesenchymal tumor” based on FNAC results. Cases those with other spindle cell tumors, and where slides were unavailable in the archive, were excluded, resulting in a series of 17 cases (28%). Sixteen of these cases were reported as spindle cell mesenchymal neoplasms, with a note that the lesion could be a schwannoma. One case was reported as “spindle cells on a fibrinous background” due to cell scarcity, with schwannoma being the primary differential diagnosis.

All samples were obtained by FNAC performed by a radiologist using 23–25-gauge needles. The clinical and demographic data of the cases were obtained from pathology reports. Each patient had conventional smear preparations, liquid-based cytology slides, and cell blocks in available materials. Air-dried smears were stained with May-Grünwald-Giemsa, whereas alcohol-fixed smears were stained using Papanicolaou staining. Immunohistochemical analysis was performed for diagnostic purposes and was not repeated in the present study. All slides of cases retrieved from archives and re-evaluated for cytomorphological characteristics. Each case was assessed for cellularity, presence of large cohesive tissue fragments, nuclear shape, nuclear palisading, and presence of filamentous cytoplasm.

The cases were re-evaluated based on their cytological features (cellularity, architecture, nuclear shape, pleomorphism, and cytoplasmic features). The histopathological follow-up was noted in available cases.

Statistical Analysis

Data analysis performed using the Statistical Package for the Social Sciences 25.0 program. Descriptive statistics for the evaluation of results were shown in the form of mean, and the nominal variables were shown as the number of cases and (%).

Ethical Approval

This study was approved by the İstanbul Training and Research Hospital Clinical Research Ethics Committee (Number: 107, Date: May 02, 2025) and was conducted under the principles of the Helsinki Declaration.

RESULTS

Of these patients, 10 were female and 7 were male. The patients’ ages ranged from 36 to 78 years (mean 54 years). The clinical features of the patients are summarized in (Table 1). In the cytological evaluation, each case was assessed for cellularity, presence of large cohesive tissue fragments, nuclear shape, nuclear palisading, and presence of filamentous cytoplasm.

The cytologic features of the patients are summarized in (Table 2). Four cases were hypercellular (23.5%), seven showed moderate cellularity (41.2%), and six were hypocellular (35.3%). In all the cases, the cells formed cohesive fragments (100%) (Figs 1–4). In 12 cases (70.5%), the tumor cells were also observed to be singly dispersed in the background. All nuclei exhibited ta-

pering ends and appeared wavy, hook-like, or comma-shaped (Figs 1–5).

In one case (5.8%), cells with relatively larger nuclei were present; however, the nuclei still showed tapered ends and fine chromatin structures, similar to the other cases. Nuclear palisading, cellular Antoni A, and hypocellular Antoni B areas were prominent in only two cases (11.7%). No prominent nucleoli were observed in any of the cases.

All cases displayed filamentous cytoplasmic extensions and syncytium-like clusters, with indistinct cytoplasmic borders (Figs 2–4). Mitosis was not observed in any of the cases. Immunocytochemical evaluation was performed in all but two cases. The cell blocks in the two cases did not contain sufficient material for further analysis. In these cases, immunohistochemical analysis was performed on the excised specimens.

S100 staining was strong in 14 cases (82%) and moderate in one (Fig. 6). Sox10 was positive in five cases (29%). No desmin, SMA, or CD34 staining was observed.

The excision materials of seven cases were also examined to confirm the diagnosis of schwannoma. One case was followed up clinically, as the patient did not consent to surgery. Clinical follow-up information was not available for the remaining nine cases.

Table 1. Clinicopathological and immunohistochemical characteristics of 17 schwannoma cases					
Case number	Age	Sex	Localization	Tumor size (cm)	Immunohistochemistry
1	77	Female	Neck	1.8	S100 + Desmin - CD34 - Ki67 <%1
2	56	Female	Neck	2.8	None
3	49	Female	Axilla	3	S100 + Desmin - SMA - CD34 - Ki67 %1
4	36	Male	Neck	3.9	S100 + CD34 -
5	44	Female	Neck	4.5	S100 + SMA - Desmin - Ki67 %2–3
6	61	Male	Neck	1.6	S100 + SMA - CD34 - Desmin -
7	36	Female	Preauricular	4.5	S100 + Desmin -
8	70	Female	Trunk	4.5	S100 + Sox10 + Desmin - CD117 - SMA - CD34 - Ki67 %1
9	59	Female	Trunk	3	S100 + Sox10 + SMA - Desmin - CD117 - DOG1 - CD34 - Ki67 %2–3
10	46	Female	Neck	2.5	S100 + Sox10 + SMA - Desmin - CD34 - Ki67: %2–3
11	47	Male	Leg	2	S100 + SMA - CD34 - Ki67 %1
12	55	Female	Trunk	4	S100 + SMA - CD34 - Ki67 %1
13	52	Male	Neck	2.7	S100 + SMA - Desmin - CD34 - Ki67 %1
14	50	Male	Axilla	1.4	Sox10 + S100 + CD34 - SMA - Desmin - Ki67%1
15	78	Female	Neck	2.1	S100 + CD68 - SMA -
16	49	Male	Neck	5.5	S100 + Sox10 + SMA - CD34 - Ki67 %1–2
17	56	Male	Neck	2	None

Cases indicated as “None” did not undergo immunohistochemical analysis.

Table 2. Cytological features of fine-needle aspiration samples in 17 schwannoma cases

Case number	Cellularity	Cohesive fragments	Wavy, hook-like nuclei	Palisading cells	Filamentous cytoplasm
1	Hypercellular	Yes	Yes	No	Yes
2	Moderate	Yes	Yes	No	Yes
3	Moderate	Yes	Yes	No	Yes
4	Hypercellular	Yes	Yes	Yes	Yes
5	Hypocellular	Yes	Yes	No	Yes
6	Moderate	Yes	Yes	No	Yes
7	Hypocellular	Yes	Yes	No	Yes
8	Hypocellular	Yes	Yes	No	Yes
9	Hypocellular	Yes	Yes	No	Yes
10	Hypercellular	Yes	Yes	Yes	Yes
11	Hypercellular	Yes	Yes	No	Yes
12	Moderate	Yes	Yes	No	Yes
13	Hypocellular	Yes	Yes	No	Yes
14	Moderate	Yes	Yes	No	Yes
15	Hypocellular	Yes	Yes	No	Yes
16	Moderate	Yes	Yes	No	Yes
17	Moderate	Yes	Yes	No	Yes

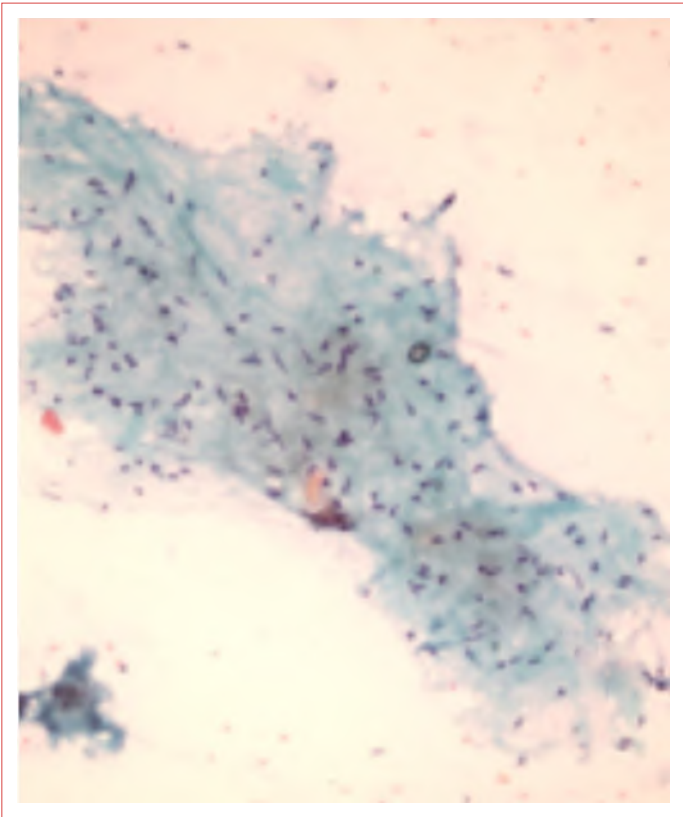


Figure 1. Spindle-like tumoral cells forming a cohesive fragment (Papanicolaou ×200).

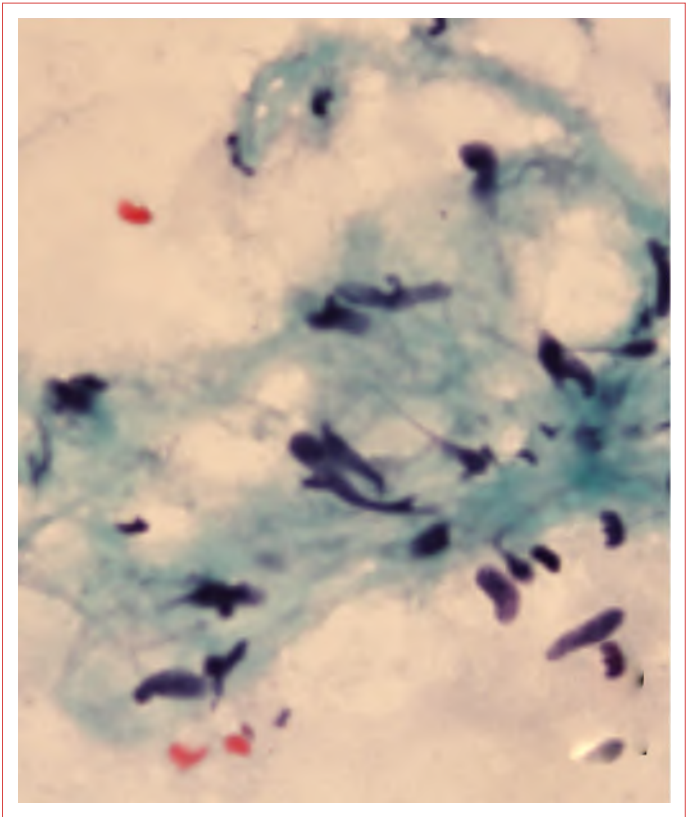


Figure 2. Fibrillar cytoplasmic extensions (Papanicolaou ×1000).

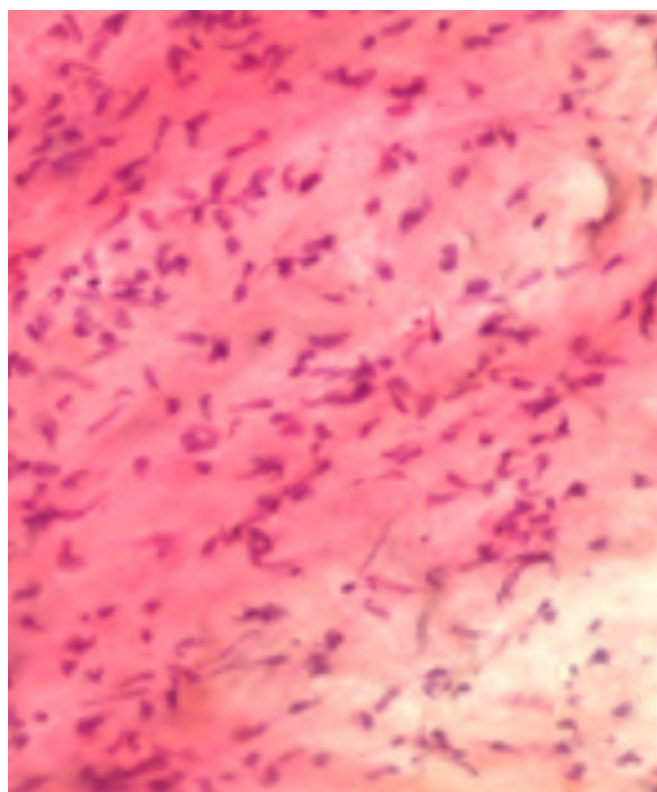


Figure 3. Cells with spindle-like nuclei in cohesive fragments (Papanicolaou ×400).

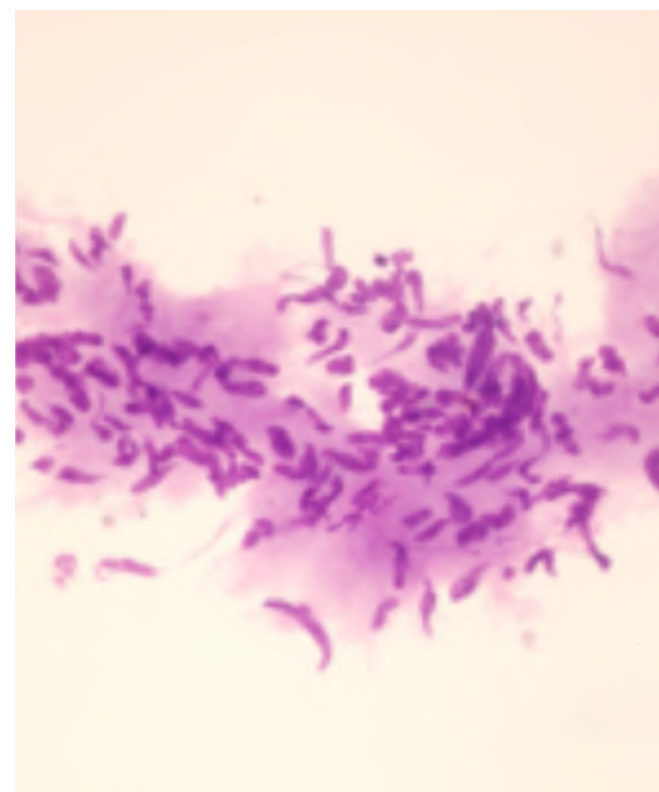


Figure 4. Wave and comma-shaped pointed nuclei (May-Grünwald-Giemsa ×400).

DISCUSSION

Schwannomas are benign, typically slow-growing tumors that originate from Schwann cells, which are specialized cells that form myelin sheaths around nerve fibers in the peripheral nervous system.^[21,22] Schwannomas are more frequently seen in adults, with the highest incidence occurring between the ages of 25 and 55.^[1] There is no preference for sex.^[1,3] In our study, the patients' age ranged from 36 to 78 years, with a mean age of 54. Although the difference was not significant, the majority of the patients were female (10 out of 17).

These tumors are generally solitary masses that can occur anywhere in the body where nerve tissue is present, although they are more commonly found in the head, neck, and extremities.^[3] Most of our cases (11/17) were located in the head-and-neck region, similar to previous reports. Three cases involved the extremities (two in the axilla and one in the thigh), while the remaining three involved the trunk.

The encapsulation of these tumors often contributes to their slow growth and can make early detection challenging, as they may not cause noticeable symptoms until they become large enough to compress the surrounding tissues or nerves.

^[3,23] In our cases, lesion sizes ranged from 1.4 cm to 5.5 cm, with a mean diameter of 3.04 cm.

The etiology of schwannomas is not fully understood, but they are generally considered to be sporadic occurrences, meaning that they arise without a clear hereditary pattern. However, they can be associated with certain genetic conditions such as NF2.^[24] None of our patients had an NF2 mutation.

Schwannomas typically exhibit a cellular composition dominated by spindle-shaped cells, which are elongated with tapered ends and oval nuclei. These cells are derived from Schwann cells, which are myelin-producing cells in the peripheral nervous system. Spindle cells are arranged in cohesive fascicles and clusters, forming a characteristic pattern that is helpful in distinguishing schwannomas from other spindle cell lesions.^[16,23] In our case series, four cases were hypercellular, seven exhibited moderate cellularity, and six were hypocellular. In all cases, the cells formed cohesive fragments. In addition to the features described in the literature, singly dispersed tumor cells in the background were observed in 12 cases.

Nuclear palisading, a distinctive feature of schwannomas, is observed in some cases in addition to their diagnostic

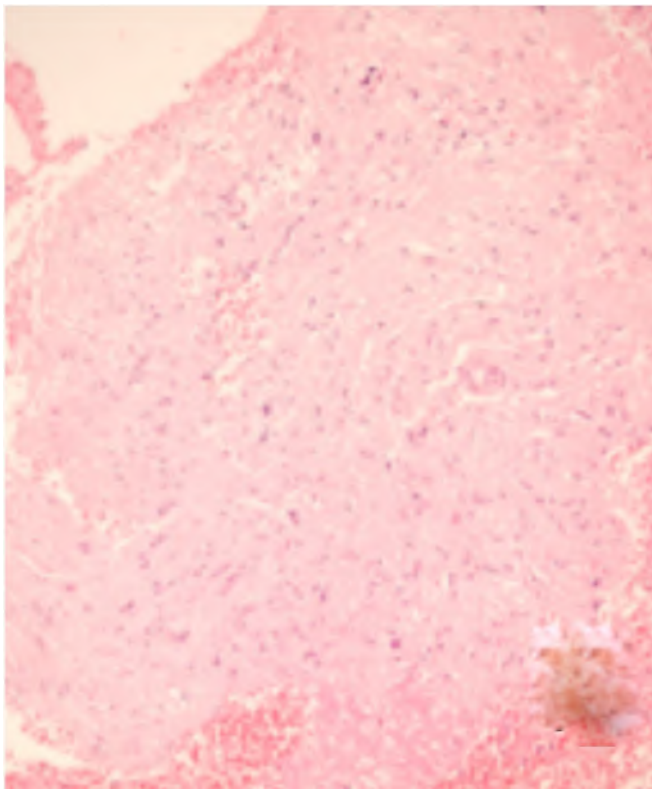


Figure 5. Fragment of spindle-like cells in cell block section (HE $\times 200$).

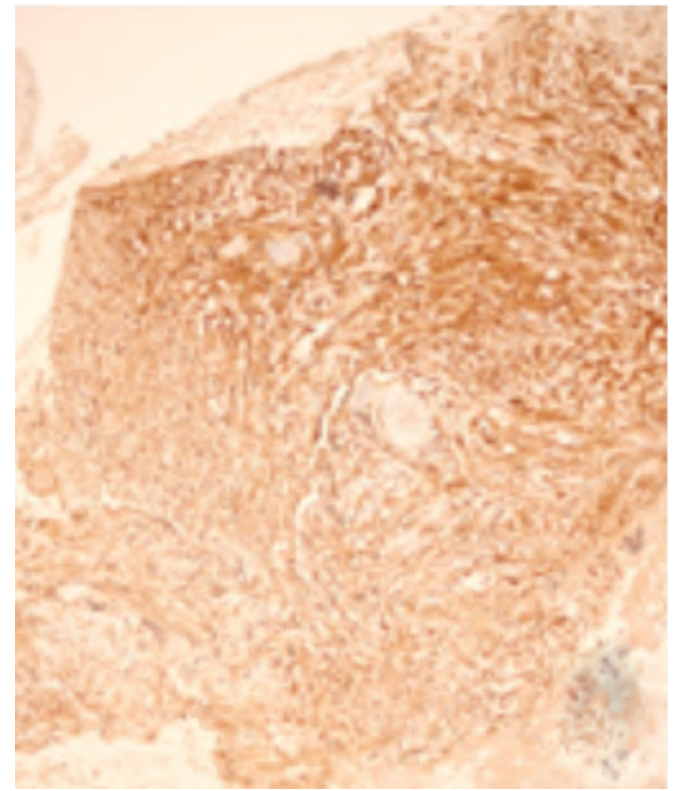


Figure 6. Tumoral cells stained with S100 ($\times 200$).

uniqueness. Nuclear palisading refers to the alignment of nuclei in parallel rows, which creates a pick fence-like appearance. This feature is particularly prominent in areas of high cellularity and is thought to be due to the tendency of Schwann cells to align along the nerve fibers. Although nuclear palisading is not entirely specific to schwannomas, its presence can be a helpful clue in the diagnosis, especially when combined with other cytological features.^[23,25] Alternating cellular (Antoni A) and hypocellular (Antoni B) areas are the characteristic histological features of schwannomas, reflecting the variable density of cells and stromal components within the tumor. Antoni A areas are characterized by high cellularity with densely packed spindle cells arranged in fascicles and clusters. Nuclear palisading and Verocay bodies were often prominent in these areas. Antoni B areas, on the other hand, are characterized by low cellularity with loosely arranged spindle cells embedded in a myxoid or edematous stroma. These areas may contain scattered lymphocytes, histiocytes, or mast cells. The presence of both Antoni A and Antoni B areas is a hallmark of schwannomas and is helpful in distinguishing them from other spindle cell lesions that may exhibit more uniform cellularity.^[5,17]

Unlike previous studies, nuclear palisading and Antoni A and B areas, which would suggest schwannoma, were observed in only two of our cases (2/17). This was thought to be related to the fact that the majority of cases had medium or hypocellular smears, and the sampling did not reflect these areas of the tumor.

Schwannoma cells are characterized by oval or elongated nuclei with pointed ends and indistinct cytoplasmic borders. The nuclei were typically uniform in size and shape, with finely granular chromatin and inconspicuous nucleoli. The nuclear contours may be smooth or slightly irregular, but marked pleomorphism or atypia is usually absent, except in certain variants, such as ancient schwannomas. The indistinct cell borders reflect the syncytial nature of Schwann cells, which are closely apposed to each other without clear cytoplasmic boundaries.^[15,16] In our cases, all the nuclei exhibited tapering tips and appeared wavy, hook-like, or comma-shaped. In one case, cells with relatively larger nuclei were present; however, the nuclei still showed tapered tips and fine chromatin structures, similar to other cases. Syncytium-like clusters with filamentous cytoplasmic extensions and indistinct cytoplasmic borders were observed in all the cases.

Nuclear enlargement and pleomorphism can be observed, especially in ancient schwannomas, potentially leading to misdiagnosis. In ancient schwannomas, degenerative changes resulted in nuclear enlargement, hyperchromasia (increased staining intensity), and irregular nuclear contours, mimicking the features of malignant tumors. However, the presence of other degenerative features, such as cystic degeneration, hyalinization, and hemorrhage, should raise suspicion of an ancient schwannoma rather than a malignant tumor.^[17,18]

A myxoid background may be observed, particularly in areas of cystic degeneration, in addition to the complexity of schwannoma stromal characteristics.^[16,26] A myxoid background was not observed in any of the cases.

Verocay bodies, representing areas of nuclear palisading with associated acellular zones, are a diagnostic clue for schwannomas.^[23,27] Verocay bodies are distinctive structures consisting of parallel rows of nuclei (nuclear palisading) alternating with zones of eosinophilic and acellular material. These are thought to represent areas of basement membrane deposition and collagen accumulation. Verocay bodies are not always present in schwannoma aspirates, but when they are observed, they are highly suggestive of the diagnosis. Verocay bodies were not observed in any case.

Schwannomas typically exhibit strong and diffuse immunoreactivity for S100 protein, a marker of neural crest origin.^[17,19,28] This immunohistochemical feature can help differentiate schwannomas from other spindle cell lesions that are S100 negative.^[17,20] Sox10 is a reliable marker of neural crest differentiation that is consistently expressed in schwannian and melanocytic tumors.^[29] Immunocytochemical evaluation was performed in all but two of our cases. S100 staining was strong in 14 cases and moderate in 1 case. Sox10 was positive in five cases. No staining was observed with Desmin, SMA, or CD34. The cell blocks of two cases did not contain sufficient material for further analysis; in these cases, immunohistochemical studies were performed on excision specimens.

The cytological features of schwannomas can overlap with those of other spindle cell lesions, such as neurofibromas, leiomyomas, gastrointestinal stromal tumors (GISTs), and fibromatosis.^[11,30,31] Neurofibromas such as schwannomas are peripheral nerve sheath tumors that can exhibit spindle-shaped cells and fibrillary stroma. However, neurofibromas typically lack encapsulation and Verocay bodies, which are often present in schwannomas.^[31]

Leiomyomas and GISTs, which are smooth muscle tumors, can also exhibit spindle-shaped cells, potentially leading to diagnostic confusion. These tumors may exhibit overlapping cytological features with schwannomas, such as elongated nuclei

and indistinct cytoplasm.^[30,31] However, leiomyomas and GISTs typically lack the characteristic Antoni A and B areas seen in schwannomas.^[30] Leiomyomas are actin, desmin, and H-caldesmon positive and negative for CD34, S100, sox10, CD117, and DOG1.^[32] GISTs, particularly in extra-gastrointestinal locations, can resemble schwannomas, posing a diagnostic challenge when they occur outside of their typical location.^[33] Immunohistochemical staining for CD117 and CD34 is crucial for differentiating GISTs from schwannomas, providing key markers for distinguishing these tumors. CD117 (KIT) is a receptor tyrosine kinase that is expressed in most GISTs, whereas CD34 is a hematopoietic progenitor cell antigen that is also expressed in a significant proportion of GISTs. In contrast, schwannomas are typically negative for both CD117 and CD34.^[33] The absence of S100 protein expression in GISTs further aids in distinguishing them from schwannomas, providing an additional marker for differentiating these lesions. While schwannomas are typically strongly positive for the S100 protein, GISTs are typically negative.^[33,34]

Fibromatosis, a benign fibrous proliferation, can mimic schwannomas owing to its spindle cell morphology and fibrous stroma.^[11,31] However, fibromatosis typically lacks encapsulation and Verocay bodies. In addition, fibromatosis may exhibit a more infiltrative growth pattern compared to the circumscribed appearance of schwannomas.^[11] In the parotid gland, myoepitheliomas can mimic schwannomas owing to their spindle cell morphology, creating a diagnostic challenge in this specific location.^[9,11] Myoepitheliomas typically exhibit a more disorganized cellular arrangement than schwannomas, with cells arranged in cords, nests, or sheets.^[17,27] Immunohistochemistry can help distinguish between these tumors and provide additional information to aid accurate diagnosis. Myoepitheliomas are typically positive for epithelial markers, such as cytokeratin and epithelial membrane antigen, as well as myoepithelial markers, such as SMA, calponin, and p63. In contrast, schwannomas are typically positive for S100 protein and negative for epithelial markers.^[25]

The differential diagnosis of schwannoma also includes malignant peripheral nerve sheath tumor (MPNST), a rare but aggressive sarcoma that arises from peripheral nerves.^[20,35,36] MPNSTs can exhibit overlapping cytological features with schwannomas, particularly in well-differentiated cases.^[20] However, MPNSTs typically exhibit more pronounced nuclear atypia, higher mitotic activity, and necrosis.^[20] Immunohistochemistry can also be helpful in distinguishing MPNSTs from schwannomas.^[20,36] While both schwannomas and MPNSTs may express the S100 protein, MPNSTs often exhibit loss of S100 expression in poorly differentiated areas.^[20] In addition, MPNSTs may express other markers such as p53, Ki-67, and nerve growth factor receptor.^[36]

However, it is important to note that S100 protein is not entirely specific for schwannomas and can be expressed in other tumors, such as melanomas, myoepitheliomas, and some soft tissue sarcomas.^[20,37] Therefore, S100 immunostaining should be interpreted in conjunction with cytomorphological findings and other clinical and radiological data.^[5,12]

In some cases, the cytological and immunohistochemical features of schwannomas may be ambiguous, making definitive diagnosis difficult. In these cases, molecular analysis can provide additional information to support diagnosis. Identification of an NF2 mutation can confirm the diagnosis of schwannoma, even in the absence of classic cytological or immunohistochemical features.^[6]

The presence of cystic degeneration and hypocellularity can lead to insufficient or inaccurate specimens, further complicating the cytological diagnosis of schwannoma. Cystic degeneration, which is a common feature of schwannomas, can result in aspiration of fluid with few or no diagnostic cells. Hypocellularity, or a low number of cells in the aspirate, can also make it difficult to evaluate the cytological features and arrive at a definitive diagnosis.^[11,16,38]

CONCLUSION

The diagnostic workup for schwannomas typically involves a combination of clinical examination, imaging studies, and cytological or histological analysis. FNAC can guide surgical planning and prevent unnecessary, extensive procedures by providing valuable information regarding the nature of the lesion before surgery. The cytological features of schwannomas include cohesive clusters of spindle-shaped cells, nuclear palisading, Verocay bodies, and a fibrillary stroma. However, the diagnosis can be challenging owing to cystic degeneration, degenerative changes, and overlapping features with other spindle cell lesions. Palisading, Antoni A and B areas, and Verocay bodies, which are cytological features expected to be seen in schwannomas, may or may not be seen rarely, as in our case series. This was not surprising for specimens with low cellularity. The presence of typical pointed nuclei and fibrillar cytoplasm with unclear boundaries are important diagnostic clues. However, these features, which are not specific to schwannomas, need to be confirmed by immunohistochemical techniques, especially by S100 immunohistochemistry. A comprehensive approach that integrates the clinical, radiological, and cytological findings is essential for the correct diagnosis and management of schwannomas.

**This study was presented as a poster presentation at the 10th National Cytopathology Congress, 21-23 April 2024, Istanbul, Turkey.*

DECLARATIONS

Ethics Committee Approval: The study was approved by İstanbul Training and Research Hospital Clinical Research Ethics Committee (No: 107, Date: 02/05/2025).

Conflict of Interest: The authors declare that there is no conflict of interest.

Funding: This research did not receive any specific grant from funding agencies in the public, commercial, or not-for-profit sectors.

Use of AI for Writing Assistance: Not declared.

Authorship Contributions: Concept – BÖ; Design – ŞED; Supervision – BÖ; Fundings – MC; Materials – BÖ, ŞED, ZBE; Data collection &/or processing – BÖ; Analysis and/or interpretation – MC; Literature search – ZBE; Writing – BÖ; Critical review – ŞED.



Peer-review: Externally peer-reviewed.

REFERENCES

1. Patnayak R, Anuradha SV, Uppin SM, Sundaram C, Raju GS, Jena A. Schwannoma of tongue - a case report and short review of literature. *Acta Oncol* 2007;46:265–6.
2. Pant A, Huda N, Aslam M. Benign solitary schwannoma of right ulnar nerve – a case report. *Acta Med Int* 2015;2:164–7.
3. Aslan G, Cinar F, Cabuk FK. Schwannoma of the submandibular gland: A case report. *J Med Case Rep* 2014;8:231.
4. Satarkar RN, Kolte SS, Vujhini SK. Cystic schwannoma in neck: Fallacious diagnosis arrived on fine needle aspiration cytology. *Diagn Cytopathol* 2011;39:866–7.
5. Wang B, Yuan J, Chen X, Xu H, Zhou Y, Dong P. Extracranial non-vestibular head and neck schwannomas. *Saudi Med J* 2015;36:1363–6.
6. Kalogeraki A, Tamiolakis D, Zoi I, Segredakis J, Kafousi M, Vakis A. Schwannoma of right cerebellopontine angle. A cytologic diagnosis. *Acta Biomed* 2018;89:411–4.
7. Abebe MW, Weldemicheal HA. Superficial peroneal nerve schwannoma. *Plast Reconstr Surg Glob Open* 2023;11:e4950.
8. Nigam JS, Bharti JN, Pradeep I, Rath A. Role of fine needle aspiration cytology in paratesticular neoplasms-a case reports-based systematic review. *Diagn Cytopathol* 2024;52:779–88.
9. Ciau N, Eisele DW, van Zante A. Epithelioid schwannoma of the facial nerve masquerading as pleomorphic adenoma: A case report. *Diagn Cytopathol* 2014;42:58–62.
10. Kang GC, Soo KC, Lim DT. Extracranial non-vestibular head and neck schwannomas: A ten-year experience. *Ann Acad Med Singap* 2007;36:233–8.
11. Chebib I, Hornicek FJ, Nielsen GP, Deshpande V. Cytomor-

- phologic features that distinguish schwannoma from other low-grade spindle cell lesions. *Cancer Cytopathol* 2015;123:171–9.
12. Manohar B, Raees A. Schwannoma neck: A diagnostic dilemma. *Int J Otorhinolaryngol Head Neck Surg* 2019;5:1422–4.
 13. Kumar YK, Rajan YRD. Intraparotid facial nerve schwannoma - A case report. *Ann Maxillofac Surg* 2024;14:252–4.
 14. Mallick D, Kumar S, Ravi R, Mukherjee AA. Isolated infra-orbital nerve schwannoma. *Bengal J Otolaryngol Head Neck Surg* 2023;31:175–8.
 15. Bhaker P, Chatterjee D, Gochhait D, Radotra BD, Dey P. Schwannoma of the parotid gland: Diagnosis by fine-needle aspiration cytology. *J Cytol* 2014;31:196–8.
 16. Chang S, Joo M, Kim H. Cytologic findings of fine needle aspiration biopsy of 23 schwannomas. *J Pathol Transl Med* 2008;19:41–6.
 17. Turkmenoglu TT, Arslankoz S. Schwannoma of submandibular gland: A rare salivary gland neoplasm diagnosed by fine needle aspiration. *J Cytol* 2022;39:84–5.
 18. Dodd LG, Marom EM, Dash RC, Matthews MR, McLendon RE. Fine-needle aspiration cytology of “ancient” schwannoma. *Diagn Cytopathol* 1999;20:307–11.
 19. Ren H, Cui X, Zhang L. Primary schwannoma of the thyroid gland: Analysis of case characteristics and review of the literature. *BMC Surg* 2024;24:234.
 20. Jiménez-Heffernan JA, López-Ferrer P, Vicandi B, Hardisson D, Gamallo C, Viguer JM. Cytologic features of malignant peripheral nerve sheath tumor. *Acta Cytol* 1999;43:175–83.
 21. Dokania V, Rajguru A, Mayashankar V, Mukherjee I, Jaipuria B, Shere D. Palatal schwannoma: An analysis of 45 literature reports and of an illustrative case. *Int Arch Otorhinolaryngol* 2019;23:e360–70.
 22. Yasumatsu R, Nakashima T, Miyazaki R, Segawa Y, Komune S. Diagnosis and management of extracranial head and neck schwannomas: A review of 27 cases. *Int J Otolaryngol* 2013;2013:973045.
 23. Gupta RK, Naran S, Lallu S, Fauck R. Fine-needle aspiration cytology in neurilemoma (schwannoma) of the breast: Report of two cases in a man and a woman. *Diagn Cytopathol* 2001;24:76–7.
 24. Douwes JPJ, van Eijk R, Maas SLN, Jansen JC, Aten E, Hensen EF. Genetic alterations in patients with NF2-related schwannomatosis and sporadic vestibular schwannomas. *Cancers* 2025;17:393.
 25. Gupta S, Borkataky S, Agarwal R, Singh S, Gupta K, Kudesia M. Rare diagnosis on aspiration cytology of parotid gland schwannoma. *Acta Cytol* 2010;54:112–4.
 26. Gong S, Hafez-Khayyata S, Xin W. Microcystic/reticular Schwannoma: Morphological features causing diagnostic dilemma on fine-needle aspiration cytology. *Am J Case Rep* 2014;15:538–42.
 27. Avila JMC. Fine needle aspiration cytology of schwannoma of the parotid gland. *Philipp J Otolaryngol Head Neck Surg* 2008;23:51.
 28. Buob D, Wacrenier A, Chevalier D, Aubert S, Quinchon JF, Gosselin B, et al. Schwannoma of the sinonasal tract: A clinicopathologic and immunohistochemical study of 5 cases. *Arch Pathol Lab Med* 2003;127:1196–9.
 29. Karamchandani JR, Nielsen TO, van de Rijn M, West RB. Sox10 and S100 in the diagnosis of soft-tissue neoplasms. *Appl Immunohistochem Mol Morphol* 2012;20:445–50.
 30. Rodriguez E, Telschow S, Steinberg DM, Montgomery E. Cytologic findings of gastric schwannoma: A case report. *Diagn Cytopathol* 2014;42:177–80.
 31. Prayaga A. Cytology of soft tissue tumors: Malignant spindle cell tumors. *J Cytol* 2008;25:87–8.
 32. Göktürk Ş, Göktürk Y, Kamaşak K, Tekelioğlu F. Rapidly growing leiomyoma mimicking schwannoma of the saphenous nerve in the lower extremity: An unusual case report. *J Musculoskelet Neuronal Interact* 2024;24:325–9.
 33. Li ZY, Liang QL, Chen GQ, Zhou Y, Liu QL. Extra-gastrointestinal stromal tumor of the liver diagnosed by ultrasound-guided fine needle aspiration cytology: A case report and review of the literature. *Arch Med Sci* 2012;8:392–7.
 34. Pakseresht K, Reddymasu SC, Oropeza-Vail MM, Fan F, Olyae M. Mediastinal schwannoma diagnosed by endoscopic ultrasonography-guided fine needle aspiration cytology. *Case Rep Gastroenterol* 2011;5:411–5.
 35. Dodd LG, Scully S, Layfield LJ. Fine-needle aspiration of epithelioid malignant peripheral nerve sheath tumor (epithelioid malignant schwannoma). *Diagn Cytopathol* 1997;17:200–4.
 36. Keel SB, Clement PB, Prat J, Young RH. Malignant schwannoma of the uterine cervix: A study of three cases. *Int J Gynecol Pathol* 1998;17:223–30.
 37. Shields JA, Font RL, Eagle RC Jr, Shields CL, Gass JD. Melanotic schwannoma of the choroid. Immunohistochemistry and electron microscopic observations. *Ophthalmology* 1994;101:843–9.
 38. Jadhav CR, Angeline NR, Kumar B, Bhat RV, Balachandran G. Axillary schwannoma with extensive cystic degeneration. *J Lab Physicians* 2013;5:60–2.

Effects of Albumin, Uric Acid, Hemoglobin, and C-Reactive Protein Levels on Rehabilitation Outcomes in Stroke: A Retrospective Clinical Study

 Selda Ciftci Inceoglu,¹  Aylin Ayyildiz,²  Cansu Adikti,¹  Banu Kuran¹

¹Department of Physical Medicine and Rehabilitation, University of Health Sciences, Sisli Hamidiye Etfal Training and Research Hospital, Istanbul, Türkiye

²Department of Physical Medicine and Rehabilitation, Basaksehir Cam & Sakura City Hospital, Istanbul, Türkiye

ABSTRACT

Objective: The aim was to explain the relationship between recovery in motor functions and ambulation skills after stroke and albumin, uric acid, C-reactive protein (CRP), and hemoglobin levels.

Materials and Methods: Patients who received inpatient rehabilitation in the physical medicine and rehabilitation (PM&R) clinic within the past 2 years were included in the study. Patients' discharge report, albumin, CRP, uric acid, and hemoglobin levels were obtained from the blood tests taken during hospitalization through the hospital system. The relationship between Brunnstrom staging (BS) and functional ambulation category (FAC) assessments before treatment and on the 15th day of rehabilitation, and the initial albumin, CRP, uric acid, and hemoglobin levels was investigated.

Results: The files of 135 patients were accessed. Six patients were excluded because they did not meet the inclusion criteria, and 4 patients were excluded because their data were incomplete. The study was completed with 125 patients. Albumin levels were low in 22 (17.6%) patients, and hemoglobin levels were low in 75 (60%) patients. CRP levels were above normal in 53 (42.4%) patients. When uric acid levels were examined, 1 (0.8%) patient was below normal, and 15 (12%) patients were above normal. There was no significant relationship between BS and albumin, CRP, uric acid, and hemoglobin levels ($p>0.05$). There was a significant positive relationship between improvements in FAC and albumin and hemoglobin levels ($p<0.05$).

Conclusion: Post-stroke FAC recovery is associated with albumin and hemoglobin levels.

Keywords: Albumin, C-reactive protein, Hemoglobin, Stroke, Uric acid

Cite this article as: Ciftci Inceoglu S, Ayyildiz A, Adikti C, Kuran B. Effects of Albumin, Uric Acid, Hemoglobin, and C-Reactive Protein Levels on Rehabilitation Outcomes in Stroke: A Retrospective Clinical Study. Eur Arch Med Res 2025;41(3):183–192.

INTRODUCTION

Stroke is a cerebrovascular disease (CVD) that causes loss of brain function due to interruption of blood flow to the brain or bleeding.^[1] It is a significant health problem worldwide. It is a significant cause of morbidity and mortality acquired

in adulthood.^[2] Most patients develop hemiplegia, affecting upper extremity functions and ambulation skills.^[3] Stroke rehabilitation is the primary treatment option recommended for functional limitations and disabilities that occur after a stroke.^[4]

Address for correspondence: Selda Ciftci Inceoglu, Department of Physical Medicine and Rehabilitation, University of Health Sciences, Sisli Hamidiye Etfal Training and Research Hospital, Istanbul, Türkiye

E-mail: seldavd@gmail.com **ORCID ID:** 0000-0002-0387-3558

Submitted: 19.05.2025 **Revised:** 20.05.2025 **Accepted:** 14.07.2025 **Available Online:** 12.09.2025

European Archives of Medical Research – Available online at www.eurarchmedres.org

OPEN ACCESS This work is licensed under a Creative Commons Attribution-NonCommercial 4.0 International License.



The success of stroke rehabilitation depends on many factors, including the severity of the stroke, emotional reasons, social aspects, early initiation of rehabilitation, and the experience of the stroke rehabilitation team.^[5] Several blood biomarkers have been used to provide prognostic information after ischemic stroke. Thirty-four different blood biomarkers are associated with physical outcomes after ischemic stroke. Increased C-reactive protein (CRP) is one of the early poor prognostic factors.^[6] Hypoalbuminemia is a strong, independent prognostic indicator of mortality and poorer functional outcomes in long-term follow-up.^[7] Serum uric acid levels are nonlinearly associated with the risk of poor functional outcome (U-shaped). This may be due to both the antioxidant and prooxidant nature of uric acid.^[8] It is known that low baseline hemoglobin levels are negatively associated with functional recovery.^[9]

This study aimed to demonstrate the relationship between albumin, CRP, uric acid, and hemoglobin levels and improvement in motor functions and ambulation skills in early stroke rehabilitation. Since stroke results are usually compared with a single blood parameter in the literature, our study makes a difference by examining the relationship with more parameters.

MATERIALS AND METHODS

Study Design

This study was designed as a retrospective clinical study. It was conducted in the Physical Medicine and Rehabilitation (PM&R) clinic between April and May 2025. Approval was obtained from the Şişli Hamidiye Etfal Training and Research Hospital Clinical Research Ethics Committee (April 22, 2025/approval no:4838). The study was conducted according to the STROBE checklist recommendations. Informed consent was obtained from the patients. The study was conducted in accordance with the principles of the Declaration of Helsinki.

Participants

Stroke patients aged 18 years and older who were admitted to the inpatient physical therapy and rehabilitation program in our PM&R department within the last 2 years were included in the study. Patients with a history of traumatic stroke, those whose rehabilitation program could not be optimally performed due to cognitive impairment, and those whose hospitalization or rehabilitation period was shorter than 15 days were not included in the study. All patients received a similar stroke rehabilitation protocol.

Clinical and Laboratory Assessments

Patients' demographic data, hospitalization, and 15th day of hospitalization were evaluated through the discharge report. Motor evaluations were evaluated with Brunnstrom staging (BS), and ambulation levels were evaluated with functional ambulation category (FAC). Brunnstrom recovery staging evaluates motor

recovery for 3 different regions: as upper extremity, the hand, and the lower extremity. Staging is done from 1 to 6 for each sub-heading. Higher levels indicate a better motor level.^[10] FAC scores ambulation from 0 to 5. While there is no functional ambulation in Stage 0, the person can ambulate independently in Stage 5.^[11]

Albumin, uric acid, hemoglobin, and CRP levels included in routine laboratory checks taken during hospitalization were obtained through the hospital system. Normal values were accepted as 35–52 g/L for albumin, 0–5 mg/L for CRP, 3.5–7.2 mg/dL for uric acid, and 130–175 g/L for hemoglobin. Patients were divided into 3 groups as those with no improvement, those with improvement, and those at the maximum stage from the beginning, in both Brunnstrom motor recovery staging and FAC. These groups were compared according to whether the albumin, CRP, uric acid, and hemoglobin levels were within the normal range. Thus, the effect of whether the laboratory values was normal or not on recovery was examined. In addition, the recovery and non-recovery groups were compared to show the effect of gender and aphasia on recovery in stroke.

Statistical Analysis

Descriptive statistics were given as numbers and percentages for categorical variables, and as mean, standard deviation or median, and interquartile range for numerical variables. In independent groups, non-parametric tests such as Mann–Whitney U and Kruskal–Wallis tests were used for numerical variables that did not conform to normal distribution. Student's T-test was applied for numerical data that conformed to normal distribution. Chi-square test was used for categorical data. In analyses where Kruskal–Wallis test was used, Dwass, Steel, Critchlow–Fligner analysis was used for post-hoc pairwise comparisons. Statistical analysis of the study was performed using "The jamovi project (2024)" jamovi (Version 2.5) [Computer Software] (Retrieved from <https://www.jamovi.org>).

RESULTS

The discharge report of 135 patients was examined. For various reasons, 6 patients whose treatment lasted <15 days and 4 patients with incomplete data were excluded from the study. A total of 125 patients were included in the study. The median age of the patients was 64 (interquartile range [IQR]=25) years. The median time since stroke was 3 (IQR=3) months. 65 (52%) of the patients were male. 93 (74.4%) of the patients had essential hypertension, 47 (37.6%) had diabetes mellitus, 21 (16.8%) had dyslipidemia, 28 (22.4%) had coronary artery disease, and 49 (39.2%) had other systemic diseases. Albumin levels were low in 22 (17.6%) of the patients, and hemoglobin levels were low in 75 (60%). CRP values were above normal in 53 (42.4%) patients. When uric acid levels were examined, 1 (0.8%) patient was below normal, 15 (12%) patients were above normal, and 109 (87.2%) were within normal limits (Table 1).

Table 1. Demographic variables of the patients and pre-treatment laboratory values

	Median (IQR)/n (%)
Age (year)	64 (25)
Gender	
Female	60 (48)
Male	65 (52)
Duration of cerebrovascular accident (month)	3 (3)
Additional diseases	
Essential hypertension	93 (74.4)
Diabetes mellitus	47 (37.6)
Dyslipidemia	21 (16.2)
Coronary artery disease	28 (22.4)
Other system diseases	49 (39.2)
Albumin	
Low	22 (17.7)
Normal	103 (82.3)
Hemoglobin	
Low	75 (60)
Normal	50 (40)
CRP	
High	53 (42.4)
Normal	72 (57.6)
Uric acid	
Low	1 (0.8)
Normal	15 (12)
High	109 (87.2)
Cerebrovascular accident etiology	
Ischemic	93 (74.4)
Hemorrhagic	30 (24)
Other	2 (16)
Number of cerebrovascular accident	
First	102 (81.6)
≥2	23 (18.4)
Clinical presentation	
Right hemiplegia	61 (48.8)
Left hemiplegia	56 (44.8)
Bilateral weakness	3 (2.4)
Loss of balance	5 (4)
Aphasia	
Motor	22 (17.6)
Sensory	2 (1.6)
Global	1 (0.8)
Dysarthria	43 (34.4)

IQR: Interquartile range.

The etiology was ischemic in 93 (74.4%) patients, hemorrhagic in 30 (24%) patients, and CVD due to other causes in 2 (1.6%) patients. While it was the first stroke in 102 (81.6%) patients, 23 (18.4%) patients had more than one stroke history. The hemiplegic side was the right in 61 (48.8%) patients, and the left in 56 (44.8%) patients. Bilateral weakness was present in 3 (2.4%) patients, and balance loss due to cerebellar stroke was present in 5 (4%) patients. Aphasia was present in 25 (20%) patients. Of these, 22 (88%) were motor, 2 (8%) were sensory, and 1 (4%) was global aphasia. In addition, 43 (34.4%) patients without aphasia had dysarthria (Table 1). The distribution of BS and FAC of the patients before treatment is shown in Table 2.

Table 2. Brunnstrom staging and FAC levels of patients before treatment

	n (%)
BS upper extremity	
Stage 1	30 (24)
Stage 2	20 (16)
Stage 3	13 (10.4)
Stage 4	12 (9.6)
Stage 5	25 (20)
Stage 6	25 (20)
BS hand	
Stage 1	42 (33.6)
Stage 2	14 (11.2)
Stage 3	15 (12)
Stage 4	7 (5.6)
Stage 5	18 (14.4)
Stage 6	29 (23.2)
BS Lower extremity	
Stage 1	9 (7.2)
Stage 2	13 (10.4)
Stage 3	30 (24)
Stage 4	16 (12.8)
Stage 5	21 (16.8)
Stage 6	36 (28.8)
FAC	
Stage 0	36 (28.8)
Stage 1	18 (14.4)
Stage 2	11 (8.8)
Stage 3	16 (12.8)
Stage 4	35 (28)
Stage 5	9 (7.2)

BS: Brunnstrom staging, FAC: Functional ambulation category.

The initial data and changes in functionality of the patients were also compared between males and females. While the mean age of female patients was significantly higher than male patients, hemoglobin and uric acid values were significantly lower than male patients ($p=0.001$, $p<0.001$, $p=0.008$, respectively). No significant difference was found in the presence of essential hypertension, presence of diabetes mellitus, CVD etiology, hospital stay, CRP, albumin pre-treatment and post-treatment BS and FAC evaluations according to gender ($p>0.05$) (Table 3). In addition, since the presence of aphasia is also important in rehabilitation, the improvements of patients with and without aphasia were also compared. When the improvements in FAC were compared between the aphasic and non-aphasic groups, no significant difference was found between them ($p=0.321$). When the improvements in BS were compared in the aphasic and non-aphasic groups, a significant difference was found between the groups ($p=0.007$). In pairwise comparisons between the groups, no difference was

found in terms of aphasia between the group with improvement and the group that was at maximum BS from the beginning ($p=0.774$), while the rate of aphasia in the group without improvement was significantly higher than in the groups with improvement and those at maximum BS from the beginning ($p=0.045$, $p=0.033$, respectively) (Table 4).

When patients with no improvement in BS, with improvement in BS, and those who were at the highest BS from the beginning were compared, no significant difference was found between the groups in terms of albumin, CRP, uric acid, and hemoglobin values ($p>0.05$). When the groups consisting of patients with no improvement in FAC, with improvement in FAC, and those who were at FAC level 5 from the beginning were compared, no significant difference was found between the groups in terms of CRP and uric acid ($p>0.05$). There was a significant difference between the groups in terms of albumin values ($p=0.027$). In post hoc pairwise comparisons, albumin values

Table 3. Pre- and post-treatment changes according to gender

	Female (n=60)	Male (n=65)	p
Age (year)	69 (IQR=16)	58 (IQR=17)	0.001m
Duration of CVE (ay)	3 (IQR=6.25)	4 (IQR=5)	0.630m
Duration of hospital stay (day)	20 (IQR=11)	22 (IQR=12)	0.462m
Presence of essential hypertension	42	51	0.279x
Presence of diabetes mellitus	23	24	0.871x
CVE etiology			
Ischemic	47	46	0.139x
Hemorrhagic	11	19	
Others	2	0	
Albumin (g/L)	37.90 (IQR=5.67)	40 (IQR=5.20)	0.116m
CRP (mg/L)	3.23 (IQR=5.67)	4.5 (IQR=6.63)	0.976m
Uric acid (mg/dL)	4.70 (IQR=1.80)	5.50 (IQR=1.60)	0.008t
Hemoglobin (g/L)	117 (IQR=16.75)	133 (IQR=20.0)	<0.001m
Pre-treatment BS			
Upper extremity	4.0 (IQR=3.25)	3.0 (IQR=4.0)	0.226m
Hand	3.5 (IQR=4.25)	3.0 (IQR=4.0)	0.597m
Low extremity	5.0 (IQR=3.0)	4.0 (IQR=2.0)	0.134m
Pre-treatment FAC	3.0 (IQR=3.0)	2.0 (IQR=4.0)	0.995m
Post-treatment BS			
Upper extremity	5.0 (IQR=4)	4.0 (IQR=4.0)	0.335m
Hand	5.0 (IQR=5)	3.0 (IQR=4.0)	0.677m
Low extremity	6.0 (IQR=2.0)	4.0 (IQR=3.0)	0.202m
Post-treatment FAC	3.0 (IQR=4.0)	4.0 (IQR=4.0)	0.462m

mMann-Whitney U test, xChi-square test; tStudent-T test; CVD: Cerebrovascular disease; CRP: C-reactive protein; BS: Brunnstrom staging; FAC: Functional ambulation category; IQR: Interquartile range.

Table 4. The effect of aphasia on clinical recovery

	Aphasic (n=25)	Non-aphasic (n=100)	p
BS			
Group 1	15	28	0.007x
Group 2	9	53	
Group 3	1	19	
FAC			
Group 1	11	33	0.321x
Group 2	14	61	
Group 3	0	6	

xChi-square test; BS: Brunnstrom staging; FAC: Functional ambulation category; Group 1: No-recovery, Group 2: Recovery, Group 3: Best level since the beginning; IQR: Interquartile range.

were significantly lower in the group with no improvement in FAC compared to the group with improvement ($p=0.022$). No significant difference was observed in other pairwise comparisons ($p>0.05$). Similarly, a significant difference was observed between the groups in terms of hemoglobin values ($p=0.042$). In post hoc pairwise comparisons, the hemoglobin level of the group with improvement in FAC was found to be significantly higher than the group with no improvement ($p=0.047$). There was no significant difference in other pairwise comparisons ($p>0.05$) (Table 5).

DISCUSSION

In this study, the relationship between motor recovery and ambulation in the early period after stroke and albumin, CRP, uric acid, and hemoglobin values was tried to be explained. No relationship was found between recovery in BS and the labo-

ratory values examined. In FAC recovery, it was seen that there was a relationship between albumin and hemoglobin levels. In addition, it was tried to show the relationship between gender and aphasia and recovery. It was seen that gender did not cause a difference in BS and FAC recovery. While aphasia did not cause a difference in FAC recovery, the aphasia rate was higher in the group without recovery in BS compared to the other groups.

It is of great importance to determine the prognostic factors of stroke, which is a significant cause of morbidity and mortality. Stroke is seen in female patients at older ages and is more mortal.^[12] In our study, the mean age of female patients was significantly higher than male patients, and uric acid and hemoglobin levels were significantly lower. However, these differences did not create a significant difference in clinical recovery. Aphasia, as a different prognostic factor, is associated with longer hospital stays and complications. Aphasia, compared to hemiparesis, may lead to poor clinical outcomes.^[13] In our study, the presence of aphasia was significantly higher in the group without recovery than in the group with recovery and in patients with maximum BS from the beginning. Perhaps these data will enable future studies to include applications for communication skills.

Low serum albumin levels are common in stroke patients^[14] and are associated with poor clinical outcomes and increased mortality.^[15] It also provides information about the premorbid nutritional status of stroke patients due to its long half-life.^[16] Our study has also shown that albumin is associated with ambulation. Globulin is also an acute-phase protein measured in serum. It increases in inflammation and is associated with hemorrhagic transformation in patients undergoing intra-arterial thrombolysis.^[17] A decrease in the albumin and globulin

Table 5. Relationship between laboratory values and clinical improvement

BS	Group 1 (n=43)	Group 2 (n=62)	Group 3 (n=20)	p
Albumin (g/L)	39.20 (IQR=4.9)	38.15 (IQR=6.08)	40.14 (IQR=5.0)	0.496†
CRP (mg/L)	2.82 (IQR=6.79)	6.82 (IQR=11.98)	2.90 (IQR=3.79)	0.074†
Uric acid (mg/dL)	4.70 (IQR=2.15)	5.30 (IQR=2.38)	5.50 (IQR=0.85)	0.117†
Hemoglobin (g/L)	118 (IQR=21.0)	128.50 (IQR=20.50)	127.0 (IQR=22.25)	0.062†
FAC	Group 1 (n=44)	Group 2 (n=75)	Group 3 (n=6)	p
Albumin (g/L)	37.10 (IQR=4.80)	40.0 (IQR=5.10)	38.0 (IQR=3.38)	0.027†
CRP (mg/L)	3.50 (IQR=13.80)	4.12 (IQR=6.35)	2.90 (IQR=1.35)	0.849†
Uric aside (mg/dL)	5.30 (IQR=1.73)	5.10 (IQR=2.0)	5.0 (IQR=1.13)	0.913†
Hemoglobin (g/L)	118.0 (IQR=25.50)	130 (IQR=25.50)	120.50 (IQR=8.0)	0.042†

†Kruskal–Wallis test; BS: Brunnstrom staging, FAC: Functional ambulation category, Group 1: No-recovery, Group 2: Recovery, Group 3: Best level since the beginning, IQR: Interquartile range, CRP: C-reactive protein.

ratio is associated with mortality.^[18] In our study, this ratio was not reversed in any patient, so the relationship with clinical outcomes could not be compared.

CRP is an acute-phase reactant that increases due to acute inflammation and tissue damage.^[19] CRP is associated with white matter lesions, stroke severity, and mortality.^[20,21] High CRP levels have been shown to lead to poor outcomes in the modified Rankin score at 3 months.^[22] However, in a study evaluating cases with intracerebral hemorrhage, it was determined that CRP was not associated with clinical and imaging results.^[23] In our study, no association was observed between CRP and either Brunnstrom motor staging or FAC. The fact that CRP is affected by many clinical conditions, the fact that patients cannot be questioned for the presence of chronic infection due to the retrospective study design, or that it is not known whether they received antibiotics for acute infection, may affect the results.

Uric acid is a product of purine metabolism. It can act as both a pro-oxidant and an antioxidant.^[24] The protection of vascular endothelial cell function and its neuroprotective effects are antioxidant effects.^[25] It has been observed that it causes a decrease in serum uric acid levels in the early phase of acute stroke, and this decrease is associated with severe stroke, large infarct volume, and poor outcomes.^[26,27] Hyperuricemia has also been reported to be associated with poor outcomes in stroke patients.^[28,29] Again, publications are showing that there is no significant relationship between uric acid and outcomes.^[24,30,31] In our study, there was no relationship between uric acid levels and clinical improvements. All these differences may be due to the bidirectional effect of uric acid, differences in study designs, or patients receiving drug therapy that affects uric acid levels. Future studies should take these differences into account and ensure that the results are more reliable.

Having abnormal hemoglobin levels increases the incidence of stroke.^[32] Low hemoglobin levels lead to an increase in infarct volume and infarct growth rate.^[33] In addition, anemia increases the risk of mortality after stroke.^[34] Low hemoglobin levels are associated with the presence of premorbid sarcopenia, prolonged hospital stay, and failure to improve dysphagia and daily living activities.^[35] Although studies generally focus on anemia, high hemoglobin levels are also associated with mortality and poor clinical outcomes. In addition, high hemoglobin levels may increase the risk of stroke recurrence and composite cardiovascular disease.^[36] In our study, the fact that the group with no improvement in FAC had significantly lower hemoglobin levels than the group with improvement supports the literature.

There are some limitations to our study. First, the study is retrospective, and only the 15th day rehabilitation results were evaluated. Second, since the study was conducted in a single

center, different results may be obtained in different locations and ethnic groups. Third, some clinical conditions, such as stroke localization, intensive care history, and recent antibiotic treatment history, were not evaluated. In addition, since the participants were only included in the inpatient rehabilitation program in the ward, the patient group consisted of those who had more severe strokes and therefore cannot be generalized to all stroke cases.

CONCLUSION

Albumin and hemoglobin levels are associated with improvements in FAC in early stroke rehabilitation. Multicenter studies with a larger number of patients and longer follow-up periods may more clearly show the relationship between laboratory parameters and clinical improvement in stroke.

DECLARATIONS

Ethics Committee Approval: The study was approved by Şişli Hamidiye Etfal Training and Research Hospital Clinical Research Ethics Committee (No: 4838, Date: 22/04/2025).

Informed Consent: Informed consent was obtained from the patients.

Conflict of Interest: The authors declare that there is no conflict of interest.

Funding: The authors received no financial support for the research and/or authorship of this article.

Use of AI for Writing Assistance: Artificial intelligence programs were not used in the study.

Authorship Contributions: Concept – SCI; Design – SCI, AA; Supervision – BK; Fundings – SCI, BK; Materials – SCI, CA; Data collection &/or processing – SCI, CA; Analysis and/or interpretation – SCI, AA; Literature search – SCI, AA; Writing – SCI, AA; Critical review – BK.

Peer-review: Externally peer-reviewed.

REFERENCES

1. Lee KE, Choi M, Jeoung B. Effectiveness of rehabilitation exercise in improving physical function of stroke patients: A systematic review. *Int J Environ Res Public Health* 2022;19:12739.
2. Murphy SJ, Werring DJ. Stroke: Causes and clinical features. *Medicine (Abingdon)* 2020;48:561–6.
3. Wolf SL, Catlin PA, Ellis M, Archer AL, Morgan B, Piacentino A. Assessing Wolf motor function test as outcome measure for research in patients after stroke. *Stroke* 2001;32:1635–9.
4. Morreale M, Marchione P, Pili A, Lauti A, Castiglia SF, Spallone A, et al. Early versus delayed rehabilitation treatment in hemiplegic patients with ischemic stroke: Proprioceptive or cognitive approach? *Eur J Phys Rehabil Med* 2016;52:81–9.

5. Clarke DJ, Forster A. Improving post-stroke recovery: The role of the multidisciplinary health care team. *J Multidiscip Healthc* 2015;8:433–42.
6. Lai YJ, Hanneman SK, Casarez RL, Wang J, McCullough LD. Blood biomarkers for physical recovery in ischemic stroke: A systematic review. *Am J Transl Res* 2019;11:4603–13.
7. Thuemmler RJ, Pana TA, Carter B, Mahmood R, Betten-court-Silva JH, Metcalf AK, et al. Serum albumin and post-stroke outcomes: Analysis of UK regional registry data, systematic review, and meta-analysis. *Nutrients* 2024;16:1486.
8. Zhang W, Cheng Z, Fu F, Zhan Z. Serum uric acid and prognosis in acute ischemic stroke: A dose-response meta-analysis of cohort studies. *Front Aging Neurosci* 2023;15:1223015.
9. Yoshimura Y, Wakabayashi H, Shiraishi A, Nagano F, Bise T, Shimazu S. Hemoglobin improvement is positively associated with functional outcomes in stroke patients with anemia. *J Stroke Cerebrovasc Dis* 2021;30:105453.
10. Brunnstrom S. Motor testing procedures in hemiplegia: Based on sequential recovery stages. *Phys Ther* 1966;46:357–75.
11. Holden MK, Gill KM, Magliozzi MR. Gait assessment for neurologically impaired patients. Standards for outcome assessment. *Phys Ther* 1986;66:1530–9.
12. Eren F, Ozguncu C, Ozturk S. Short-term prognostic predictive evaluation in female patients with ischemic stroke: A retrospective cross-sectional study. *Front Neurol* 2022;13:812647.
13. Boehme AK, Martin-Schild S, Marshall RS, Lazar RM. Effect of aphasia on acute stroke outcomes. *Neurology* 2016;87:2348–54.
14. Alcázar Lázaro V, del Ser Quijano T, Barba Martín R. Hypoalbuminemia and other prognostic factors of mortality at different time points after ischemic stroke. *Nutr Hosp* 2013;28:456–63.
15. Abubakar S, Sabir A, Ndakotsu M, Imam M, Tasiu M. Low admission serum albumin as prognostic determinant of 30-day case fatality and adverse functional outcome following acute ischemic stroke. *Pan Afr Med J* 2013;14:53.
16. Dziedzic T, Slowik A, Szczudlik A. Serum albumin level as a predictor of ischemic stroke outcome. *Stroke* 2004;35:e156–8. Erratum in: *Stroke* 2005;36:689.
17. Xing Y, Guo ZN, Yan S, Jin H, Wang S, Yang Y. Increased globulin and its association with hemorrhagic transformation in patients receiving intra-arterial thrombolysis therapy. *Neurosci Bull* 2014;30:469–76.
18. Wang A, Zhang Y, Xia G, Tian X, Zuo Y, Chen P, et al. Association of serum albumin to globulin ratio with outcomes in acute ischemic stroke. *CNS Neurosci Ther* 2023;29:1357–67.
19. Koenig W. High-sensitivity C-reactive protein and atherosclerotic disease: From improved risk prediction to risk-guided therapy. *Int J Cardiol* 2013;168:5126–34.
20. Fornage M, Chiang YA, O'Meara ES, Psaty BM, Reiner AP, Siscovick DS, et al. Biomarkers of inflammation and MRI-defined small vessel disease of the brain: The cardiovascular health study. *Stroke* 2008;39:1952–9.
21. Idicula TT, Brogger J, Naess H, Waje-Andreassen U, Thomassen L. Admission C-reactive protein after acute ischemic stroke is associated with stroke severity and mortality: The “Bergen stroke study.” *BMC Neurol* 2009;9:18.
22. Löppönen P, Qian C, Tetri S, Juvela S, Huhtakangas J, Bode MK, et al. Predictive value of C-reactive protein for the outcome after primary intracerebral hemorrhage. *J Neurosurg* 2014;121:1374–9.
23. Fonseca S, Costa F, Seabra M, Dias R, Soares A, Dias C, et al. Systemic inflammation status at admission affects the outcome of intracerebral hemorrhage by increasing perihematomal edema but not the hematoma growth. *Acta Neurol Belg* 2021;121:649–59.
24. Zhong J, Cai H, Zhang Z, Wang J, Xiao L, Zhang P, et al. Serum uric acid and prognosis of ischemic stroke: Cohort study, meta-analysis and Mendelian randomization study. *Eur Stroke J* 2024;9:235–43.
25. Shah A, Keenan RT. Gout, hyperuricemia, and the risk of cardiovascular disease: Cause and effect? *Curr Rheumatol Rep* 2010;12:118–24.
26. Brouns R, Wauters A, Van De Vijver G, De Surgeloose D, Sheorajpanday R, De Deyn PP. Decrease in uric acid in acute ischemic stroke correlates with stroke severity, evolution and outcome. *Clin Chem Lab Med* 2010;48:383–90.
27. Fernández-Gajardo R, Matamala JM, Gutiérrez R, Lozano P, Cortés-Fuentes IA, Sotomayor CG, et al. Relationship between infarct size and serum uric acid levels during the acute phase of stroke. *PLoS One* 2019;14:e0219402.
28. Karagiannis A, Mikhailidis DP, Tziomalos K, Sileli M, Savvatanos S, Kakafika A, et al. Serum uric acid as an independent predictor of early death after acute stroke. *Circ J* 2007;71:1120–7.
29. Arévalo-Lorido JC, Carretero-Gómez J, Robles NR. Cardiovascular risk assessment after one-year acute ischemic stroke based on uric acid levels and renal dysfunction. A clinical study. *Int J Neurosci* 2021;131:609–14.
30. Dawson J, Lees KR, Weir CJ, Quinn T, Ali M, Hennerici MG, et al. Baseline serum urate and 90-day functional outcomes following acute ischemic stroke. *Cerebrovasc Dis* 2009;28:202–3.
31. Miedema I, Uyttenboogaart M, Koch M, Kremer B, de Key-

- ser J, Luijckx GJ. Lack of association between serum uric acid levels and outcome in acute ischemic stroke. *J Neurol Sci* 2012;319:51–5.
32. Panwar B, Judd SE, Warnock DG, McClellan WM, Booth JN 3rd, Muntner P, et al. Hemoglobin concentration and risk of incident stroke in community-living adults. *Stroke* 2016;47:2017–24.
33. Bellwald S, Balasubramaniam R, Nagler M, Burri MS, Fischer SDA, Hakim A, et al. Association of anemia and hemoglobin decrease during acute stroke treatment with infarct growth and clinical outcome. *PLoS One* 2018;13:e0203535.
34. Barlas RS, Honney K, Loke YK, McCall SJ, Bettencourt-Silva JH, Clark AB, et al. Impact of hemoglobin levels and anemia on mortality in acute stroke: Analysis of UK regional registry data, systematic review, and meta-analysis. *J Am Heart Assoc* 2016;5:e003019.
35. Yoshimura Y, Wakabayashi H, Nagano F, Bise T, Shimazu S, Shiraishi A. Low hemoglobin levels are associated with sarcopenia, dysphagia, and adverse rehabilitation outcomes after stroke. *J Stroke Cerebrovasc Dis* 2020;29:105405.
36. Zhang R, Xu Q, Wang A, Jiang Y, Meng X, Zhou M, et al. Hemoglobin concentration and clinical outcomes after acute ischemic stroke or transient ischemic attack. *J Am Heart Assoc* 2021;10:e022547.